Gas chromatographic analysis of phospholipid fatty acids in human serum

Serum phospholipid fatty acid composition in relation to overweight, semen quality and weight loss

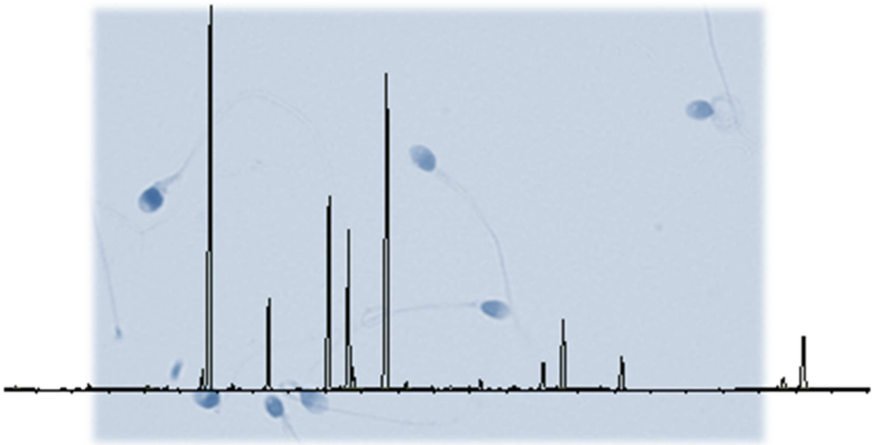

Siri Davidsen Bekken

May 2013

OSLO AND AKERSHUS
UNIVERSITY COLLEGE
OF APPLIED SCIENCES

Gas chromatographic analysis of phospholipid fatty acids in human serum

Serum phospholipid fatty acid composition in relation to overweight, semen quality and weight loss

by

Siri Davidsen Bekken

Master of biomedicine

Oslo and Akershus University College of Applied Sciences

Faculty of Health Sciences

Supervisors: Oliwia Witczak and Per Ola Rønning

Thesis submitted for the Master degree, 60 ECTS

May 2013

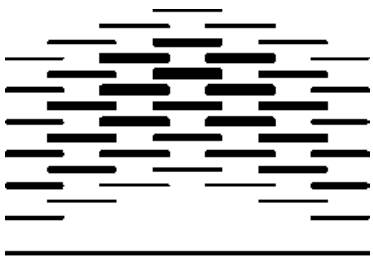

OSLO AND AKERSHUS
UNIVERSITY COLLEGE
OF APPLIED SCIENCES

Cover figures: Sperm cells stained with Papanicolaous staining method for examination of sperm morphology. Sperm cell nucleus obtains a dark blue/violet color. The sperm cell picture is overlaid by a chromatogram representing a typical participant sample analyzed in this master study.

ACKNOWLEDGEMENTS

The work presented in this master thesis has been carried out at the Faculty of Health Sciences, Oslo and Akershus University College of Applied Sciences (HiOA) from August 2012 to May 2013. The thesis is for the Master's degree in Biomedicine at HiOA.

I wish to thank Trine B. Haugen for welcoming me into her research group "Male reproductive health" and the research project "Effect of overweight on male reproductive function". A special thanks goes to my supervisors Associate Professor Oliwia Witczak and Per Ola Rønning for giving me the opportunity to work within an exciting research field, and for their encouraging support and thorough guidance throughout my study period. Thank you for your time and for willingly sharing your knowledge. Thanks to Professor emeritus Hans J. Grav for sharing his expertise in the field of fatty acid analyses.

I would also like to thank Hilde Herning for sharing her lab expertise and for always answering my many questions with a smile. Thanks to Jorunn M. Andersen for invaluable suggestions and advice, and to Elin L. Aschim for guidance through the confusing world of statistics. A thank you goes to my fellow student Linda for good laughs and support during this period.

Finally, I would like to thank my dearest friend Kine for her endless encouragement and for lending me her ear whenever needed. My heartfelt gratitude goes to my husband Per Kristian for reminding me that there are more to life than this master thesis, and for taking care of our daughter while I was working late nights. I could not have done this without you.

Oslo, May 20th 2013

Siri D. Bekken

ABSTRACT

Introduction: The increasing prevalence of overweight and obesity has become one of the major health concerns in modern times. Male obesity has been associated with decreased male reproduction function and fertility in some studies. Fertilizing ability may depend on a certain level of semen quality, and a link between male obesity and lowered semen characteristics has been suggested in several studies, although results are conflicting. Little is known on the influence of diet on semen quality in human males, and if weight loss will lead to an improvement in male reproduction function. Serum phospholipid fatty acid composition in some degree reflects dietary intake. The aim of this study was to investigate association between serum phospholipid fatty acid composition and semen quality, and to see whether the two parameters are affected by weight loss. Prior to this, a qualitative and quantitative method for analyses of serum fatty acid methyl esters (FAMEs) had to be established.

Methods: Serum samples from men with body mass index (BMI) in the normal, overweight or obese range were collected at baseline and after weight loss, and analyzed in this study. Qualitative and quantitative analyses of serum phospholipid FAMEs were performed by using gas chromatography coupled flame-ionization detector (GC-FID). Qualitative results were confirmed by using GC-mass spectrometry, and capabilities of the two detector types were compared. BMI and serum phospholipid fatty acid composition were investigated for association with semen quality data, and fatty acid composition and semen quality were examined at baseline and after weight loss.

Results: GC-MS presented a lower limit of detection and a more secure identification of FAMEs compared to GC-FID. At baseline, after adjusting for potential confounders, BMI in the obese range was inversely associated with semen volume, sperm concentration, total sperm count, total motility, progressively motile sperm count, sperm morphology and total normal morphology count, compared to men with normal BMI. The proportion of n-6 FAMEs in serum phospholipids showed an inverse association with sperm motility and normal morphology parameters. Increasing n-6/n-3-ratio was negatively, and the proportion of n-3 FAMES positively, related to sperm motility parameters. Weight loss was not found associated with any significant changes for neither serum phospholipid fatty acid composition nor semen quality.

Conclusion: GC-MS is a powerful tool for fatty acid analysis in complex sample material compared to GC-FID. This study found association between obesity and decreased semen quality. A high proportion of n-6 FAMEs and a high n-6/n-3-ratio in serum phospholipids, which is typical for a Western diet today, were inversely associated with sperm motility. Weight loss did not alter the serum phospholipid FAME composition or semen quality, but the lack of significant effects may be due to few participants and the fact that participants remained overweight or obese after weight loss. Participants going through weight loss should be followed until a normal BMI is reached to reveal any effects of weight loss on the two investigated parameters.

SAMMENDRAG

Introduksjon: Forekomsten av overvekt og fedme er blitt en av de største utfordringene innen helse i den moderne tid. En del studier har assosiert mannlig overvekt med nedsatt reproduksjonsfunksjon og fertilitet. Evnen til fertilisering kan være avhengig av et visst sædkvalitetsnivå. Flere studier har presentert en sammenheng mellom mannlig overvekt og nedsatt sædkvalitet, men det finnes også motstridende resultater. Det er lite kjent hvilken påvirkning kosthold har på human sædkvalitet, og om kostholdsendring og/eller vektnedgang vil føre til et forbedret mannlig reproduksjonspotensiale. Fettsyresammensetningen i serum fosfolipider reflekterer til en viss grad fettinntak via kosthold. Målet for dette studiet var å undersøke om det er en assosiasjon mellom fettsyresammensetningen i serum fosfolipider og sædkvalitet, samt om de to parameterne separat er påvirket av vektnedgang. For å gjøre dette mulig måtte en kvalitativ og kvantitativ analysemetode for serum fosfolipid fettsyre metylestere (FAME) etableres.

Metoder: Menn med kroppsmasseindeks (body mass index, BMI) karakterisert som normal, overvektig eller fedme avga blodprøver før og evt. etter vektnedgang, og serum ble benyttet i denne oppgaven. Kvalitative og kvantitative FAME-analyser ble utført ved gasskromatografi med flammeionisasjonsdetektor (GC-FID). Kvalitative analyser ble bekreftet med GC med massespektrometer (GC-MS) og de to instrumentene ble sammenliknet. BMI og FAME-sammensetningen i serum fosfolipider ble undersøkt i forhold til sædkvalitet, og FAME-sammensetning og sædkvalitet ble sett på separat før og etter vektnedgang.

Resultater: GC-MS førte til en sikrere identifikasjon av FAME og en lavere nedre deteksjonsgrense sammenliknet med GC-FID. BMI karakterisert som fedme før vektnedgang, viste invers assosiasjon med sædvolum, sædcellekonsentrasjon, total antall sædceller, total motilitet, totalt progressive sædceller, normal morfologi og totalt antall sædceller med normal morfologi sammenliknet med menn med normal BMI. Andelen n-6 FAME i serum fosfolipider var inverst assosiert med motilitet- og morfologiparametere. Økende n-6/n-3-ratio viste en negativ assosiasjon med motilitetsparameterne, mens økende andel n-3 FAME viste motsatt effekt. Vekttap førte ikke til noen signifikante endringer i verken serum fosfolipid FAME-sammensetning eller sædkvalitet.

Konklusjon: GC-MS ser ut til å være et kraftig verktøy for fettsyreanalyser i komplekst prøvemateriale sammenliknet med GC-FID. I dette studiet ble det funnet en assosiasjon mellom BMI og nedsatt sædkvalitet. En høy andel n-6 FAME og n-6/n-3-ratio i serum fosfolipider, noe som er typisk for dagens vestlige kosthold, var inverst assosiert med motilitet. Vekttap førte ikke til signifikante endringer i serum fosfolipid FAME-sammensetning eller sædkvalitet. En medvirkende årsak til mangelen på signifikant effekt av vekttap kan være få deltakere og at deltakerne fortsatt hadde en BMI karakterisert som overvektig eller fedme etter vekttapet. Deltakerne som går ned i vekt bør følges til de har oppnådd en normal BMI for å avsløre effekt av vekttap på de to aktuelle parameterne.

ABBREVIATIONS

AZF	azoospermia factor
BMI	body mass index
C	carbon
EFA	essential fatty acid
EI	electron ionization
eV	electron volts
FAME	fatty acid methyl ester
FID	flame-ionization detector
FSH	follicle-stimulating hormone
GC	gas chromatography
ISTD	internal standard
LH	luteinizing hormone
MS	mass spectrometry
MUFA	monounsaturated fatty acid
NA	not analyzed
ND	not detected
NP	non-progressive motility
NS	not separated
PC	phosphatidyl choline
PE	phosphatidyl ethanolamine
PR	progressive motility
PS	phosphatidyl serine
PUFA	polyunsaturated fatty acid
QMF	transmission quadrupole/mass filter (GC-MS)
ROS	reactive oxidative species
RSD	relative standard deviation
RT	retention time
RTL	retention time locking
SFA	saturated fatty acid
SIM	selected ion monitoring
TGCT	testicular germ cell tumor/cancer
TIC	total ion current
v/v	volume/volume
WCOT	wall coated open tubular column
WHO	World Health Organization
wt%	percentage weight of total

Contents

1 INTRODUCTION

The increasing prevalence of overweight and obesity has become one of the major health concerns in modern times (1). In the same time period, a decrease in semen quality has been observed (2, 3) Body mass index (BMI) over the normal range (Table 1.1) has been associated with lowered semen quality and altered hormone balance, which both can contribute to reduced reproduction potential (4-6). The pathophysiological mechanisms underlying the relation between obesity and semen quality are not yet clarified, but knowledge in the field is increasing (7). Studies on the reversibility of obesity-associated male infertility in response to weight loss are few (6), and weight loss by lifestyle changes or surgery as a treatment need to be explored further.

1.1 Overweight and obesity

Overweight and obesity have become one of the major public health concerns both in developed and developing countries, and worldwide obesity has more than doubled since 1980. Data from the World Health Organization (WHO) suggests that more than 1.4 billion adults, 20 years and older, were overweight per 2008. Of those more than 200 million males and 300 females were classified as obese. Overweight and obesity are defined as abnormal or excessive fat accumulation that may impair health, and are characterized as body mass index (BMI) ≥25 kg/m^2 and ≥30 kg/m^2, respectively (Table 1.1) (1).

Table 1.1 Body mass index (BMI) classification modified from the World Health Organization (12).

BMI classification	kg/m^2
Underweight	<18.5
Normal range	18.5-24.9
Overweight	25.0-29.9
Obese	≥30.0

Overweight and obesity are related to substantial health risks. Links have been established between overweight and increased risk of diseases including cancer, cardiovascular diseases and metabolic syndrome (8). Metabolic syndrome is defined as a cluster of disorders including obesity, hypertension, dyslipidemia and impaired insulin sensitivity (9). Impaired insulin sensitivity may develop further into type 2 diabetes (10). Known causes that contribute to development of overweight and obesity are an increased intake of fat-rich nutrients, combined with a decreased physical activity level due to sedentary work situations and increasing urbanization (1). In obese individuals these causes are often combined with an unfavorable genotype that predisposes individuals to obesity (11). Actions to reduce overweight and obesity have traditionally been mainly diet and lifestyle changes, but recently the use of bariatric surgery to lose weight has advanced. Bariatric surgery is usually performed to treat morbid

obesity (BMI ≥35 kg/m^2) (12). The most commonly performed bariatric procedure is Roux-en-Y gastric bypass surgery (Figure 1.1). A bariatric surgery is proven to be an effective treatment to reduce obesity-related health conditions for the patient group categorized as obese (13).

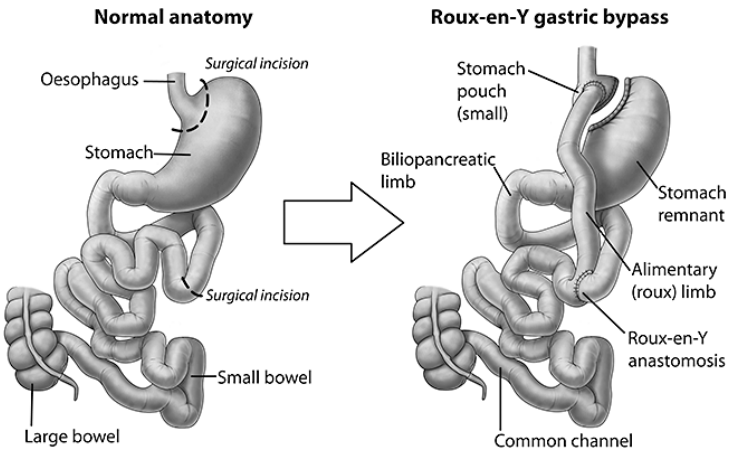

Figure 1.1 Roux-en-Y gastric bypass involve a rearrangement of the gastrointestinal tract. Ingested nutrition goes directly to the small bowel after passing a small stomach, leading to altered nutrition absorption (14).

1.2 Overweight in relation to subfertility or infertility

In developed countries, infertility is diagnosed in 10-15 % of couples who are trying to conceive (15). A couple are regarded infertile when they are unable to conceive during one year of regular intercourse without use of contraceptive methods, and there is no other obvious reason present (16). Women and men are each the sole cause of infertility in approximately 30 % of the cases, respectively, while 10 % is due to a combined factor. As much as approximately 25 % of infertile couples have no obvious cause (Figure 1.2).

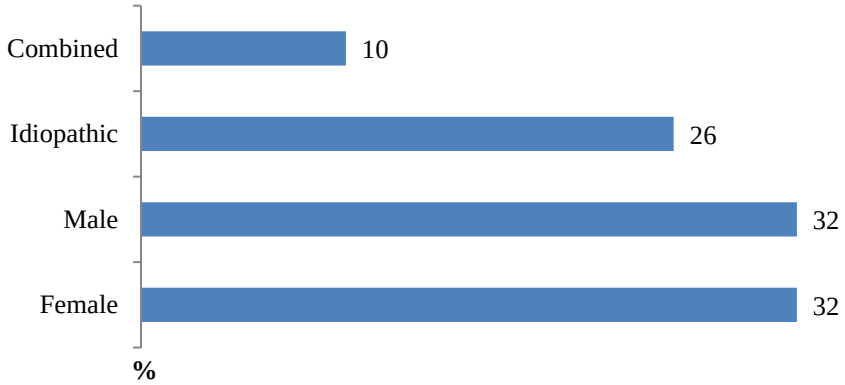

Figure 1.2 Unintentional causes of infertility may lie with the female, male or the couple combined. Approximately 25 % of infertile couples have no known cause (idiopathic infertility) (17).

Overweight and obese couples have an increased risk of experiencing subfertility (18). Several studies show that overweight in women leads to decreased fertility and prolonged time to pregnancy (19, 20).

High BMI for women prior to contraception is also associated with adverse outcomes of pregnancy. Today, weight loss before contraception is recommended for women with a BMI in the overweight or obese range to improve chances of a successful outcome both of natural pregnancies and assisted reproduction (21, 22). Overweight and its effect on male fertility have been studied to a lesser extent; however the body of evidence for a negative effect is growing. A 3-unit increase in BMI was associated with infertility in a study by Sallmen et al. (23). The observation was strengthen when results from the Norwegian Mother and Child Cohort Study showed an increased odds ratio for infertility for overweight and obese men compared to men with BMI 20.0-22.5 kg/m^2 (24). Several studies suggest that increased BMI has a negative effect on semen quality in general, but affected parameters vary (6, 25-27). These results are challenged by studies finding no significant correlation between increased BMI and semen quality (28-30). Varying inclusion factors, study populations and exposures make it difficult to reach a conclusion (7). Metabolic syndrome, which has a high prevalence in overweight and obese men, has also been associated with a decreased reproduction function (31). The observed decline in male fertility in parallel with increasing rates of obesity suggests that obesity is a cause of reduced male reproduction function, but the biological mechanisms responsible for the effect are not yet defined (11).

1.3 Human male reproduction function

1.3.1 Factors contributing to impaired male reproduction function and male infertility

A male factor is the sole cause of approximately 30 % of infertility cases, as shown in Figure 1.2 (15). Causes for disrupted male reproduction function are many (Figure 1.3), but 25 % of men presenting infertility have abnormal semen parameters for no known reason (male idiopathic infertility) (15).

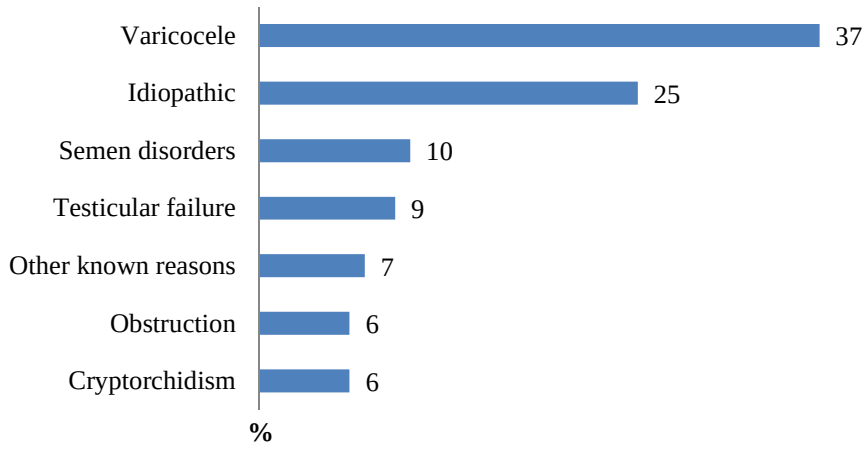

Figure 1.3 There are several known contributors to male infertility, but 25 % of presenting infertility have reduced semen quality without an obvious reason (32) .

Genetic disorders that affect male infertility are among others chromosomal abnormalities, Y chromosome microdeletions and cystic fibrosis mutations. Klinefelter syndrome is the most frequent sex chromosome abnormality in men, often followed by impaired spermatogenesis and azoospermia. Microdeletions in the long arm of the Y chromosome (azoospemia factor [AZF] deletions) are strongly associated with spermatogenetic failure. Classical AZF deletions are never found in normozoospermic males and the presence of AZF deletions are rare in males with sperm concentration $>5 \cdot 10^6$sperm/ml (the lower reference limit defined by WHO is $15 \cdot 10^6$sperm/ml). Cystic fibroses is the most common genetic disease of Caucasians and one of the symptoms following the diagnosis is infertility (15).

The number of young males diagnosed with testicular germ cell cancer (TGCT) has increased drastically during the last 15-20 years in Western Europe. TGCT as a disease involves a high risk of poor semen quality before cancer treatment. Chemotherapy and radiation as treatment for cancer in general have shown to negatively affect fertility in cancer survivors through gonadal damage, resulting in impaired spermatogenesis, germ cells damage and even permanent sterility in male patients. Post-treatment fertility for cancer patients is depending on pre-treatment fertility and type of cancer treatment the patient has received (33).

Two physiological abnormalities are associated with decreased reproduction function in men; varicocele and cryptorchidism. Varicocele is a common abnormality that may lead to reduced fertility and varicocele has been correlated with decreased sperm quality and increased sperm DNA damage. The effect of varicocele on reproduction function seems to be reversed after surgical correction (34). Cryptorchidism is a frequent congenital abnormality of the male genitalia. Lowered sperm quality parameters are often seen in men with a history of cryptorchidism (15).

The effects of overweight and obesity on male reproduction function are less clear than the causes mentioned above. Several mechanisms are suggested, and some of them are briefly described here.

Sperm DNA integrity and mitochondrial activity are important measurements of sperm function (35). Subfertile men have shown a higher total DNA fragmentation index in sperm than fertile semen donors (36). Increased BMI has been proven to correlate with a higher percentage of sperm DNA damage and decreased mitochondrial activity compared to normal weight men (37, 38).

The excess of nutrients associated with obesity lead to elevated cell stress and ROS production (39). Oxidative stress is a pathophysiologic process that arises when there is an excess concentration of reactive oxidative species (ROS) compared to the level of anti-oxidant defense in a defined physiologic environment (40). ROS are molecules with an unpaired electron, which makes the molecule reactive and unstable. ROS can induce great cellular damage to their surroundings, for example in the testicular microenvironment (41). The spermatozoa plasma membrane is very rich in polyunsaturated fatty acids (PUFAs) and is therefore vulnerable to damage caused by lipid

peroxidation (42, 43). Oxidative stress can result in sperm membrane lipid peroxidation that may lead to decreased sperm motility, impaired sperm-oocyte interaction and DNA damage (41, 44).

Sex hormones play a fundamental role in human reproduction and the hypothalamic-gonadal axis that regulates spermatogenesis and secretion of testosterone in men is shown in Figure 1.4. Obesity is associated with profound alterations in male reproductive hormone profile. Several androgens are secreted from the testes and the most significant androgen is testosterone. Testosterone stimulates the development of male sexual characteristics (45), and a decreased testosterone level leads to retention and phagocytosis of spermatids and reduced sperm counts (46, 47).

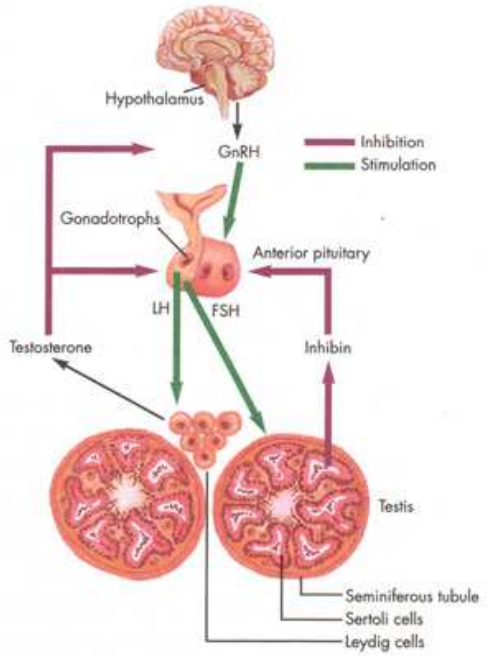

Figure 1.4 The hypothalamic-pituitary-gonadal axis regulates spermatogenesis and secretion of testosterone. Testosterone has a negative feedback effect on the release of gonadotropin-releasing hormone from the hypothalamus and luteinizing (LH) and follicle-stimulating (FSH) hormone from the pituitary gland. Inhibin B is produced and secreted by the Sertoli cells during FSH stimulation and has a negative feedback on the release of FSH from the pituitary gland (48, 49).

Free and total testosterone levels are shown to decrease with increasing BMI. Inhibin B, a marker of Sertoli cell function and spermatogenesis, decreases with increasing BMI and estrogen levels are elevated (25). White adipose tissue express high levels of an aromatase enzyme and increased estrogen/testosterone-ratio in obese males is a result of the increased conversion of androgens into estrogen (50). Increased estrogen levels may decrease both testosterone production and spermatogenesis (11, 51). Several environmental toxins are lipophilic and accumulate in fat-rich food and in fat tissue (5, 52). Such contaminants have been associated with decreased sperm production through their endocrine disrupting effect (53). Obese men have a high frequency of sleep apnea, and the fragmented sleep course leads to a disrupted nightly rise of testosterone. The disrupted testosterone rise is associated with abnormal spermatogenesis (54).

Overweight and obese men make out about 2/3 of men reporting erectile dysfunction, but the pathophysiological link between obesity and erectile dysfunction is not fully known (11, 55). Obesity is associated with a sedentary lifestyle (1). In combination with increased amount of scrotal fat, that may lead to increased testicular temperature, which has shown to be associated with reduced sperm concentration (56). Fever, sexually transmitted diseases and use of anabolic steroids can also contribute to decreased semen quality (15, 57).

Studies have shown that fertilizing ability depends on a certain level of sperm quality (58, 59). WHO has generated reference limits for measurements performed on semen samples (Table 1.2). The reference limits are based on semen samples from fertile men whose partner conceived within 12 months after ended use of contraception, as defined by Cooper et al. (60).

Table 1.2 WHOs lower reference limits for semen parameters, with 5 centiles (95 % confidence interval) [1] (60, 61).

Semen quality parameter	Lower reference limit
Semen volume (ml)	1.5 (1.4-1.7)
Total sperm count (10^6/ejaculate)	39 (33-46)
Sperm concentration (10^6 per ml)	15 (12-16)
Total motility (PR+NP %)	40 (38-42)
Progressive motility (PR %)	32 (31-34)
Vitality (live spermatozoa, %)	58 (55-63)
Sperm morphology (normal forms, %)	4 (3.0-4.0)

[1]The values are from non-weighted raw data. For a two-sided distribution the 2.5th and 97.5th centiles provide the reference limits; for a one-sided distribution the fifth centile provides the lower reference limit.
PR=progressive motility
NP=non-progressive motility

Men with semen characteristics below these reference limits are not necessarily infertile, and results must be interpreted in conjunction with additional clinical information. Neither do semen characteristics above the reference limits guarantee fertility. The reference limits are used as a tool to decide patient management, and as a threshold for clinical trials and investigations (61). The WHO laboratory manual for the examination and processing of human semen emphasizes that total number of progressively motile spermatozoa (total PR count) and the total number of spermatozoa with normal morphology (total normal morphology count) in the ejaculate are of biological significance, but do not define reference limits for the two calculated parameters.

WHO has also defined different variants of semen quality and the nomenclature and explanation of the most prevailing variants are listed in Table 1.3 (61).

Table 1.3 Definition of semen quality by the World Health Organization (61).

Name	Definition
Aspermia	No semen
Asthenozoospermia	Percentage of progressively motile spermatozoa below the lower reference limit
Asthenoteratozoospermia	Percentages of both progressively motile and morphologically normal spermatozoa below the lower reference limits
Necrozoospermia	Low percentage of live, and high percentage of immotile, spermatozoa in the ejaculate
Normozoospermia	Total number (or concentration) of spermatozoa, and percentages of progressively motile and morphologically normal spermatozoa, equal to or above the lower reference limits
Oligoasthenozoospermia	Total number (or concentration) of spermatozoa, and percentage of progressively motile spermatozoa, below the lower reference limits
Oligoasthenoteratozoospermia	Total number (or concentration) of spermatozoa, and percentage of both progressively motile and morphologically normal spermatozoa, below the lower reference limits
Oligoteratozoospermia	Total number (or concentration) of spermatozoa, and percentage of morphologically normal spermatozoa, below the lower reference limits
Oligozoospermia	Total number (or concentration) of spermatozoa below the lower reference limit
Teratozoospermia	Percentage of morphologically normal spermatozoa below the lower reference limit

1.3.2 Male reproduction system

Male external genitalia consist of penis and scrotum. Scrotum holds the testes and epididymis, as shown in Figure 1.5. The primary functions of the testes are spermatogenesis and the production of androgens. Scrotum is located outside the body because spermatogenesis is most efficient at a temperature 1-2 °C below body temperature (62).

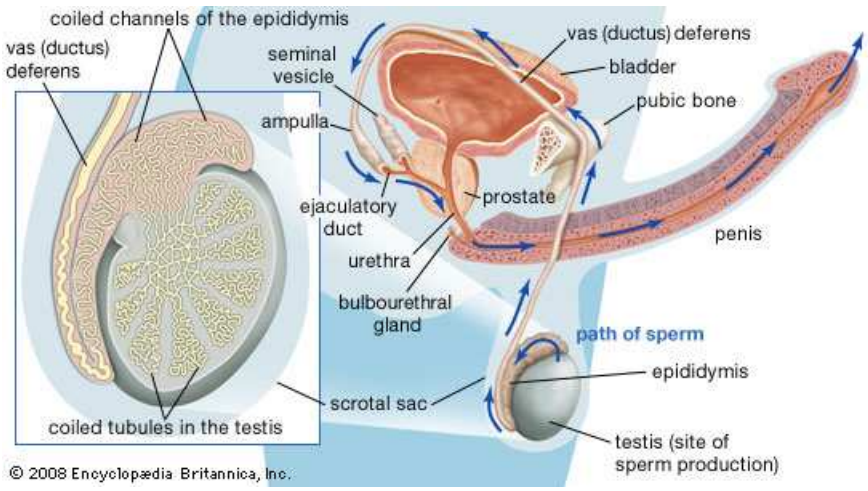

Figure 1.5 Adult human male reproductive system with an enlarged cross section of a normal testicle. Coiled seminiferous (coiled) tubules lead spermatozoa to the epididymis during maturation and spermatozoa are eventually transported through the vas deferens towards the urethra for ejaculation (63).

Testes contain a network of 12-20 fine coiled tubes called seminiferous tubules (64). Seminiferous tubules are lined with Sertoli cells that nourish developing spermatozoa. Spermatozoa are then led into the epididymis for further maturation. From epididymis spermatozoa pass through vas deferens and during ejaculation muscle contractions push spermatozoa further out through the urethra. When in urethra spermatozoa are mixed with a fluid from the prostate that activates sperm motility, called seminal fluid (62).

1.3.3 Spermatozoa

Spermatogenesis

Spermatogenesis occurs at puberty and continues through lifetime. In human males the production of spermatozoa takes approximately ten weeks, and a fertile male produces several hundred million spermatozoa each day (62). The development of spermatozoa from primordial germ cells is called spermatogenesis and can be divided into different stages, as shown in Figure 1.6. Primordial germ cells are located in testis early in embryogenesis. At the onset of puberty the stem-cell spermatogonia (Type A) profilerates and produces daughter cells that either remains Type A spermatogonia or become Type B spermatogonia. Type B spermatogonia go through a limited number of mitotic divisions before they enter meiosis as primary spermatocytes. Primary spermatocytes develop to secondary spermatocytes through meiotic division I. Secondary spermatocytes turn into haploid spermatids when meiotic division II is completed. The spermatids differentiate to mature spermatozoa (65).

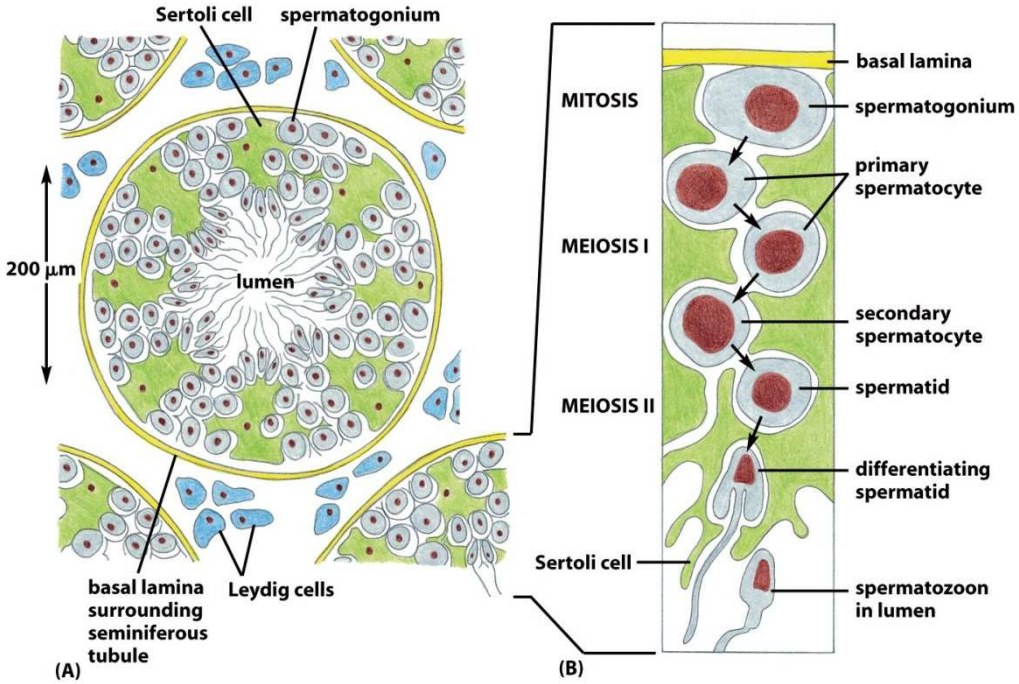

Figure 1.6 A simplified drawing of a cross section of a seminiferous tubule in a mammalian testis. The stages of spermatogenesis take place in close relationship with Sertoli cells (green). The maturing gametes move from the basal lamina towards the lumen of the seminiferous tubule. Sperm goes though further maturation in the lumen and become motile in the epididymis (not shown) (65)

Spermatozoa structure and function

Spermatozoa plasma membrane is in general stable and metabolically inert. There is no renewal of proteins, phospholipids, cholesterol or other membrane analytes in mature spermatozoa. During maturation spermatozoa have lost most organelles and the capacity of DNA transcription, protein synthesis and lipid synthesis. Despite the lack of these functions the spermatozoa plasma membrane acts as a dynamic compound that change in composition during maturation in the epididymis, and especially when the spermatozoa is moving towards the oocyte in the female reproduction system. The dynamic behavior of the spermatozoa plasma membrane is due to the ability to absorb proteins and lipids from the surroundings to modify its composition (42). The biochemical composition of the sperm membrane is of interest in the field of sperm physiology and pathology (66). It is suggested that lipids play an important role in sperm functionality and thus in male fertility (67, 68).

1.4 Lipids and fatty acids

1.4.1 Lipids

Lipids are amphipathic organic molecules present in all cell types. They provide cells with fuel, function as thermal insulators and contribute to cellular structure and communication in cell membranes. Lipids also have an important role as fat-soluble vitamins, hormones and biological regulators (69). Lipids are a diverse group of organic compounds that amongst others consists of neutral lipids including triacylglycerol and cholesterol, and the more polar phospholipids and sphingolipids (69).

1.4.2 Phospholipids

The term phospholipids is often used for lipids with phosphate-containing head groups. Phospholipids can be divided into glycerophospholipids (also called phosphoglycerides) which are lipids built on glycerol, and sphingomyelin (SM), which is built on sphingosine, both shown in Figure 1.7 (69).

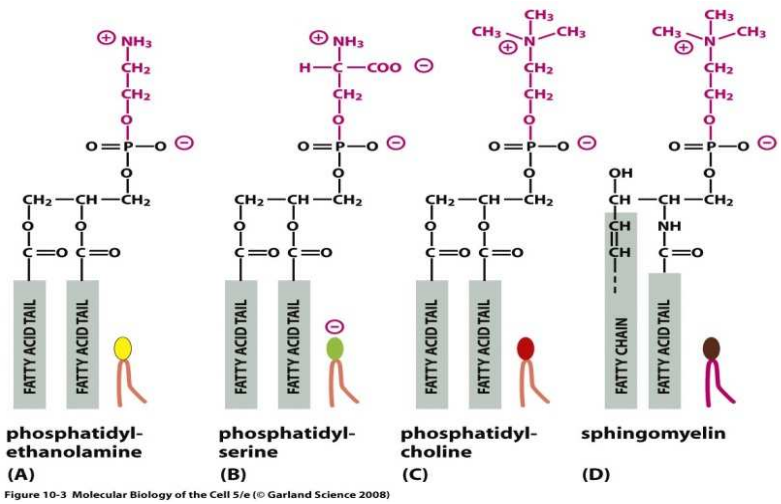

Figure 1.7 The four major phospholipids in mammalian plasma membranes, with the varying head groups denoted in different colors; Ethanolamine (yellow), serine (green), choline (red) and sphingomyelin with a choline head group (brown) (70).

SM will not be further discussed here, and the term phospholipids is used in this it will refer to glycerophospholipids. The polar head group is an earmark the phospholipid class, and consists of phosphoric acid attached at the sn-3 position (Figure 1.8) by a phosphate ester bond and a complex amino alcohol or amino acid bonded to the phosphate by a second phosphate ester bond (69).

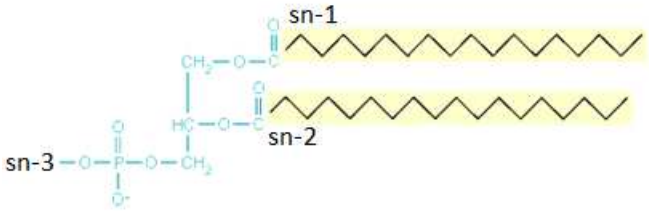

Figure 1.8 Glycerophospholipid structure with hydrophobic fatty acids (yellow) attached to position sn-1 and -2 on the glycerol backbone (blue), and sn-3 is the position where the hydrophilic head group binds to the phosphate group with a phosphate ester bond (69) .

The most common amino alcohols are choline and ethanolamine, and the most common amino acid is serine. Their following molecular names are phosphatidyl choline (PC), phosphatidyl ethanolamine (PE) and phosphatidyl serine (PS) (Figure 1.7). Each phospholipid class comprises several types of phospholipids with the same polar head group, but with different aliphatic acyl side chains, most commonly one saturated fatty acid (SFA) and one unsaturated fatty acid (69).

Glycerolipids and the following main subgroup glycerophospholipids are the most abundant membrane lipids in higher animals (69). Phospholipids, with their hydrophilic head group and hydrophobic tail, spontaneously form bilayers in aqueous environment because of their amphipathic nature (Figure 1.9) (70).

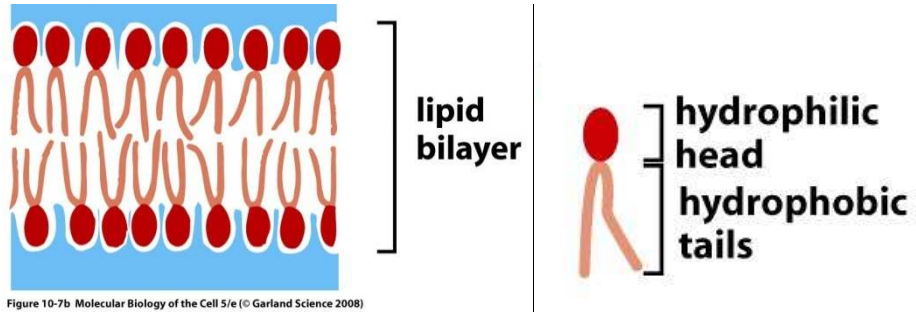

Figure 1.9 Left: A cross section of lipid bilayer of the membrane, the blue area represents an aqueous environment. Right: The most abundant membrane lipids are phospholipids with its hydrophilic phosphate head group and hydrophobic fatty acid tail. The straight tail is a saturated fatty acid and the tail with a kink contains a fatty acid with a *cis*-double bond (70).

1.4.3 Fatty acid nomenclature and structure

For many fatty acids there are trivial names, numeric symbols and systematic names. The shorthand nomenclature common in GC analysis of fatty acids will be used in this thesis. The shorthand annotation system is C*A*:*B* n-*X*, where *A* is the number of carbon (C) atoms in the fatty acid chain, *B* is the number of double bonds and n-*X* is the location of the double bond when counting from the methyl end of FAMEs (71). Trivial names, abbreviations and numeric names of common fatty acids in biology are listed in Table 1.4.

Table 1.4 Fatty acid nomenclature often used in biological and nutritional context.

Trivial name	Abbreviation	Numeric name
Palmitic acid	-	C16:0
Stearic acid	-	C18:0
Oleic acid	OLA	C18:1n-9
Linoleic acid	LA	C18:2n-6
α-Linolenic acid	ALA	C18:3n-3
Arachidonic acid	AA	C20:4n-6
Eicosapentaenoic acid	EPA	C20:5n-3
Clupanodonic acid	DPA	C22:5n-3
Docosahexaenoic acid	DHA	C22:6n-3

Saturated fatty acids (SFAs) contain no double bonds and they are mostly straight chain structures with an even number of carbon atoms. Examples of naturally occurring SFAs are C16:0 and C18:0 (72).

Monounsaturated and polyunsaturated fatty acids (MUFAs and PUFAs) contain one or more double bonds, respectively (73). In naturally occurring unsaturated fatty acids the double bond have a *cis*-configuration (Figure 1.10b) (69). *Cis* is from Latin and means “on the same side”. The most common MUFAs and PUFAs have an even number of carbon atoms. A double bond restricts motion at its acyl chain location. The *cis*-configuration gives the chain an angle of 120 °C in the average molecular shape, as shown in Figure 1.10b. Unsaturated fatty acids with *cis*-configuration are less thermodynamically stable and have lower melting points than SFAs with the same carbon number (72).

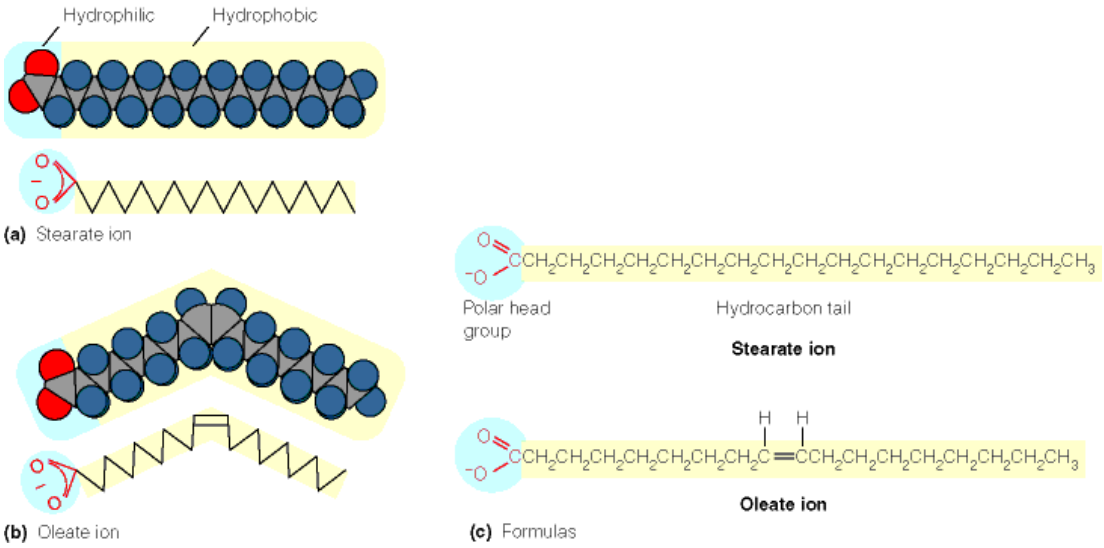

Figure 1.10 Structures (a,b) and formulas (c) for the ionized forms of two of the most abundant fatty acids in animals. The hydrophilic head groups are marked in pale blue and hydrophobic tails in yellow. Oleate ion has one *cis* double bond (69).

Fatty acids are weak acids and present in their anionic form ($RCOO^-$) at physiological pH, as shown in Figure 1.10 (69).

1.4.4 Serum lipids and serum phospholipid fatty acid composition

The percentage distribution of the major phospholipid classes in blood plasma is reported to be PC (70-72 %)>SM (16-21 %)>PE (2-4%)≥ PS (2 %)>other minor phospholipids (74). Fatty acids with a chain length from C8:0 to C26:1n-9 have previously been identified in plasma (75). The most abundant fatty acids found in plasma phospholipids were C16:0 with a median of 24.8 percentage weight of total fatty acids (wt%) with range 21.5-29.6 wt%, C18:0 [13.8 (10.6-16.9) wt%], C18:1n-9 [7.8 (6.3-13.3) wt%], C18:2n-6 [23.0 (17.1-29.1) wt%], C20:3n-6 [3.3 (1.5-5.5) wt%], C20:4n-6 [11.6 (7.0-17.1) wt%], and C22:6n-3 [3.1 (1.9-4.6) wt%] (76). These findings are confirmed in a review where 16 studies are compared and the most abundant fatty acids in plasma phospholipids were C16:0 [31.2 (26.3-38.5) mol%] and C18:2n-6 [21.9 (17.3-24.8) mol%]. The presence of C18:0 [14.3 mol%] was found to be larger than C18:1n-9 [10.1 mol%] and C20:4n-6 [8.3 mol%] (74).

1.4.5 Fatty acid metabolism

Mammalian cells lack the enzyme that converts n-6 fatty acids to n-3 fatty acids. Cells are dependent of two metabolically and functionally unequal, fatty acids provided through diet (77). The two essential fatty acids (EFAs) are C18:2n-6 (linoleic acid) and C18:3n-3 (linolenic acid) and they are precursors for the n-6 and n-3 families, respectively (Figure 1.11). Both C18:2n-6 and C18:3n-3 can be converted to more important active members of their n-families through desaturation and elongation (77, 78). The two EFAs are substrate for the same rate-limiting enzymes Δ6- and Δ5-desaturase in the synthesis of PUFAs (78, 79).

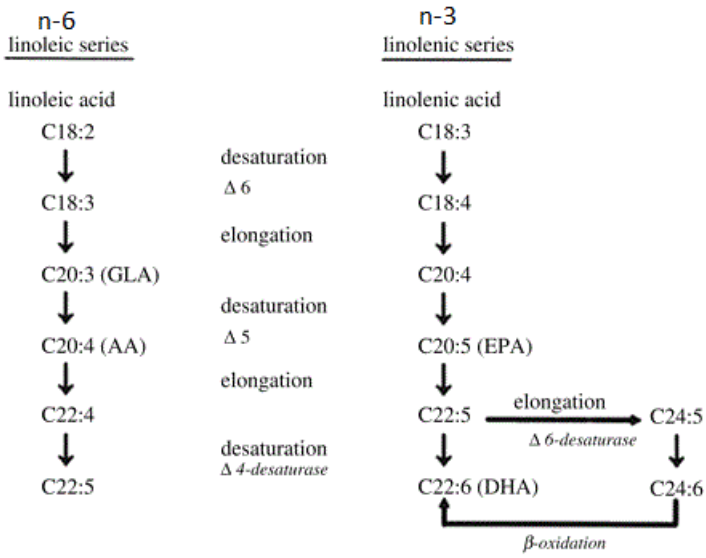

Figure 1.11 Desaturation and elongation of n-6 and n-3 fatty acids. Both pathways are competing for Δ6- and Δ5-desaturase, while the role of Δ4-desaturase is not clarified. Modified after Simopoulos (80).

These enzymes have a greater affinity for highly unsaturated fatty acids in the order C18:3>C18:2>C18:1 and should lead to a higher content of n-3 fatty acid in tissues, but that also depends on the ratios of the two EFAs provided through diet (77, 78). Long-chained SFAs and MUFAs can be endogenously synthesized from precursors mainly derived from carbohydrate, and C16:0 and C18:0 is desaturated to C16:1n-7 and C18:1n-9, respectively, by a Δ9 desaturase. Fatty acid ratios has been proposed as a measurement of desaturase enzyme activity; C20:4n-6/C20:3n-6 for Δ5 desaturase, C18:3n-6/C18:2n-6 for Δ6 desaturase and both C18:1n-9/C18:0 and C16:1n-7/C16:0 for Δ9 desaturase, but the use of these ratios is controversial when dietary fat intake is unknown (74). There are several factors that may influence the fatty acid composition in serum phospholipids, such as metabolic disorders, smoking, gender and enzyme activity for desaturases and elongases, together with dietary intake (74).

1.4.6 Dietary intake of fatty acids

Lipids in the human diet are structural and stored lipids from animals and plants (78). The fatty acid composition in serum phospholipids reflects dietary intake in previous weeks or months prior to blood collection for a selection of FAs, notably long chain n-3 PUFAs and C18:2n-6 (9, 81). Most SFAs and MUFAs can be endogenously synthesized; saturates can be derived from carbohydrates and be further derivatized to monounsaturates. In a study by Thiébaut et al. there was found no relation between the amount measured in serum phospholipids and dietary intake of C16:0 and C18:0. C16:1n-7 and C18:1n-9, which are products of the two SFAs, were directly related to dietary intake of C16:0 and C18:0 (81). C20:5n-3 and C22:6n-3 levels in serum are considered as biological indicators of nutritional status (82). The plasma phospholipids C20:5n-3 and C22:6n-3 are both shown to be effective biomarkers in response to dietary intake and supplementation of the corresponding FAs (83).

An n-6/n-3-ratio of approximately 16/1 is normal in the Western world diet today, compared to a 1/1-ratio during early human evolution. The elevated ratio is caused by a high percentage intake of cereal grains like maize, rice and wheat and vegetable seed oils, all rich in n-6 fatty acid, and modern food preparation methods used by the food industry (84). Fish and fish oil are rich in n-3 FAs, especially C20:5n-3 and C22:6n-3, and an increase in n-3 and a decrease in n-6 FAs in diet leads to replacement of n-6 FAs in cell membranes by n-3 FAs (77). The increased shift in n-6/n-3-ratio is linked to inflammation symptoms and pathogenesis of many diseases (77).

The dietary intake of fat from different food sources is often assessed by using self-reporting methods like validated food intake questionnaires. These methods are associated with a substantial measurement error (85). Measurement of the fatty acid composition in serum phospholipids is objective and potentially independent of these errors, but the fatty acid composition may be affected by other factors than just dietary intake. Non-dietary factors that contribute to the fatty acid composition are endogenous metabolism, genetic background, metabolic diseases and other lifestyle

factors (86), and results from analyses of serum phospholipid fatty acids should be interpreted with caution.

1.4.7 Serum and spermatozoa phospholipid fatty acids versus semen quality

Fatty acids in sperm and seminal plasma versus sperm quality

Several studies concerning fatty acid composition in seminal plasma and spermatozoa membrane have shown that C22:6n-3 is significantly lower in oligozoospermic and asthenozoospermic compared to normozoospermic men (68, 87) and the ratio of PUFAs/SFAs was lower in men with decreased sperm quality compared to men with normal sperm quality (67, 82, 88). Asthenozoospermic males are also shown to have a higher spermatozoa n-6/n-3-ratio than normozoospermic males (68, 82, 89). Normal sperm motility is shown to positively correlate with the amount of C22:6n-3 and total PUFAs in spermatozoa (67, 88). Some studies also found significant positive correlation between sperm morphology (87), sperm concentration and the amount of C22:6n-3 in spermatozoa (68).

Fatty acids in serum versus fatty acids in sperm and seminal plasma

A study on the effects of C22:6n-3 supplementation found increased serum and slightly increased seminal plasma phospholipid C22:6n-3 levels. The increased C22:6n-3 levels in serum and seminal plasma did not seem to affect the incorporation of C22:6n-3 into spermatozoa phospholipids (90). A study on rabbits reported that a diet with increased n-3/n-6-ratio led to a rearrangement of sperm fatty acid composition and a twice as high n-3/n-6-ratio in sperm membrane phospholipids compared to the control diet group (91). Safarinejad (2009) reported that 32 weeks of n-3 fatty acid supplementation gave an increase in C20:5n-3 and C22:6n-3 levels in seminal plasma and spermatozoa in humans (92).

Dietary fatty acids and semen quality

A correlation between fatty acid status in serum and sperm quality is not yet established. An analysis of human phospholipid fatty acids in serum, seminal plasma and spermatozoa found similar C22:6n-3 levels in serum of normozoospermic and asthenozoospermic males, suggesting a similar intake of dietary C22:6n-3. Levels of the same fatty acid in seminal plasma and spermatozoa were lowered in the asthenozoospermic males, maybe due to a metabolic difference rather than dietary variations (82). Early studies in rats showed that an EFA-deficient diet lead to degeneration of seminiferous tubules and absence of spermatozoa in the lumen of seminiferous tubules and epididymis (66). A study on benefits of different dietary n-3/n-6-ratios on male rat reproduction function showed that a ratio of 1.52 gave increased sperm density, motility and amount of morphologically normal sperm compared to both higher and lower ratios. The ratio of 1.52 also led to other improved reproduction function parameters, including improved serum reproductive hormone levels (93). Two recent human studies found that a high intake of SFAs seems negatively correlated to sperm concentration and total sperm count (94, 95). One of the studies also found that dietary intake of n-3 fatty acids positively correlated

with sperm morphology (95), while the other study found that a high intake of energy from monounsaturated fat was associated with lower percentage of sperm with normal morphology (94).

2 METHODS; INTRODUCTION AND THEORY

Fatty acids in biological sample material are traditionally analyzed with gas chromatography (GC) after being extracted and trans methylated to their fatty acid methyl ester (FAME) derivates (71, 96).

2.1 Sample preparation

2.1.1 Lipid extraction

Extraction involves transfer of a solute from one phase to another, often with the purpose to isolate or concentrate an analyte. The most common procedure is extraction of an aqueous solution with an organic solvent, and in this study chloroform-methanol was used to extract lipids from serum. Lipids in hydrophobic structures like membranes can readily be extracted by a non-polar solvent, while non-polar lipids surrounded by polar regions, or somehow bound in a structure protected from the non-polar solvent, will not be extracted. Chloroform-methanol is a polar-nonpolar solvent system that results in a quantitative extraction of lipids. The solvent system also denatures proteins and results in an insoluble protein residue that easily can be discarded. Unsaturated fatty acids must be protected against autoxidation during extraction and two precautionary approaches are 1) keep the sample and extraction solvent cold and 2) add an antioxidant to the solvent system before sample material is introduced. Sample material should be stored in -80 °C prior to extraction (97, 98).

2.1.2 Lipid fractionation

The separation of lipid fractions with ion-exchange chromatography is based on differences in polarity between the lipid classes. Polarity determines the degree of interaction with the functional group of the stationary phase. The stationary phase is in this study a non-polar matrix with positively charged NH_2-groups added; an anion-exchange matrix that retain fatty acids. Solvents lower the affinity for lipids to the stationary phase and wash lipids out of the column. Lipid classes are separated by adding solvents of varying polarity (99).

2.1.3 Derivatization of fatty acids

Fatty acids have the ability to make hydrogen bonds with the stationary phase in capillary columns used in GC. Hydrogen bonding leads to slow equilibrium processes and results in long retention times (100). Polar fatty acids are also unstable at the high temperatures used with GC. To avoid hydrogen bonding and degradation of unstable, polar fatty acids the phospholipids are transmethylated to stable derivatives of fatty acid methyl esters (FAMEs) by acid catalysis with methanolic HCl. The hydrogen atom in the hydroxyl group of the fatty acids is replaced with a methyl group (CH_3, R' in Figure 2.1) (101).

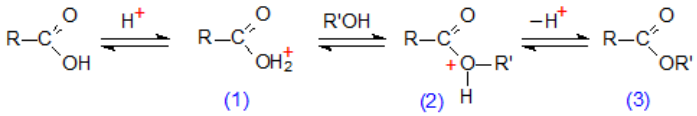

Figure 2.1 General mechanism for an acid-catalysed esterification of fatty acids (102).

All fatty acids are esterified at approximately the same rate by methanolic HCl, so differential losses of specific fatty acids during the esterification step are unlikely (102).

2.2 Gas chromatography (GC)

2.2.1 Principles of gas chromatography

GC is a separation method where compounds are separated by distribution between two phases; a gaseous mobile phase and a liquid or solid stationary phase. The separation takes place in a heated column. There are two main modes of GC depending on type of stationary phase; 1) gas-solid chromatography where the stationary phase is a solid adsorbent, and 2) gas-liquid chromatography, where the stationary phase is a non-volatile liquid (103, 104). To be separated on a gas chromatograph analytes must be sufficiently volatile and stable at the high temperatures used during analysis (105).

A gas chromatograph is composed of an injector/injection port, a heated oven where the column is placed, and one or more detectors. The chromatograph is connected to a computer with relevant software to process and display the results. A schematic presentation of a gas chromatograph is displayed in Figure 2.2.

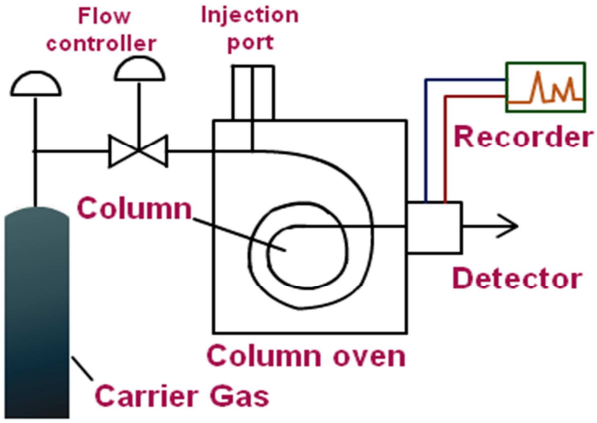

Figure 2.2 A schematic presentation of a gas chromatograph (106). The carrier gas transports the vaporized sample from the injection port through the heated column and to the detector.

Sample material is introduced to a heated injection port and rapidly vaporized. Vaporized sample material is transferred from the injector on to the column by a chemically inert gaseous mobile phase, often referred to as the carrier gas. The most commonly used carrier gases are helium (He), nitrogen gas (N_2) and, in fewer cases, hydrogen gas (H_2). The selection of carrier gas depends on detector used and desired resolution. The correlation between column efficiency and gas velocity is given in van

Deemter's plot for nitrogen, helium and hydrogen in Figure 2.3 (103). Height equivalent theoretical plate (HEPT), also called plate height, is mainly affected by mass transfer of analytes between the stationary phase and the mobile phase during separation. Plate height can be described as the length of a column needed to achieve one equilibration of analyte between the mobile and stationary phase. The smaller the plate height, the narrower the band width (104).

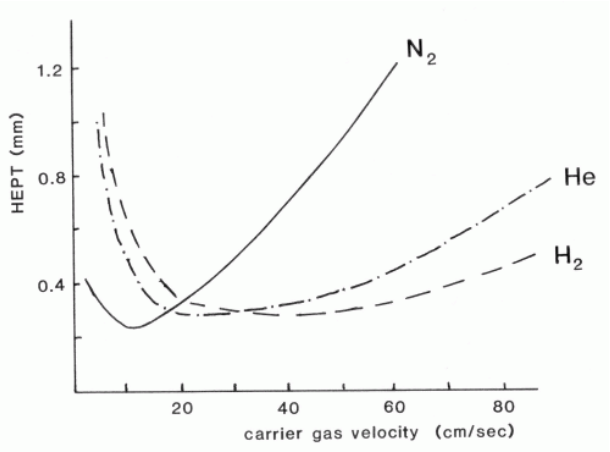

Figure 2.3 Van Deemter's plot showing optimum carrier gas flow to obtain maximum column efficiency. HEPT (height equivalent theoretical plate), is mainly affected by mass transfer of analytes between the stationary phase and the mobile phase during separation, and low HEPT gives high column efficiency (105).

Stationary phase is chosen based on its chemical characteristics. The stationary phase should facilitate interaction with analytes so they are separated within an acceptable analysis time (107). Intermolecular forces between stationary phase and sample analytes are based on Coulombs law; like attracts like. The distribution ratio (K) of analyte between carrier gas (C_{MP}) and stationary phase (C_{SP}) determines the analytes retention time (equation 1).

Equation 1

$$K = \frac{C_{SP}}{C_{MP}}$$

Analytes with high solubility in the stationary phase will progress slowly through the column and conversely; analytes with low solubility will travel with the carrier gas and elute early. K is dependent on temperature, analyte vapour pressure and analyte affinity for the stationary phase. When column temperature rises relative retention decreases and analytes in a sample elute closer together (107). A detector registers analytes as they elute from the column. The signals registered by the detector are converted to peaks in a chromatogram. The chromatogram displays retention time and signal strength, which is further used for identification and quantification of analytes (108).

2.2.2 Instrumentation

Injection techniques for GC

A split/splitless injector is the most common injector type for capillary columns (Figure 2.4). A split/splitless injector makes it possible to switch between two injection modes depending on sample concentration. Splitless is an injection technique for trace analysis and splitless means all injected material is transferred to the column. Split injection is used for samples with relatively high analyte concentration. Both injection modes are held at a temperature high enough to vaporize sample material and solvent, and the temperature is held constant trough out the GC run (105).

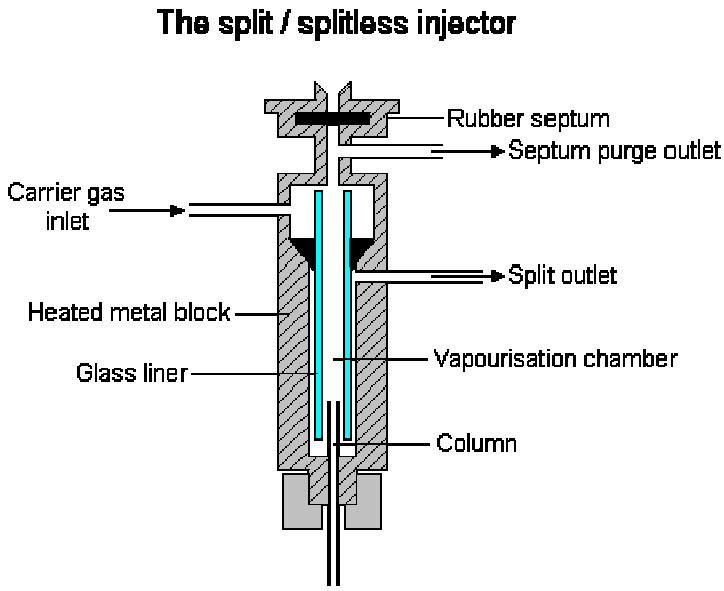

Figure 2.4: Split/splitless injector where sample is vaporized and transferred to the capillary column by an inert carrier gas (109).

A challenge when using splitless mode is the long transfer time of the analyte from the vaporization chamber to the column inlet, due to the reduced gas flow in the injector during the splitless transfer time. This results in excessive band broadening unless sample refocusing techniques are used. The most common refocusing technique is “solvent effect”, often in combination with the use of a retention gap. A retention gap column can minimize band broadening and refocus analytes. A retention gap contains no stationary phase and the fused silica tube is deactivated to avoid any analyte retardation. Non-volatile analytes condense in the retention gap to avoid contamination in the analytical column. The column temperature should be approximately 40 °C below solvent boiling point, and the low initial column temperature and the retention gap leads to solvent focusing. Solvent condenses at the column inlet and analytes are trapped in the solvent (“solvent effect”). When the temperature rapidly increases solvent is vaporized and analytes are focused to a narrow band before they are transferred on to the analytical column (108, 110).

Capillary columns

Analytes in a sample are separated in a heated column. Today open tubular capillary columns made of fused silica dominate. There are three different open tubular columns based on the shape and type of the stationary phase; wall-coated (WCOT), support-coated (SCOT) and porous-layer (PLOT). WCOT has a liquid stationary phase coated on the inside of the column and was used in this study, so WCOT will be further described in this text. A column length is between 15-100 m, with 30 m being the most common choice. A long capillary column provides better resolution, but also longer retention times and more time consuming analysis. Column inner diameter is often between 0.10 and 0.53 mm. Narrow columns gives better resolution, but require a higher pressure and have lower sample capacity than wider columns. Width of the column also depends on detector type, a mass spectrometer gets overloaded when using a column with diameter >0.32 mm. A capillary column consists of a fused silica coated with heat resistant polyimide (Figure 2.5), a material that provides mechanical strength to the long and thin column (105, 108).

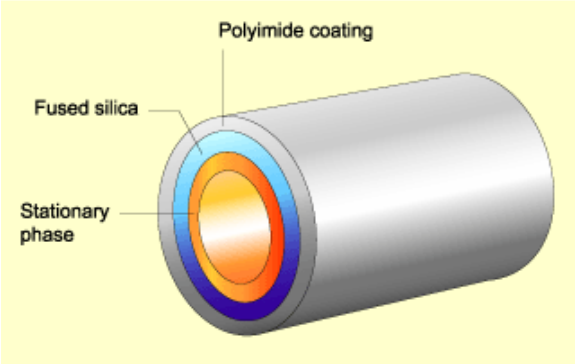

Figure 2.5 Cross-section of a capillary column showing the stationary phase coated on the inside wall of a fused silica column with polyimide coating (111).

Thickness of the stationary phase can vary within a range of 0.1-5 µm, but 0.25 µm is standard. A thick stationary phase increases sample capacity and retention times, and is mostly used for volatile analytes (108). The combination of long capillary column and a thin film of liquid stationary phase attached to the inner wall results in high resolution, great sensitivity and shorter analysis time (104). BPX70 (SGE International), the column used in this study, is a long capillary column. The columns stationary phase consist of 70 % dicyanopropyl 30% dimethyl polysilphenylene-siloxane (Figure 2.6) (112).

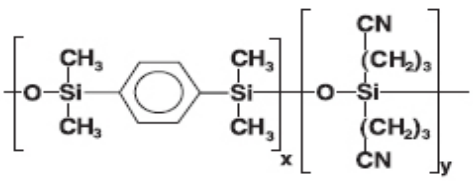

Figure 2.6 70 % Dicyanopropyl 30% Dimethyl Polysilphenylene-siloxane (112).

BPX70 is a polar phase column (Figure 2.7) designed especially for separation of FAMEs. The main advantage of a polar stationary phase compared to less polar stationary phase is their high resolution capability of unsaturated FAMEs (96). The high resolution capability may be due to interaction between pi bonds in the stationary phase phenyl group and double bonds in unsaturated FAMEs (113).

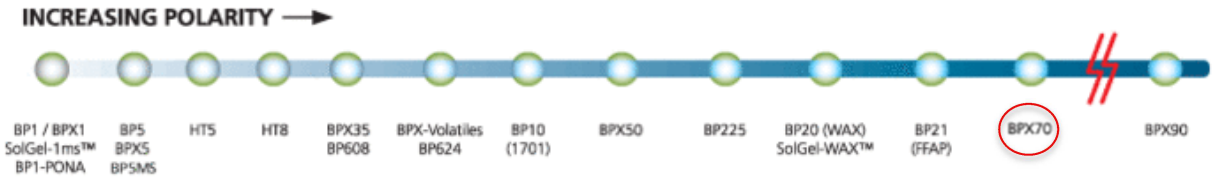

Figure 2.7: Polarity scale for columns made by SGE International. BPX70 is a polar phase-column, marked with a red circle (114).

2.3 Flame-ionization detector

2.3.1 Principles of flame-ionization detector

Flame-ionization detector (FID) is a mass sensitive detector that responds proportionally to the number of carbon atoms in a compound and is often used for general routine analyses (107). FID is sensitive to a wide range of organic compounds, it is not significantly affected by temperature and gas flow fluctuations and has a linear response covering seven orders of magnitude (10^7) (96). The limit of detection (LOD) for FID is approximately 10^{-12} g/ml and the lowest LOD is achieved when N_2 is used as carrier gas (107, 108). Occurrence of heteroatoms like O and S, and halogens in a compound will lead to reduced response in the detector. FID do not detect compounds such as H_2, O_2, N_2, NO_2, NH_3, H_2S and CO_2 (107). H_2O is not detected, but may interfere with other detectable compounds that elutes at the same time (103). Figure 2.8 show a schematic display of a FID.

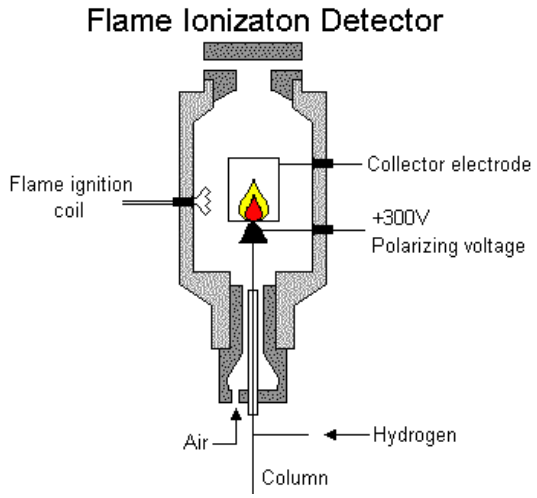

Figure 2.8 A schematic display of a flame ionization detector, where gaseous sample eluted from the column is burned in a flame of hydrogen and air (109).

Hydrogen is introduced to the column eluent. The mix meets the air stream and the sample is burned in a flame of H_2 and air (1:10) (105, 108). When an organic compound burns in the flame it produces ions. Carbon atoms produce CH radicals that are thought to further produce CHO^+ ions and electrons as shown in equation 2:

Equation 2:

$$CH + O \rightarrow CHO^+ + e^-$$

Only 1 in 10^5 carbon atoms produce an ion, but ion production is proportional with the number of available carbon atoms burned in the flame (C in carbonyl- and carboxyl groups will not produce CH radicals) (108). Between the flame and a collector electrode a current of 10^{-14} A flows when there is no organic compounds present. Burning of molecules containing carbon atoms produce a current of 10^{-12} A and the collector registers the alteration. The current is converted to voltage and the detector amplifies and translates the signal to a digital signal and displayed by the GC software in form of a chromatogram (108).

A disadvantage with the FID is the lack of selectivity; the detector responds to most carbon atom containing compounds. This is a challenge when complex sample material is analyzed. GC with mass spectrometry (GC-MS) will might be a better alternative for identification and quantification of FAMEs in complex samples (115).

2.3.2 Identification of FAMEs analyzed with GC-FID

Retention times are affected by several parameters; changes in temperature, flow-rate, column length, choice of stationary phase and film thickness. Retention time is not comparable between different columns, so identification of eluted compounds must be performed when test condition changes (107). The elution order of FAMEs depends on the polarity of the stationary phase. In general, FAMEs with the lowest molecular weight elutes first. For unsaturated FAMEs the retention time will increase with increasing number of double bonds. FAMEs with the same number of double bonds the fatty acid with double bond furthest away from the methyl end will elute first, as displayed in Figure 2.9. When a highly polar column like BPX70 is used, FAMEs with a high number of double bonds is strongly retained and C22:6n-3 elutes after C24:0, in spite of lower molecular weight (96).

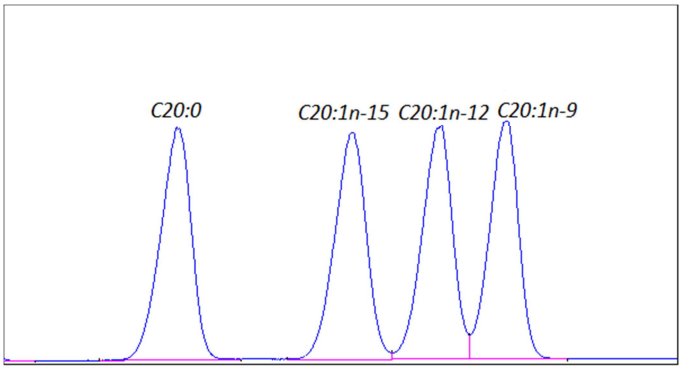

Figure 2.9: FAMEs with the lowest molecular weight elutes first. For unsaturated FAMEs every additional double bond leads to increased retention time, and if same amount of double bonds, FAME with double bond furthest from to the methyl end (n) elute first; C20:0<C20:1n-15<C20:1n-12<C20:1n-9.

There are several ways to identify unknown peaks in a chromatogram. Identification of unknown FAMEs can be performed by comparing their retention times to retention times of known analytes. A commercially available purified standard solution or natural products containing a spectra of well characterized fatty acids can be used for retention time comparison, assuming reproducible test conditions (96).

Alternative ways to identify unknown peaks in a chromatogram are 1) relative retention time (RRT), where the ratio between a reference peak retention time and the unknown peak retention time is calculated and compared to ratios for FAMEs in literature, 2) equivalent chain length (ECL) where the unknown peak is placed relative to straight-chain SFA peaks (C16:0, C18:0 and so on). Calculated ECL value is compared to ECL values in literature and 3) Kovats retention index (RI), where retention time of an analyte is related to retention time for linear alkanes. The latter option is not commonly used for identification of FAMEs (96, 107). A technique that makes identification of unknown peaks more reliable is retention time locking (RTL), a feature of the Agilent ChemStation software used in this study. A compounds retention time shows significant variations from run to run, due to fluctuations in GC-parameters such as pressure and temperature, and decomposition of stationary phase. RTL minimize the effect of these variations. RTL is based on that small adjustments in inlet pressure during analysis will keep retention time within a very narrow time range to the desired retention time (116). Even with the use of RTL, identification of unknown FAMEs with GC-FID is sensitive for contaminants behaving like FAMEs. Identification of unknown analytes should therefore be confirmed with mass spectrometry (96).

2.4 Mass spectrometry

Gas chromatography combined with mass spectrometry (GC-MS) is an analytical technique used for separation, identification and quantification of organic compounds in complex samples. GC separates analytes in complex samples and MS give qualitative and quantitative information that can lead to

identification and quantification of analytes (117). A schematic display of a mass spectrometer is shown in Figure 2.10.

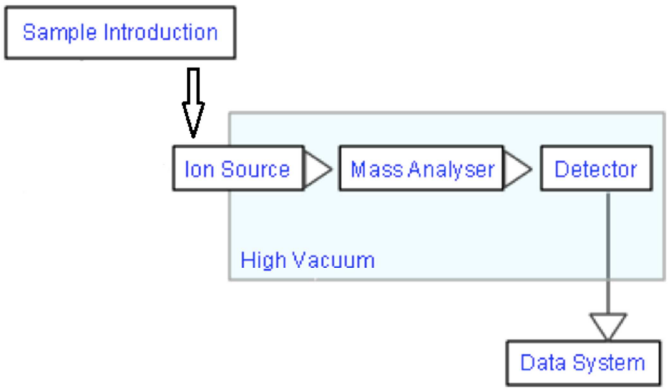

Figure 2.10 A schematic display of a mass spectrometer. Sample elute from the GC-column and analyte molecules are fragmented and ionized by the ion source. Fragments are separated according to their mass-to-charge ratio, detected and displayed as a mass spectrum.

To obtain a mass spectrum, gaseous sample material eluted from the GC-column is ionized. Ions are accelerated by an electric field and separated according to their mass-to-charge ratio (*m*/*z*) (118). If all charges are +1, *m*/*z* is numerically equal to the mass.

2.4.1 Ionization techniques

The ionization technique used in this study was electron ionization. When the gas-phase eluate enters the MS molecules are ionized by electron ionization (EI). EI is the most commonly used ionization technique in GC-MS. A heat-induced beam of electrons (e^-) from a hot filament are accelerated through a 70 V electric field before they come in proximity with the gaseous molecules eluted from the GC-column. Molecules (M) absorb energy from interaction with electrons and 12-15 eV (electron volts, 1 eV = 96.5 kJ/mol) provide enough energy for ionization:

Equation 3:

$$\underset{70\ \text{eV}}{M + e^-} \rightarrow \underset{\sim 55\ \text{eV}}{M^{+\cdot}} + e^- + \underset{0.1\ \text{eV}}{e^-}$$

$M^{+\cdot}$ designates the molecular ion, which is a radical ion with an odd number of electrons. Maximum fragmentation occurs when the ionization potential is approximately 30 eV, so $M^{+\cdot}$ often have residual energy and break into both neutral and ion fragments (118). The reaction pathway in equation 4 is an example of a general sequence of fragmentation, the specific fragment reactions depends of the original molecule structure.

Equation 4

$$M^{+\cdot} \overset{\nearrow R\cdot}{\longrightarrow} m_1^+ \overset{\nearrow n_1}{\longrightarrow} m_2^+ \overset{\nearrow n_2}{\longrightarrow} most\ stable\ fragment\ ion\ (base\ peak)$$

where $R\cdot$ is a radical fragment, *m* is ion fragments and *n* is neutral molecules. The use of 70 eV secures a reproducible EI spectrum according to specific reaction pathways. The reproducible pattern of fragments can be used for identification. EI efficiency is only 0.01 % to 0.001 %, but despite the low efficiency a very low analyte amount (pg-range) gives a spectrum that can be matched against available mass spectral databases. A great advantage with the EI technique is large commercially available databases of EI spectra, compared to other ionization techniques with smaller available databases (119).

To increase the abundance of the molecular ion, the energy of electrons in the ionization source can be lowered to 20 eV, which will lead to less fragmentation. Another option is to change ionization technique to chemical ionization. Chemical ionization is a soft ionization technique, resulting in less fragmentation than EI and is the preferred ionization technique when studying molecule masses (118).

2.4.2 Mass analyzers

There are several different types of mass analyzers commonly used in combination with GC on the market. Three common bench top alternatives are; transmission quadrupole GC-MS (QMF), quadrupole ion trap GC-MS and time-of-flight GC-MS (118, 119).

QMF was used in this study and is one of the most common mass analyzers, mostly because of its robustness, low cost and usability (119). The quadrupole consists of four parallel electric poles. The poles are arranged in pairs, so two poles across from each other have the same direct current potential (positive or negative) and the two other poles the opposite potential as shown in Figure 2.11. At the same time a radio frequency oscillating voltage is applied to all four poles, creating an alternating electric field leading ions into oscillating trajectories as they move from the ionization chamber towards the detector (118).

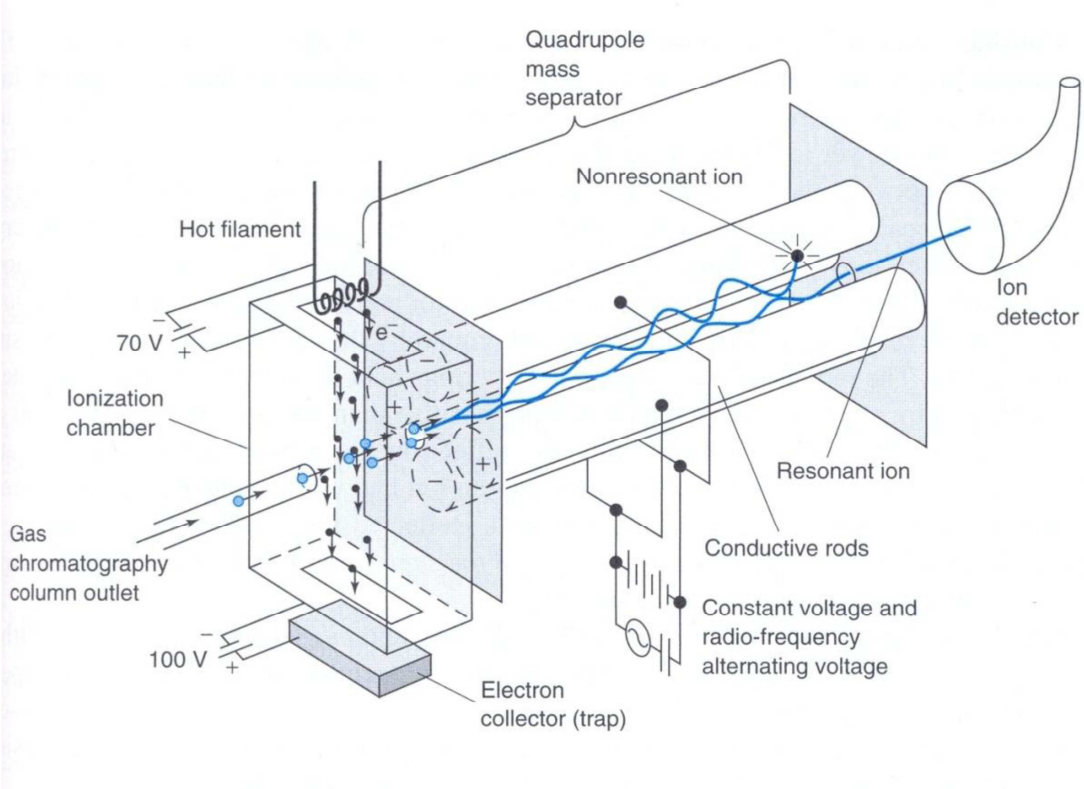

Figure 2.11: An illustration of a transmission quadrupole GC-MS (QMF). Gaseous molecules from the GC column are ionized and lead into the quadrupole mass separator. Metal poles with pared electric potential (+/-) give ions with a certain m/z-ratio stable oscillations so it reaches the detector. By varying the electric potential different ions are detected (118).

The chosen electric field allows only ions with a specific *m/z*-ratio to get stable oscillations and be transmitted to the detector. By rapidly changing voltages ions with different *m/z*-ratio are sent to the detector and a QMF can register 2-8 spectra per second and covers a range of up to 4000 *m/z* units (118).

2.4.3 MS data acquisition

Total Ion Current chromatogram

A total ion current (TIC) chromatogram is constructed from the intensity of consecutively detected mass spectra in a full scan mode for the range of *m/z*-values entered in the method. A TIC displays the abundance of analyte as a function of retention time. Analysis performed in TIC-mode detects all compounds in a sample, and provide limited information for complex samples where compounds may co-elute. It is possible to extract the ion current of a single *m/z*-value post-acquisition to obtain a mass chromatogram, often called extracted ion chromatogram (EIC). EIC can be used to visualize and resolve suspected co-eluting substances, or to provide clean chromatograms of compounds of interest. To increase selectivity and signal-to-noise ratio for both qualitative and quantitative purposes more specific methods like selected ion monitoring (SIM) can be used (119, 120).

Selected Ion Monitoring

The MS detector can scan a sample for one or a few ions characteristic for target compound(s). Selected ion monitoring (SIM) results in selective chromatograms displaying only the peaks providing ions with the targeted *m/z*-values. SIM is often used for trace analysis and is convenient because only the information of interest is recorded, which results in a method with high selectivity. With SIM the quadrupole analyzer toggles between the one or few chosen *m/z*-values instead of full scan for a great range of *m/z*-values as with TIC. In complex samples like human serum some FAMEs may coelute. Co-elution can be recognized by ion traces and co-eluting compounds can be separated by SIM if they differ in ion fragmentation. More time to monitor a few *m/z*-values results in improved sensitivity, lower detection limit and more defined chromatogram peak profiles because the background noise is decreased compared to TIC and EIC (118, 119). Mass spectra from SIM chromatograms cannot be used for library searches because a complete spectrum is lacking. This is not considered a problem if full scan analyses are performed for the same sample material, while SIM is used specifically for quantitative measurements for selected quantitation and qualification ions based on the full scan analysis.

2.4.4 Interpreting FAME mass spectra

When identifying an unknown analyte from a mass spectrum it is necessary to gather information about the analyzed sample. Knowledge about origin, collection and chemical and structural characteristics will come in handy in the analyte identification process. Mass spectra are read from right to left and a mass spectrum for C16:0 is shown in Figure 2.12. The molecular ion ($M^{+\cdot}$) gives us the molecular mass of an unknown. If present, the molecular ion peak can be found to the right in a mass spectrum (ion with the highest *m/z*-value) (120). If the $M^{+\cdot}$ is not visible, its fragments are also important clues to the structure of the unknown (118). Examples are M^+-18 (loss of H_2O), M^+-31 (loss of a methoxygroup), M^+-43 (loss of propyl) and M^+-74 (loss of a McLafferty fragment). An ion in a mass spectrum is not represented with a single peak, but a cluster of peaks where the peak with the lowest *m/z*-value is the monoisotopic mass peak. The percentage relationship between peaks relative to the monoisotopic peak in a cluster can be used in identifying the elemental ion composition (118).

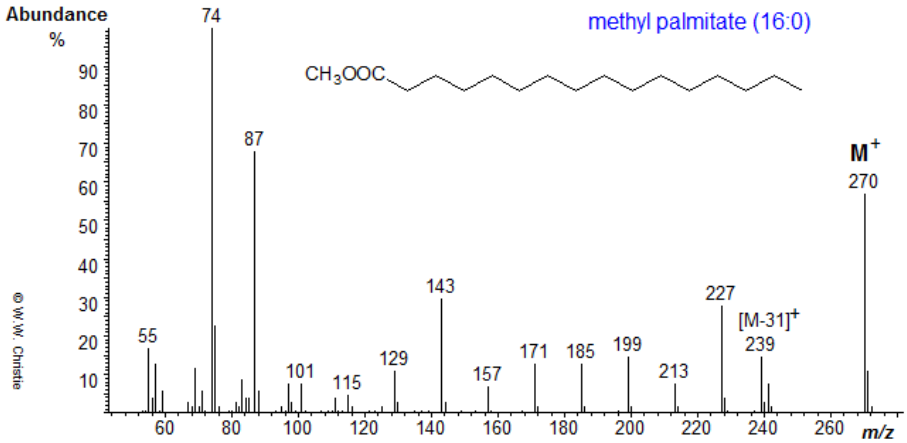

Figure 2.12: Mass spectrum of the fatty acid methyl ester methyl palmitate (C16:0). The molecular ion has m/z-value of 270 (121).

The highest peak in a spectrum is called the base peak and in Figure 2.12 *m/z* 74 (McLafferty rearrangement ion) is the base peak. A search in a mass spectral database against known mass spectra often gives good clues to identify the unknown analyte. Successful matches should always be verified by analyzing the pure expected analyte to see if that mass spectrum is in accordance to the spectrum from the database, as well as a to verify a matching retention time.

A large number of FAMEs often produce similar mass spectra and the molecular ion ($M^{+\cdot}$) is seldom abundant. Even though the molecular ion often is missing, FAMEs provide a characteristic fragmentation pattern and there are some features that give information about the identity of an unknown FAME (122). Characteristic features for FAMEs are listed in Table 2.1.

Table 2.1: Characteristic features* that are of diagnostic relevance for interpreting mass spectra of FAMEs (71, 122).

FAME[a]	Base peak m/z	M+[b]	No ions with m/z:	Mass differences[c]	Mass relations to M
X:0	74	weak (lower MW) visible (higher MW)	90, 103	43>41 87>143	(M-43)>(M-31)≥(M-29)
X:1	55 (d>6) 74 (d<6)	visible	90, 103	**41**>43 **69**>67(d>6) **96**>69 (d<6)	(M-32)>(M-31)>M (M-32):M≈4:1 (M-74)≈(M-116)
X:2	67	visible	75, 90, 103	41>43 **81**>95, 55, 82	
X:3	79	visible	75, 90	41>43 **79≥67**>80, 55, 93 **80**>**93**(n-6) 80<**93**(n-3) 150>149(n-6) 108<107 (n-3)	M>(M-31) M≈(M-98)(n-6) M≈(M-56) (n-3)
X:4,5,6	79	weak	75, 90	41>43 **79**>**91, 67**, 80, 93>55 **80**>**93**(n-6) 80<**93**(n-3) 150>149(n-6) 108<107(n-3) 150>161(n-6) 150<161 (n-3)	

[a]FAMEs sorted by number of double bonds and distance from the carboxyl end (d) or methyl end (n).
[b]The quantity of M is designated by weak (<2 %) and visible (2-50 %).
[c]The m/z-values in bold print have a relative abundance >50 %.
*All features are verified within the chain length (X) range of C10-20 by Härtigs group (122), above this range shifts in details may occur.

The main challenges when identifying fatty acids separated by GC lies in determination of the position and geometry of double bonds of unsaturated fatty acids (71). The characteristics listed in Table 2.1 may confirm identification by retention time comparison with the use of standard solutions as described in section 2.3.2.

2.5 Quantification of fatty acids

2.5.1 Internal standard method

Internal standard (ISTD) method provide the most accurate quantification for both GC-FID and GC-MS (123). The use of an ISTD is a prerequisite to relate analysis results to the situation as it was in the original sample material, assuming that the concentration ratio between analyte and ISTD remain constant during sample preparation and analysis. Chromatography response to an analyte varies slightly from run to run and the use of an ISTD will correct for differences in gas flow, sample amount injected, temperature fluctuations and other variations. The internal standard method is also a good

choice when there are expected variations in the sample preparation method that can lead to loss of sample material and varying recovery of analyte. The relationship between analyte and added ISTD, and the detectors relative response to the two compounds, is usually constant over a wide range of conditions (124). A high quality ISTD is a compound chemically similar to the analyte, so when analyzing FAMEs the ISTD is often an odd numbered FAME that is not present naturally in the sample material. The ISTD should elute in an available space in the chromatogram near the peaks of interest, and in most biological samples where C16:0 and C18:0 is predominant, C17:0 is a commonly chosen ISTD, such as the ISTD used in this study; 1,2-diheptadecanoyl-sn-glycero-3-phosphatidylcholine (96). If the sample material contains a great specter of fatty acids there might be necessary to use several internal standards, and C19:0 and C21:0 are possible choices. The ISTD is added both to the calibration standards and to sample material, and goes through the sample preparation steps (124). ISTD concentration should be in the mid-range of what is expected for compounds in the samples (115, 123).

2.5.2 System performance

Retention factor (k)

The retention factor (*k*, previously called capacity factor) describes the actual retention properties of the stationary phase by adjusting the analyte retention time with respect to the time needed by the unretained solvent to pass through the column. The retention factor is a more convenient way of describing retention characteristics than the distribution ratio (*K*) described earlier. A high retention factor describes a stationary phase with great ability to retain the analyte. The ChemStation software (Agilent) used for GC-FID analyses calculate retention factor using equation 5:

Equation 5

$$k = \frac{T_R - T_0}{T_0}$$

Where T_R is analyte retention time and T_0 is retention time for the unretained solvent, both given in minutes. A k <1 means that the elution of analyte is so fast that an accurate determination of retention time is difficult, while a k >20 indicates long retention times and a long total analysis time (125).

Peak width and plate number

A peak in a chromatogram actually shows the distribution of analyte as a band when the analyte elute from the column. The analyte distribution is affected by small variations in injection, column temperature and retention ability of the stationary phase amongst others (100). The ChemStation software calculates peak width at half peak height (equation 6):

Equation 6

$$W_{50.0} = width\ of\ peak\ at\ height\ 50.0\ \%\ of\ total\ height$$

where $W_{50.0}$ is given in minutes. The half-height peak width ($W_{50.0}$) can also be expressed as 2.35 sigma (2.35σ). Sigma is the standard deviation of the peak.

The number of theoretical of separation steps, or plates, in a column (*N)* designates the columns separation capabilities. In other words, *N* describes the column efficiency. An efficient column has a high *N*, little band broadening and lead to narrow peaks in a chromatogram (103). The ChemStation software defines the number of theoretical plates as in equation 7:

Equation 7

$$N = 5.54\left(\frac{T_R}{W_{50.0}}\right)^2$$

Calculation of *N* assumes that the peak has a normal distribution.

An alternative way of expressing the column efficiency is by using plate height (*H*), as described in section 2.2.1. The plate height is not dependent of column length and can be used for comparison of efficiency for column with varying lengths. The relationship between plate height and column length is displayed in equation 8:

Equation 8

$$H = \frac{L}{N}$$

where *L* is the column length (104).

Resolution

Chromatographic separation of two adjacent peaks (*a* and *b*) is defined by peak resolution (*R*). The resolution is a quantifiable measurement on whether the two peaks are resolved so sufficiently that peak areas can be obtained (100). The ChemStation software calculates resolution by using the half-width method as showed in equation 9, pertaining to peaks *a* and *b*, T_R of peak *a* < T_R of peak *b*:

Equation 9

$$R = \frac{\left(\frac{2.35}{2}\right)\left(T_{R(b)} - T_{R(a)}\right)}{W_{50.0(b)} + W_{50.0(a)}}$$

Resolution for quantitative analyses should be >1.5. A resolution >1.8 indicate too much separation, which can lead to band broadening of later eluting peaks and long total analysis time (100).

Peak symmetry

The analyte band moving through a column in a normal dispersion elutes as a bell-shaped Gaussian peak, as shown in Figure 2.13.

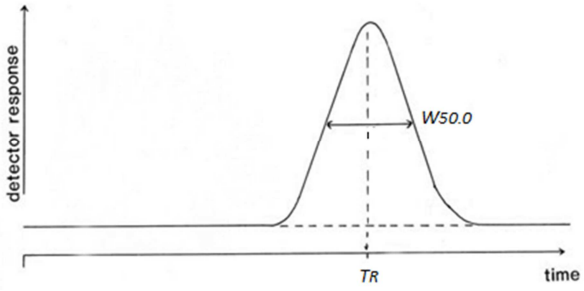

Figure 2.13 A chromatographic peak with an ideal Gaussian shape (126).

If a part of the analytes in a band is more strongly retained than predicted by the distribution ratio (*K*), for example due to hydrogen bonding, they will travel slower through the column and form a tail on the main peak; peak tailing. The opposite, peak fronting, is a result of analyte moving ahead of the main band. Fronting peaks occur when the sample capacity of the analytical column is exceeded. Peak asymmetry is a measure of fronting or tailing and is commonly used to describe peak shape. Peak asymmetry is calculated by comparing peak half-widths at 10 % or 5 % of the peak height. On the contrary, the ChemStation software only calculates a peak symmetry factor (equation 10):

Equation 10

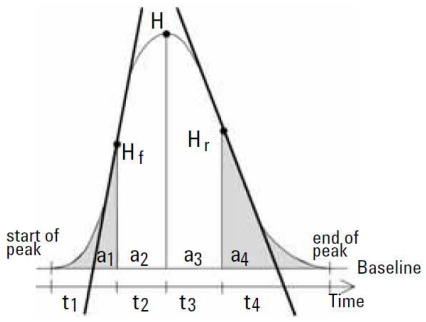

$$Peak\ symmetry = \frac{a_1 + a_2}{a_3 + a_4}$$

where $a_{1\text{-}4}$ is area of the slice. The four areas are calculated as shown in the Figure above equation 10, where $t_{1\text{-}4}$ is time of slice, H_f is height of front inflection point, H_r is height of rear inflection point and H is height at peak apex. ChemStation does not state any peak symmetry limits and the most important factor is the quality of peak integration. Satisfying peak symmetry must be evaluated within each laboratory and adjusted to meet the requirements of the specific analysis (oral communication with Geir Skagestad, Matrix AS, Norway April 16th 2013).

Signal/noise-ratio and limits of detection and quantification

The mean noise level for a base line must be established in order to calculate the signal-to-noise ratio and determine the limit of detection. Limit of detection (LOD) is defined as the smallest concentration of analyte that give a signal significantly different from the signal for a blank sample (noise, N) (124). LOD is commonly described as a signal that is three times the noise for a sample (S/N>3). A signal at the limit of detection is still too low to be accurately measured and the limit of quantitation (LOQ) is set to 10 times the N of a sample (S/N>10). The challenge is to achieve a reliable measurement of the noise, and there are several techniques offered by different software programs.

The ChemStation software calculates N by using six times the standard deviation of the linear regression of all data points in a given time range:

Equation 11

$$N = 6 \times std.dev$$

The slope of the linear regression is the drift in the samples base line and when the six times deviation method is used the calculated N is drift-corrected (127). See Figure 2.14 for illustration of the calculation method.

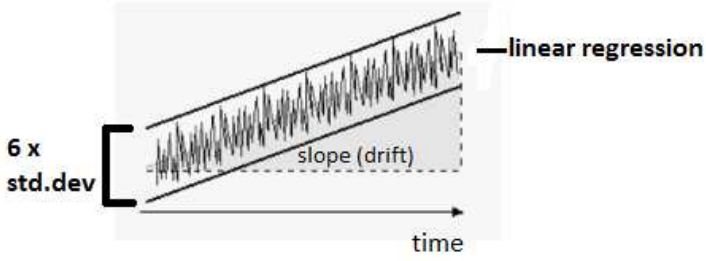

Figure 2.14 Noise is calculated as six times the standard deviation for the linear regression of the drift by the ChemStation software (127).

N is calculated for seven time ranges within the total analysis time, defined by the software user. The time range closest to each peak is selected for signal/noise-ratio calculation. The Xcalibur software used for GC-MS-analysis provided a different calculation method. To be able to compare the LOD for the two instruments ChemStation calculation procedure was performed manually on the chromatograms produced by the GC-MS.

2.5.3 Quantification of FAME analyzed with GC-FID

Quantification of FAMEs analyzed with GC-FID is usually determined based on the peak height or area. Quantification is often based on calibrated calculation procedures and two common methods use external or internal standard(s). External standard procedure use absolute response factors obtained from a calibration with standards containing a known amount of FAMEs, covering the concentration

range expected in the unknown samples (128). Internal standard method is a more robust quantification method and is described in section 2.5.1.

2.5.4 Quantifiation of FAME analyzed with GC-MS

Quantification can be performed using any type of ionization technique and mass analyzer. Quantification can be performed both in TIC and SIM mode. In TIC mode the total signal for each peak is used for quantification. In SIM mode, a quantification ion is used to quantitate an analyte. A quantification ion is present in abundance. The quantification ion can be uniquely characteristic for a molecule, or present in several analytes as long as they are chromatographically separated. The base peak is often used as a quantification ion. Quantification ions must be well separated from matrix interference. In biologic samples matrix interference may be present for ions with *m/z*-value below 200, which makes the selection of good quantification ions challenging because only a small percent of the total ion current have *m/z*-values over 200 (123). Qualifier ions can confirm that the signal registered is due to a fatty acid and not interferences. Qualifier ions are set to lie within a specified percentage range of the quantifier ion to confirm the peak identity.

GC-MS has several advantages compared to GC-FID when you want to perform qualitative and quantitative analyses. With GC-MS good separation is not as crucial as when using GC-FID; characteristic ions can still be sorted by mass. GC-MS also give a greater confirmation of analyte identity. GC-FID methods are based primarily on retention times for identification. GC-MS provide identification based on both the retention time, mass spectra and matches found by searching mass spectral databases contributes to confirm analyte identity (123).

2.6 Aim of the HiOA-study "Effect of overweight on male reproductive function"

A relation between for overweight and prolonged time to fertilization has been established in females, and the adverse effects may be reversible with weight loss (20, 22). There are a number of studies on male overweight and obesity, and their effect on male reproduction function (4, 23, 30). As of today there are few published studies investigating whether weight loss will improve factors within male reproduction function (6, 129). If results indicate that weight loss will improve semen quality and contribute to increased male reproduction function, there will be evidence to advise overweight men to lose weight if they wish to increase chances of conceiving.

The overall aim of the HiOA study is to investigate if overweight affects male reproduction function by comparing overweight and obese men to normal weight men. The HiOA study also explore whether weight loss by diet, bariatric surgery and/or lifestyle intervention can counteract possible observed negative effects.

2.6.1 Ethical considerations

The research project is approved by The Regional Committees for Medical and Health Research Ethics (REC) and is reported to The Data Protection Official for Research. The Norwegian Directorate of Health has approved establishment of a research biobank for collected sample material. The lower age limit for participating in this study is 18 years, and all participants have signed an informed consent before data was collected. They have the right to withdraw from the study at any time, and participant data will be deleted and collected sample material will be destroyed. Anonymized published data will not be withdrawn. Participants get feedback on their test results if wanted and they are recommended to contact their regular general physician if they want the results further investigated.

Relevant legislation for this study is the Act on medical and health research (130) and the Act on ethics and integrity in research (131).

2.7 Research material

2.7.1 Subjects and sample collection

Men with a BMI >25 kg/m^2 who had taken action to lose weight were recruited from Grete Roede AS, VG Weight club, advertisement in media, and at different training facilities before the start of this master study. Men with a BMI >35 kg/m^2 who were going through a lifestyle intervention program or bariatric surgery were recruited from The Morbid Obesity Center, South-Eastern Regional Health Authority, Norway, dep. Tønsberg and Aker, and Center for learning and achievement (LMS) dep.

Aker. Men with normal BMI (18.5-24.9 kg/m^2) were recruited by advertisements in media, and from The Fertility Clinic South, Telemark Hospital, from couples with known female factor as the cause of infertility.

Participants to the study were enrolled over a time period of three years, 2009-2012. Men who lost weight by self-induced life style changes or controlled life style intervention returned for a second blood sample after weight loss and the second semen sample three months later. The blood sample will in that way reflect the blood status at early spermatogenesis. Participants who went through bariatric surgery delivered the first blood and semen sample before they underwent surgery and the second set of samples after approximately one year postoperative. The overweight participants will contribute as their own control group in regard to the effect of weight loss.

Twenty three men with normal BMI (18.5-24.9 kg/m^2) were recruited as a control group for reproductive function and fatty acid status in serum phospholipids. All participants were administered a lifestyle and medical questionnaire when visiting the research facilities. Weight, height and waist circumference, percent body fat and blood pressure were obtained during their visit. The semen sample was provided by masturbation at home or at the research facilities. Participants were asked to refrain from ejaculation 2-7 days, preferably 3 days, before sample collection and to keep the semen sample close to their body during transportation. The semen sample was to be delivered within 2 hours after collection. Blood samples were drawn at the research facilities by authorized staff.

Sample material collected for research is stored at -80 °C in a biobank at HiOA.

2.7.2 Semen analysis

All semen parameters except motility were performed by trained staff at HiOA and determined according to the World Health Organization (WHO) (132) procedures, described in a manual by Nordic Association for Andrology in collaboration with European Society of Human Reproduction and Embryology (133). Motility analysis were performed at The Center for Reproduction Medicine at Skåne University Hospital (Sweden) and determined according to WHO procedures updated in 2010 (61).

Volume was determined by weighing and subtracting the weight of the empty tube, assuming that 1 ml semen = 1 g. Sperm motility was performed by microscopy and graded as follows; progressive motility (PR), non-progressive motility (NP) and immotility (IM). Total PR count is calculated by multiplying the percentage score of PR with the total sperm count.
Vitality was determined by microscopy after eosin-nigrosin staining to differentiate between viable and non-viable sperm cells. Smears were Papanicolao stained before evaluation of morphology was performed. Morphology was classified as defect head, mid piece or tail, and presence of cytoplasmic residues. Sperm concentration was assessed by using a Neubauer Improved Haemocytometer after

liquefaction. Total normal sperm morphology is calculated by multiplying the percentage score for normal morphology with the total sperm count.

2.8 Aim of this master study

Studies on dietary fat intake and semen quality suggest a negative relation between a high intake of SFA and decreased semen quality (94, 95). Serum phospholipid fatty acids can in some degree be used as a marker of short-term dietary fat intake (134). There is a lack of studies on serum phospholipid fatty acid composition and semen quality and changes in both parameters after weight loss. The general aim of this study was to:

- Optimize the method used to extract serum phospholipid fatty acids and chemically modify extracted fatty acids for GC-analysis.
- Establish a qualitative and quantitative method for FAME analyses using a GC with flame-ionization detector and ChemStation software for data processing.
- Verify qualitative results by using GC-mass spectrometry with Xcalibur software, and compare flame-ionization detector and mass spectrometry considering ability for identification of FAMEs, and limits of detection and quantification.
- Investigate if BMI show associations with semen quality or serum phospholipid FAME composition, and explore whether levels of serum phospholipid FAMEs correlate with any semen quality parameters.
- Study what effect weight loss may have on the composition of serum phospholipid FAME composition and semen quality.

3 EXPERIMENTAL

Chemicals, equipment and stock standard solutions used in this study are listed in appendix 1.

3.1 Serum phospholipid fatty acid preparation

A detailed step-by-step procedure for preparation of serum phospholipid fatty acids for GC-analyses can be found in appendix 2, a summary of the procedures is given in this section.

3.1.1 Lipid extraction

Lipids were extracted according to a method modified after Folch (97). The method used was modified and adapted to the sample material based on experience from professor emeritus Hans J. Grav (formerly University of Oslo) and work by Almendingen et al. 2007 (135). Each set up also contained a method blank where neither serum nor internal standard were added. Serum samples were thawed at 4-6 °C. Fifteen µl butylated hydroxytoluene (BHT in 1 % ethanol, an antioxidant) and 200 µl serum were added to 20 times the sample volume (4 ml) of cold chloroform/methanol (2:1) in acid washed glass tubes. 30 µl 1 mg/ml 1,2-diheptadecanoyl-sn-glycero-3-phosphatidylcholine in chloroform/methanol (2:1) was used as ISTD. The mix was vortexed for 30 sec and incubated in room temperature for 30 min.

The sample solution was washed with four times the sample volume (800 µl) of 0.9 % NaCl and vortexed for 30 sec before 10 min incubation in room temperature. All test tubes were centrifuged for 5 min, 10 % U/min (~2500 rpm). The chloroform phase was transferred to new test tubes by suction and evaporated to dryness under a stream of N_2. Lipids were dissolved in 300 µl n-hexane. 200 µl were used for lipid fractionation, while 100 µl containing the total lipid profile were derivatized without fractionation.

3.1.2 Lipid fractionation

Ion-exchange chromatography was used to separate lipid fractions. The method is based on work done by Kaluzny et al. (99). Columns used were bonded-phase columns (Supelclean TM LC-NH_2 Tubes, 1 ml from Supelco, Bellefonte, PA, USA). Columns were equilibrated with 4x1 ml n-hexane. 200 µl of the total lipid extract was then added to the column before the columns were flushed with 4x200 µl chloroform. Neutral lipids were eluted by adding 4x1 ml chloroform/2-propanol (2:1) and the free fatty acids by 4x1 ml 2 % acetic acid in ethyl ether, both eluents were discharged. Finally phospholipids were eluted by adding 4x1 ml methanol to the columns.

3.1.3 Derivatization of fatty acids

The transmethylation method is based on work by Hoshi et al. (101) and the experience passed on from professor emeritus Hans J. Grav.

Both total lipid and phospholipid samples were vaporized to complete dryness under N_2 and resolved in 1 ml benzene, 200 µl 2,2-dimetoxypropane and 2 ml 3 M methanolic HCl, in that order. Solutions were vortexed for 30 sec and left dark and in room temperature overnight. The following day solutions were neutralized by adding 4 ml 6 % $NaHCO_3$. FAMEs were extracted in 2 ml n-hexane and vaporized to dryness under N_2. The extraction step was repeated three times. Samples were dissolved in 200 µl n-hexane (blank samples were dissolved in 400 µl n-hexane) and transferred to 100 µl crimp vials. Before capping, air in the vials was replaced with N_2 to avoid deterioration of the sample material. Phospholipid samples were stored until GC analysis, and total lipid samples are stored for later studies, both in -80° C.

3.2 GC analyses of fatty acid methyl esters

3.2.1 Gas chromatography with flame ionization detection (GC-FID)

To perform fatty acid separation in this study a 7890A gas chromatograph with flame-ionization detector from Agilent Technologies (Santa Clara, CA, USA) were used together with AutoSampler 7693 from the same company. Sample material was injected in split less mode and split less time was set to 0.7 min. After spilt less time the injector switched to split mode with a split ratio of 1:40. An increase of split less time to 1.0 min was investigated, but did not improve separation.

Injector temperatures of 250° C and 280° C was tested, and the injection temperature was set to 280 °C to avoid discrimination of long, less volatile FAMEs. The injection volume was 1 µl. Nitrogen gas (N_2) was used as carrier gas with a gas flow of 1.4 ml/min. The GC was set to constant flow mode, meaning the gas flow was kept constant during time of analysis, while the column pressure shifted as a result of increasing column temperature. Initial column pressure was 165.48 kPa. FAMEs were separated on a 60 m × 0.25 mm polar BPX70 column with stationary phase film thickness of 0.25 µm (SGE International, UK). To minimize band broadening and refocus analytes in the samples, a precolumn from Supelco (Bellefonte, PA, USA) was mounted. Column temperature was held at 50 °C for one minute, 19 °C below solvent boiling point during injection to achieve a “solvent effect”. The temperature program used to separate FAMEs is listed in Table 3.1; total analysis time was 76.5 min.

Table 3.1 Temperature program used for separation of FAMEs from serum phospholipids on a flame-ionization detector coupled gas chromatograph.

Temperature ramp	°C/min	°C	Hold time (min)
Initial temperature		50	1
Ramp 1	40	120	3
Ramp 2	2	180	0
Ramp 3	1	220	0
Ramp 4	20	235	0

3.2.2 Retention time locking

A retention time versus pressure calibration was performed to lock the optimized method. C17:0 FAME was the compound used for this purpose and for later relocking procedures. C17:0 FAME is easy identifiable, gives a symmetrical peak and elutes in a critical part of the chromatogram. Five calibration runs were performed under identical conditions, except for varying inlet pressures listed in Table 3.2.

Table 3.2: Five different inlet pressures were used for retention time versus pressure calibration. Retention time vs. pressure-calibration was further used to retention time lock the calibrated GC-FID method used for FAME analysis.

Calibration run	Variants of target pressure	Actual inlet pressure (kPa)
1	Target pressure – 20 %	132.00
2	Target pressure – 10 %	149.00
3	Target pressure (as nominal method pressure)	165.48
4	Target pressure + 10 %	182.00
5	Target pressure + 20 %	198.50

The retention time for C17:0 was registered for each run and the five pairs of inlet pressures and retention times were plotted in ChemStation software as a part of the method.

3.2.3 Response factor

A 1 mg/ml total FAME concentration of the commercially available standard solution GLC #411 was spiked with FAME C17:0 to obtain a 40.0 µg/ml ISTD concentration. The spiked standard solution was used in determination of relative response factors for saturated FAMEs to evaluate the response dependence of GC-FID to the FAME carbon number, according to equation 12:

Equation 12

$$RRF = \frac{A_x\, C_{ISTD}}{A_{ISTD} C_x}$$

where RRF of an analyte is given in terms of the analyte area (A_x), the ISTD area (A_{ISTD}) and the concentrations of the analyte and the ISTD (C_x and C_{ISTD}, respectively). GLC #411 is a mix of 31 equally weighed fatty acid methyl esters from Nu-ChekPrep (MN, USA) and list of the FAMEs can be found in appendix 3.

3.2.4 Quantification of FAMEs

Three different stock solutions were used to prepare standard solutions that covered all expected FAMEs in the unknown samples; 1) cis-5,8,11,14,17-eicosapentaenoic acid methyl ester (C20:5n-3), 2) methyl cis-7,10,13,16,19-docosapentaenoate (C22:5n-3), both single standards from Supelco (Bellafonte, USA) and 3) GLC #411. The ISTD that was added to all samples prior to sample preparation was C17:0, as explained in section 3.2.1. The ISTD added to standard solutions was methyl heptadecanoate, a C17:0 FAME from Fluka Analytical. Nine concentration levels of the

standard solutions were used to provide calibration curves. Area of each FAME peak was calculated and area ratio for the known analyte to the ISTD was plotted against the corresponding known concentration ratio by the ChemStation software. Quantification was performed by calculating µg/ml FAME-equivalents in serum, with the assumption that the ISTD provided two C17:0 FAME-equivalents when added to the serum samples (appendix 4). The area sum for a selected number of FAMEs detected for all participants, with exception of the ISTD, was considered equal 100 %. The percentage distribution of serum phospholipid FAMEs was calculated based on the concentrations in µg/ml and used for statistical analyses.

3.2.5 Gas chromatography with mass spectrometry

To verify qualitative results from the GC-FID, an identical analytical method was transferred to the GC combined with a mass spectrometer (GC-MS). Helium was used as carrier gas at a constant flow rate of 1.4 ml/min. 1 µl sample was injected in split less mode, and the split valve was closed for 0.7 min and then opened to 1:50 split ratio. After 2 min the gas saver flow was set to a split ratio of 1:20. For details on the temperature program used for sample analysis, see section 3.2.1 and Table 3.1. A 6 min solvent delay was applied to the method to avoid detecting the solvent peak. Analysis was carried out using a BPX70 column as described in section 2.2.2. The quadrupole MS was operated with 70 eV electron ionization (EI), and FAMEs were analyzed with both TIC and SIM mode. In TIC mode the data acquisition was performed in the *m/z*-range from 35-420. Scan time was set to 4.0 sec with 2.5 scans/sec in TIC. Ions acquired during SIM were *m/z* 67, 74 and 79.

Mass spectra from the TIC chromatogram were used to select the most characteristic ion pattern belonging to each FAME. The ion pattern was used to identify FAMEs with the highest selectivity by comparing spectra with the common features listed in Table 2.1. The most abundant ions were selected to be able to perform quantification of FAMEs in SIM mode at a later stage in the study.

3.3 Processing of raw data

Method blank samples were analyzed first and last for every analysis sequence. The method blank samples all presented small amounts of C16:0 and C18:0. After several attempts to eliminate the contamination without success it was decided to increase the serum volume by a fourfold to be able to perform blank subtraction. The average measured area (A) for C16:0 and C18:0 was subtracted from the measured area for corresponding peaks in participant chromatograms. New concentrations (C) and percentage distribution of FAMEs were calculated by using the equation given by the calibration curve:

Equation 13: C16:0

$$\frac{A_{C16:0}}{A_{ISTD}} = 1.34908 \times \frac{C_{C16:0}}{C_{ISTD}} - 0.15637$$

Equation 14: C18:0

$$\frac{A_{C18:0}}{A_{ISTD}} = 1.38573 \times \frac{C_{C18:0}}{C_{ISTD}} - 0.15766$$

Blank subtraction was performed prior to statistical analysis.

3.4 Statistical analysis

The cut-off level for statistical significance in this master thesis was $p \leq 0.05$. Percentage FAMEs are calculated based on quantified amounts (µg/ml), and defines percentage weight of a selection of nine FAMEs detected in all participant samples set to equal 100 %.

In the cross-sectional study, participants were divided into three groups according to BMI at baseline (1: 18.5-24.9 kg/m^2, 2: 25.0-29.9 kg/m^2 and 3: ≥30.0 kg/m^2). In crude analysis, non-parametric tests were used for group comparisons due to the small sample sizes. Median and range for all semen quality parameters and FAMEs were calculated for participants in each group, and median for men in the three groups were compared by using Kruskal Wallis Test. Any statistically significant results ($p \leq 0.05$) by Kruskal Wallis Test, were investigated with follow-up Mann-Whitney U Tests between pairs of groups to see which group that significantly differed from the others.

Semen quality is known to decrease with increasing age, and the parameters sperm motility and normal sperm morphology are affected by abstinence time before semen sample delivery (136, 137). The comparison of semen quality for men divided into three BMI groups was repeated with multiple linear regression with semen quality parameters as dependent continuous variable and BMI groups as an independent dichotomous variable, adjusted for the two confounders age and abstinence time.

Multiple linear regression was also used to investigate the participant group as a whole for associations between semen quality parameters as dependent continuous variable and BMI or percentage FAMEs as independent continuous variable, adjusted for age and abstinence time.

The results from multiple linear regression are presented with the unstandardized B-coefficient (B) and the corresponding *p*-value. The B-coefficient indicates the average change in the dependent variable associated with a 1 unit change in the independent variable after adjusting for other independent variables (138). Residuals for semen quality parameters that did not meet the distributional assumptions of linear regression were square root transformed, log transformed, reflected and square

root transformed or reflected and log transformed, dependent of the shape of the parameters original distribution. The B-coefficient for transformed variables provide information on the average change in the dependent variable associated with a 1 unit change in the transformed variable, and is difficult to relate to the real life situation. There is considerable controversy concerning back transforming of adjusted variables, and back transforming was not performed for results given in this master thesis. The B-coefficient for transformed variables listed in Tables 4.11, 4.12 and 4.14-4.16 provide only information on the direction of the association (negative or positive), not the average change in the dependent variable as explained earlier in this section.

In the longitudinal study, the percent weight loss was calculated and participants were divided into three groups; 1) low: <10 %, 2) high: ≥10 % and 3) bariatric surgery with a following weight loss. Median with 25-75 percentiles is provided for each variable and Wilcoxon Signed Rank Test was used to perform within-group comparisons of serum phospholipid fatty acid composition and of semen quality parameters at baseline and after weight loss.

Microsoft Excel 2010 and IBM SPSS for Windows (version 20.0) were used for statistical analysis.

4 RESULTS

4.1 Analytical process

Blood and semen sample collection, and semen analyses, were performed prior to the start of this master study. Sixty-one serum samples were prepared and analyzed using GC-FID. Statistical analyses were done for semen quality and FAME data. Three samples from a total of two participants were excluded based on disagreement in FAME identification (two baseline and one follow-up sample(s)). All together 59 participants provided FAME chromatograms for further analysis. Nineteen of 59 participants provided FAME chromatograms both at baseline and after weight loss.

Prior to GC-analysis serum phospholipid fatty acids had to be extracted, separated and chemically prepared. The sample preparation protocol was modified from a four day- to the two day-procedure described in section 3.1, and the amount of serum used was increased by a fourfold to enhance analyte recovery. After getting familiar with the ChemStation software, a satisfying temperature program and a calibration procedure were compiled for qualitative and quantitative GC-FID analysis. Standard solutions and four participant samples were analyzed with GC-MS to confirm FAME identity and compare signal-to-noise ratio for GC-FID and GC-MS in both TIC and SIM mode.

Results from the method development are presented in section 4.2-4.5. Participant baseline results are presented in section 4.6-4.7 and the effect of weight loss described in section 4.8.

4.2 Recovery of the internal standard

Recovery of ISTD expanded over a range from 29.9-68.9 %, with 32 of a total of 59 analyzed baseline samples with a recovery higher than 50 %.

4.3 Optimization of gas chromatographic separation

The criteria parameters considered in the GC–FID method optimization were to obtain the highest resolution between the different FAMEs, suitable peak integration and the shortest possible analysis time. The retention times of FAMEs depends mainly on their chain length, number of double bonds and double bond position as described in section 2.3.2. The optimal temperature program used for FAME separation on a BPX70 column is described in Table 3.1. Baseline separation of FAMEs in GLC # 411 was achieved between 7 and 61 minutes with exception of the following FAMEs; C18:1n-12, n-9 and n-7; C20:1n-15, n-12 and n-9; C22:3n-3 and C22:4n-6. A chromatogram for 1 mg/ml total FAME concentration of GLC # 411 is displayed in Figure 4.1.

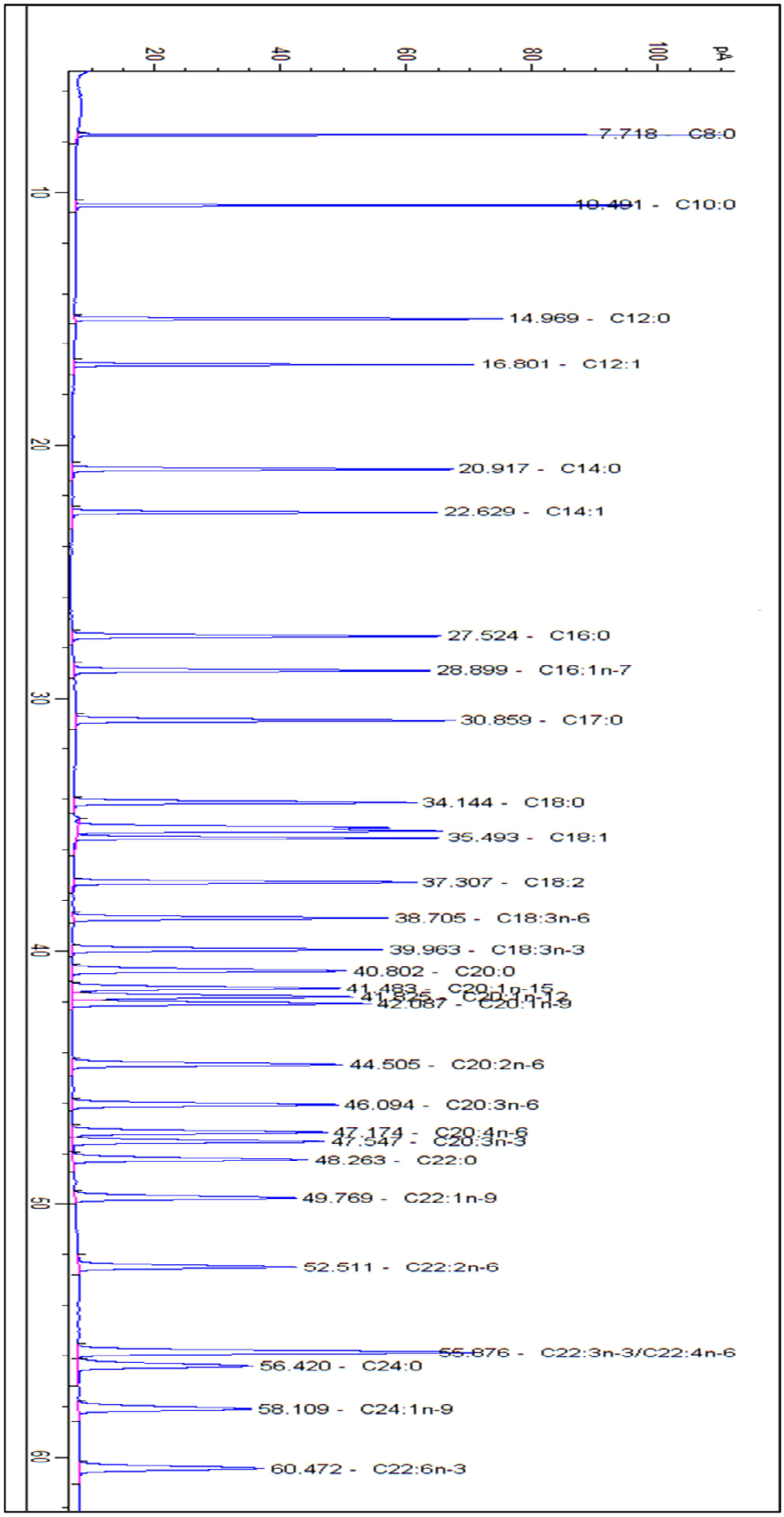

Figure 4.1 Chromatogram obtained for a 1 mg/ml total FAME concentration of the standard solution GLC # 411, where signal (pA/s) is plotted against time in minutes. GLC #411was used to calibrate the GC-method for quantification of human serum phospholipid FAMEs. All FAMEs in GLC #411 are equally weighted (3.23 wt%).

The three peaks in the C18:1 fraction were visibly separated, but because of their structure similarity they eluted so close together that their retention time windows overlapped and they did not achieve a satisfactory resolution for quantification (100). The area and concentration for C18:1n-12, n-9 and n-7 were combined for quantification and will be referred to as C18:1 throughout this master thesis. Peaks for the three variants of C20:1 showed a resolution slightly beneath the required 1.5, but were still quantified separately (System performance, appendix 5).C22:3n-3 and C22:4n-6 co-eluted completely and concentrations were combined for quantification.

Two single standards were used to quantitate C20:5n-3 and C22:5n-3 and their chromatograms are shown in Figure 4.2. They eluted in the time window between C22:1n-9 and C22:2n-6, and C24:1n-9 and C22:6n-3, respectively.

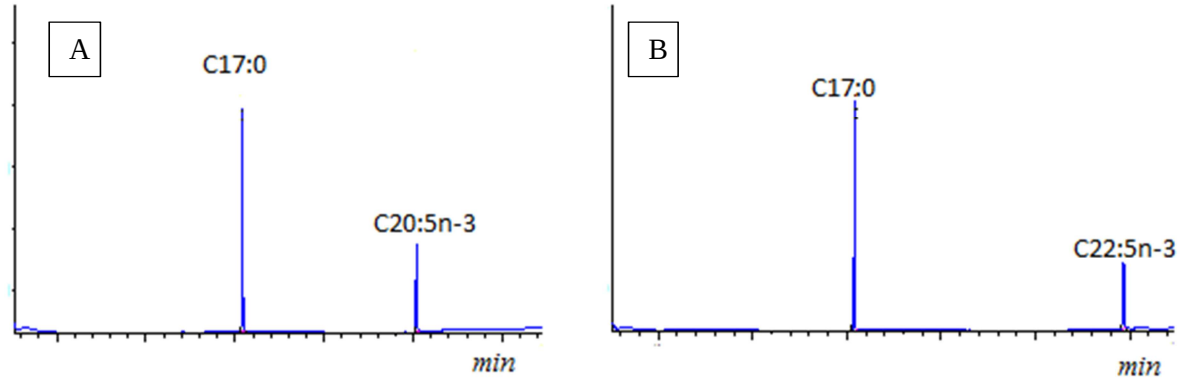

Figure 4.2 Chromatogram obtained for the two single standards; A) C20:5n-3 and B) C22:5n-3, both used to calibrate the GC-method for quantification of human serum phospholipid FAMEs. Concentration of each FAME was 32.3 µg/ml and the peak to the left in both chromatograms are the ISTD 40 µg/ml C17:0 FAME.

4.4 Identification and characterization of human serum phospholipid FAMEs

Retention time locking and identification of FAMEs by GC-FID

Human serum phospholipid FAMEs were identified by comparing their retention times with those of FAMEs in commercially available standards mentioned in section 3.2.4. Small fluctuations in chromatographic conditions can affect analyte retention time and may lead to misidentification. A procedure for retention time locking (RTL) was performed to minimize shifts in retention time. RTL resulted in closely matched retention times with a maximum standard deviation of 0.007 minutes when comparing 5 individually prepared replicates of a serum sample (data not shown). Average retention time and the relative standard deviation (RSD %) for identified FAMEs are listed in Table 4.1.

Table 4.1 Average retention times (RT), standard deviation and relative standard deviation (RSD %) for identified FAMEs in five replicates of a serum sample.

FAME	Average RT (min)	RSD %
C14:0	20.934	0.012
C16:0	27.631	0.016
C16:1n-7	28.903	0.008
C18:0	34.227	0.018
C18:1	35.494	0.004
C18:2n-6	37.401	0.018
C18:3n-6	38.520	0.005
C20:3n-6	46.092	0.007
C20:4n-6	47.212	0.011
C20:5n-3	50.434	0.007
C22:5n-3	59.398	0.008
C22:6n-3	60.482	0.009

Identification of FAMEs by using GC-MS

MS detection was performed by EI both in full scan mode and SIM mode. The GC method used with GC-FID was adapted to the GC-MS to be able to compare the two detector types.

Mass spectra for peaks present in the GLC #411 standard solution were compared to expected features listed in Table 2.1. All features were compatible except the expectation that *m*/*z* 108<107 for n-3 FAMEs with three or more double bonds, which turned out to be *m*/*z* 108>107 for all n-3 FAMEs in this study (see spectrum for C18:3n-3 as a representative example in appendix 6).

Four serum samples were analyzed with GC-MS and mass spectra for each sample were compared with both spectra from GLC #411 and expected features to confirm peak identification. The peak identified as FAME C20:1n-9 by the GC-FID method turned out to be an unidentified contamination present in all four serum samples as shown in appendix 6. FAME C20:1n-9 was excluded from all participant result calculations based on this observation.

The theoretical elution order; 1) C20:3n-6, 2) C20:3n-3 and 3) C20:4n-6 when polar columns are used for separation of FAMEs was challenged when spectra from GLC #411 were compared with the expected features. The results indicate that the elution order was 1) C20:3n-6, 2) C20:4n-6 and 3) C20:3n-3. EIC from the TIC chromatogram for the molecular ion for FAME C20:3 (*m*/*z* 320) was performed and only peak 1 and 3 of the three FAMEs were visible, which support the second elution order. The TIC and EIC chromatograms are displayed in appendix 6.

4.5 Quantification of FAMEs in human serum phospholipids

4.5.1 Response factors for FAMEs analyzed with the GC-FID method

RRF for saturated FAMEs is plotted in Figure 4.3, and RRF for C18 variants are plotted in Figure 4.4.

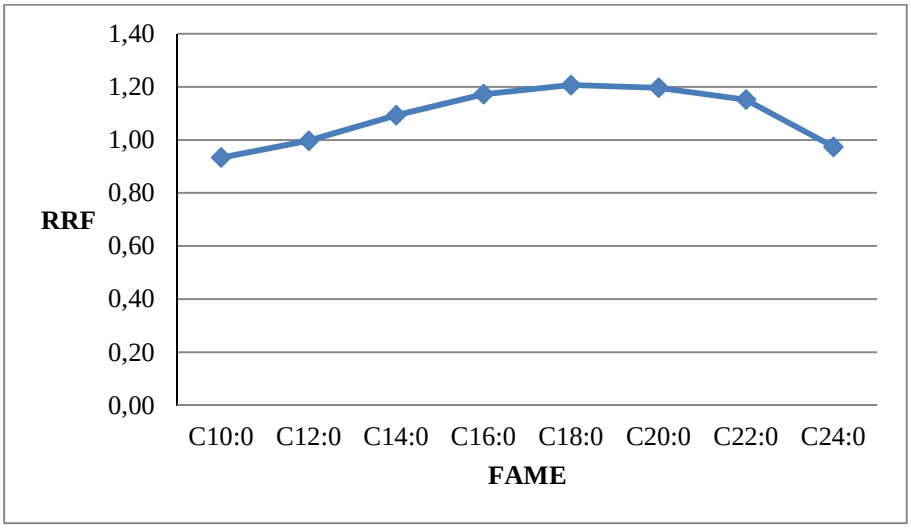

Figure 4.3 Relative response factors for a series of saturated FAMEs determined by GC-FID.

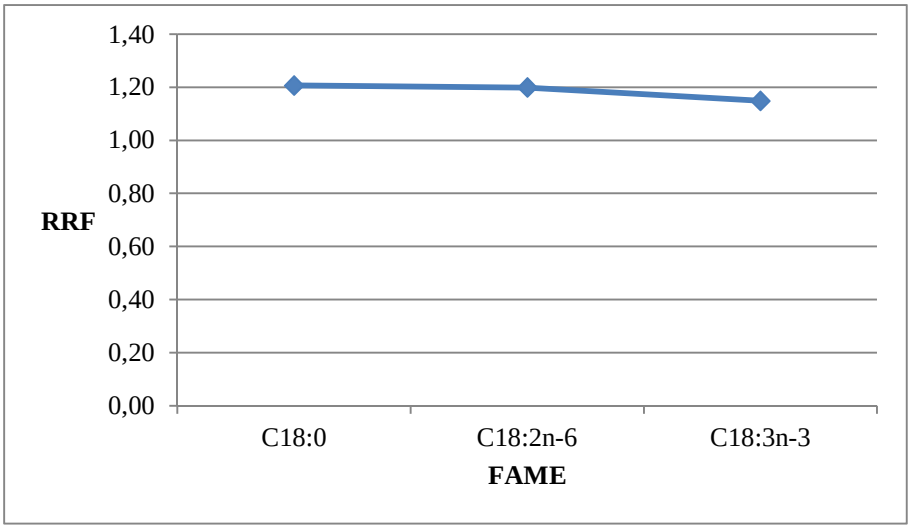

Figure 4.4 Relative response factors for a saturated and unsaturated FAMEs with identical chain length determined by GC-FID.

4.5.2 Calibration and linearity for the GC-FID method

To each calibration level 40 µg/ml FAME C17:0 ISTD was added. A calibration curve of nine levels was analyzed with duplicates of level 1, 4, 6 and 9. Concentrations for each level are listed in Table 4.2 and the calibration curve for C18:0 is displayed in Figure 4.5 as a representative example. The FID calibration exhibited a linear response over the entire concentration range examined (7.8-201.3 µg/ml).

Table 4.2 Nine concentration levels of fatty acid methyl esters (FAMEs) were used to make a calibration curve for quantification of FAMEs in unknown serum samples. 20 µl 1 mg/ml ISTD was added to all levels.

Standard	Level	FAME-concentration
GLC #411, EPA and DPA	1	7.8 µg/ml
	2	15.5 µg/ml
	3	23.2 µg/ml
	4	31.0 µg/ml
	5	61.9 µg/ml
	6	92.9 µg/ml
	7	123.9 µg/ml
	8	154.8 µg/ml
	9	201.3 µg/ml

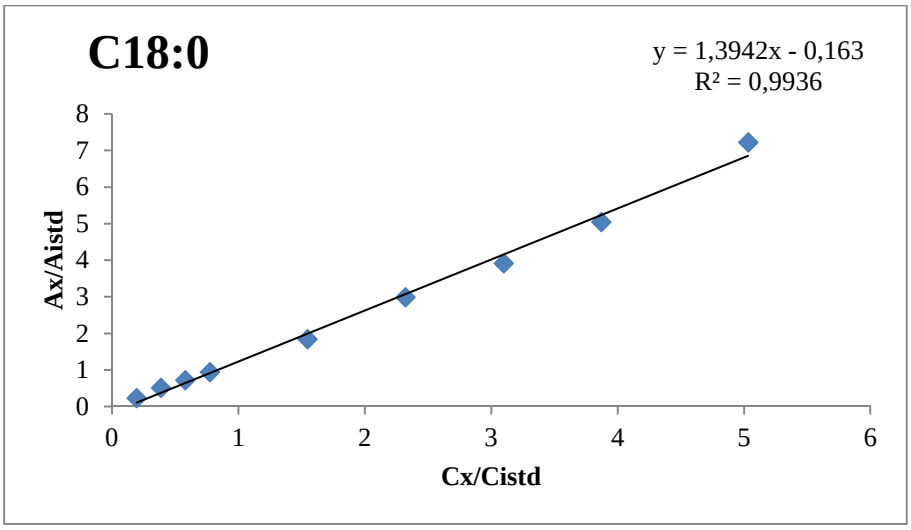

Figure 4.5 Calibration curve for nine levels of C18:0 FAME analyzed with GC-FID with R^2 and the linear function for the curve. Area ratio (A) is plotted against concentration ratio (C) for FAME (x) relative to the internal standard (istd).

The correlation coefficients (R^2) for the calibration curves were >0.99 for all FAMEs except C20:1n-15, who had R^2 = 0.971. The GC-FID method was recalibrated after 8 weeks of analyzing, and area ratio for the old and new calibration curve was compared by regression analysis. The compared area ratios for C20:0, C20:1n-15, n-12 and n-9, C22:1n-9 and C22:2n-6 presented a slope with 95 % confidence intervals different from 1; hence area ratios measured at the two time points are significantly different at a 5 % level. Intercept confidence intervals all contain the value 0.0 and are considered not significantly different. Slope and intercept for the compared areas are listed in Table 4.3, and calibration curves for both calibrations, with corresponding linear function and R^2, can be found in appendix 7.

Table 4.3: Slope and intercept with standard deviation and 95 % confidence interval (CI) for area comparison curves, comparing areas produced by first and second calibration of the GC-method.

FAME	Slope	std.dev	CI	Intercept	std.dev	CI
C8:0	0.99	0.01	(0.97-1.01)	0.01	0.02	(-0.04-0.06)
C10:0	1.00	0.01	(0.99-1.01)	0.00	0.02	(-0.04-0.04)
C12:0	1.00	0.01	(0.99-1.01)	-0.01	0.02	(-0.04-0.03)
C12:1	1.00	0.01	(0.98-1.01)	-0.01	0.02	(-0.05-0.04)
C14:0	1.01	0.01	(0.99-1.02)	-0.01	0.02	(-0.05-0.03)
C14:1n-5	1.00	0.01	(0.99-1.02)	0.00	0.02	(-0.05-0.05)
C16:0	1.01	0.01	(0.99-1.02)	-0.01	0.02	(-0.05-0.03)
C16:1n-7	1.01	0.01	(0.99-1.02)	-0.01	0.02	(-0.04-0.03)
C18:0	1.01	0.01	(0.99-1.02)	0.00	0.02	(-0.04-0.04)
C18:1	0.99	0.01	(0.98-1.01)	0.07	0.05	(-0.05-0.19)
C18:2n-6	1.01	0.01	(0.99-1.02)	-0.01	0.02	(-0.05-0.04)
C18:3n-6	1.01	0.01	(0.99-1.03)	-0.01	0.02	(-0.06-0.03)
C18:3n-3	1.01	0.01	(0.99-1.02)	-0.01	0.02	(-0.05-0.04)
C20:0	1.03	0.01	(1.01-1.05)	-0.03	0.03	(-0.09-0.03)
C20:1n-15	1.07	0.01	(1.04-1.10)	-0.09	0.05	(-0.22-0.03)
C20:1n-12	1.01	0.01	(1.00-1.01)	0.00	0.02	(-0.01-0.01)
C20:1n-9	0.95	0.02	(0.91-0.99)	0.06	0.05	(-0.06-0.18)
C20:2n-6	1.00	0.01	(0.99-1.02)	0.00	0.02	(-0.05-0.05)
C20:3n-6	1.00	0.01	(0.99-1.02)	0.00	0.02	(-0.05-0.05)
C20:4n-6	1.00	0.01	(0.99-1.02)	0.00	0.02	(-0.05-0.04)
C20:3n-3	1.00	0.01	(0.99-1.02)	0.00	0.02	(-0.05-0.05)
C22:0	1.01	0.01	(0.99-1.02)	0.00	0.02	(-0.05-0.05)
C22:1n-9	0.95	0.01	(0.94-0.97)	0.00	0.02	(-0.06-0.07)
C22:2n-6	1.03	0.01	(1.02-1.04)	0.00	0.02	(-0.05-0.04)
C22:3n-3/C22:4n-6	1.00	0.01	(0.99-1.02)	0.00	0.04	(-0.08-0.09)
C24:0	1.00	0.01	(0.97-1.03)	0.00	0.02	(-0.09-0.08)
C24:1n-9	1.00	0.01	(0.98-1.01)	0.02	0.02	(-0.03-0.06)
C22:6n-3	1.00	0.01	(0.99-1.02)	-0.01	0.02	(-0.05-0.03)

4.5.3 Limits of detection and quantification for GC-FID and GC-MS

Limits of detection (LOD) are given in µg/ml for a number of detected FAMEs (Table 4.4). All methods are capable of detecting low concentrations of FAMEs. When LOD for FID and MS were compared, MS presented a lower LOD for FAMEs up to a chain length of C22, while FID had a lower LOD for C22-24. When MS was operated in SIM mode LOD was improved by a factor of 2.2 to as much as 57.7, rivaling both FID and MS-TIC. LOQ data showed the same trends and Δ-values (Table 4.5).

Table 4.4 Limits of detection (LOD) for standard solution FAMEs. LOD for GC-FID and GC-MS, and for the two MS modes total ion current (TIC) and selected ion monitoring (SIM), were compared and ratios for their LODs are given to the right (ΔLOD).

	GC-FID	GC-MS TIC	GC-MS SIM*	Δ LOD		
Name	LOD (µg/ml)	LOD (µg/ml)	LOD(µg/ml)	FID/MS	FID/SIM	TIC/SIM
C8:0	0.075	0.039	0.001	1.9	53.9	28.3
C10:0	0.086	0.048	0.001	1.8	58.0	32.4
C12:0	0.079	0.059	0.002	1.3	48.2	36.0
C12:1	0.084	0.051	ND	1.6	-	-
C14:0	0.088	0.076	0.001	1.2	67.2	57.7
C14:1n-5	0.092	0.067	ND	1.4	-	-
C16:0	0.106	0.081	0.001	1.3	71.4	54.0
C16:1n-7	0.110	0.069	ND	1.6	-	-
C17:0	0.104	0.061	0.009	1.7	12.0	7.1
C18:0	0.115	0.075	0.011	1.5	10.6	6.9
C18:1	0.107	NS	ND	-	-	-
C18:2n-6	0.121	0.112	0.025	1.1	4.8	4.4
C18:3n-6	0.131	0.109	0.021	1.2	6.3	5.3
C18:3n-3	0.134	0.122	0.024	1.1	5.6	5.1
C20:0	0.151	NS	0.006	-	24.2	-
C20:1n-15	0.213	NS	ND	-	-	-
C20:1n-12	0.202	NS	ND	-	-	-
C20:1n-9	0.190	NS	ND	-	-	-
C20:2n-6	0.211	0.126	0.057	1.7	3.7	2.2
C20:3n-6	0.214	0.117	0.021	1.8	10.4	5.6
C20:4n-6	0.204	0.110	0.018	1.8	11.4	6.2
C20:3n-3	0.206	0.118	0.016	1.7	13.1	7.5
C22:0	0.221	0.358	0.019	0.6	11.8	19.1
C22:1n-9	0.235	0.356	ND	0.7	-	-
C20:5n-3	0.189	NA	NA	-	-	-
C22:2n-6	0.238	0.338	0.036	0.7	6.5	9.3
C22:3n-3/C22:4n-6	0.147	0.271	0.047	0.5	3.2	5.8
C24:0	0.336	0.505	ND	0.7	-	-
C24:1n-9	0.338	0.445	ND	0.8	-	-
C22:5n-3	0.233	NA	NA	-	-	-
C22:6n-3	0.317	0.312	ND	1.0	-	-

* m/z 67, 74, 79
ND=Not detected because its base peak was not monitored during SIM mode analysis.
NS=Not separated.
NA=Not analyzed.

Table 4.5 Limits of quantification (LOQ) for standard solution FAMEs. LOQ for GC-FID and GC-MS, and for the two MS modes total ion current (TIC) and selected ion monitoring (SIM), were compared and ratios for their LOQs are given to the right (ΔLOQ).

	GC-FID	GC-MS TIC	GC-MS SIM *	Δ LOQ		
FAME	LOQ (µg/ml)	LOQ (µg/ml)	LOQ (µg/ml)	FID/MS	FID/SIM	TIC/SIM
C8:0	0.249	0.130	0.005	6.4	53.9	8.5
C10:0	0.288	0.161	0.005	6.0	58.0	9.7
C12:0	0.262	0.196	0.005	4.5	48.2	10.8
C12:1	0.280	0.170	ND	5.5	-	-
C14:0	0.294	0.252	0.004	3.9	67.2	17.3
C14:1n-5	0.307	0.225	ND	4.5	-	-
C16:0	0.355	0.269	0.005	4.4	71.4	16.2
C16:1n-7	0.368	0.232	ND	5.3	-	-
C17:0	0.347	0.205	0.029	5.6	12.0	2.1
C18:0	0.384	0.250	0.036	5.1	10.6	2.1
C18:1	0.356	NS	ND	-	-	-
C18:2n-6	0.402	0.372	0.084	3.6	4.8	1.3
C18:3n-6	0.437	0.363	0.069	4.0	6.3	1.6
C18:3n-3	0.445	0.407	0.080	3.6	5.6	1.5
C20:0	0.504	NS	0.021	-	24.2	-
C20:1n-15	0.709	NS	ND	-	-	-
C20:1n-12	0.672	NS	ND	-	-	-
C20:1n-9	0.634	NS	ND	-	-	-
C20:2n-6	0.702	0.420	0.192	5.6	3.7	0.7
C20:3n-6	0.712	0.389	0.069	6.1	10.4	1.7
C20:4n-6	0.679	0.368	0.060	6.1	11.4	1.9
C20:3n-3	0.687	0.393	0.052	5.8	13.1	2.2
C22:0	0.738	1.194	0.062	2.1	11.8	5.7
C22:1n-9	0.784	1.186	ND	2.2	-	-
C20:5n-3	0.631	NA	NA	-	-	-
C22:2n-6	0.794	1.125	0.121	2.4	6.5	2.8
C22:3n-3/C22:4n-6	0.489	0.905	0.155	1.8	3.2	1.8
C24:0	1.119	1.684	ND	2.2	-	-
C24:1n-9	1.126	1.484	ND	2.5	-	-
C22:5n-3	0.778	NA	NA	-	-	-
C22:6n-3	1.057	1.039	ND	3.4	-	-

* m/z 67, 74, 79
ND=Not detected because its base peak was not monitored during SIM mode analysis.
NS=Not separated.
NA=Not analyzed.

4.5.4 Quantifier and qualifier ions for quantification by GC-MS

Mass spectra from analysis of GLC #411 in TIC mode was used to specify each FAMEs quantifier ion, which was defined as the ion of highest abundance (the base peak). Two or three characteristic ions of relatively high abundance were chosen as qualifier ions. Quantifier and qualifier ions listed in Table 4.6 can further be used for identification and quantification of unknown FAMEs in serum samples analyzed in by using GC-MS in SIM mode.

Table 4.6 Name, *m/z*-value, quantifier (base peak) and qualifier ions for FAMEs in the standard solution GLC #411.

FAME	*m/z* (Da)	Quantifier ion	Qualifier ions
C8:0	158	74	87, 127
C10:0	186	74	87, 143
C12:0	214	74	87, 143, 171
C12:1	212	74	55, 87, 138
C14:0	242	74	87, 143, 199
C14:1n-5	240	55	74, 87
C16:0	270	74	87, 143, 227
C16:1n-7	268	55	69, 87, 236
C18:0	298	74	87, 143, 255
C18:1	296	55	69, 110
C18:2n-6	294	67	81, 95
C18:3n-6	292	79	67, 80, 93
C18:3n-3	292	79	67, 80, 93
C20:0	326	74	55, 87, 143
C20:1n-15	324	74	55, 96, 292
C20:1n-12	324	55	69, 74, 292
C20:1n-9	324	55	69, 74, 292
C20:2n-6	322	67	81, 95
C20:3n-6	320	79	67, 93, 150
C20:4n-6	318	79	67, 91
C20:3n-3	320	79	67, 95, 108
C22:0	354	74	87, 143
C22:1n-9	352	55	69, 97
C22:2n-6	350	67	81, 95
C22:3n-3	348	79	67, 80, 108
C22:4n-6	346	79	67, 80, 150
C24:0	382	74	87, 143
C24:1n-9	380	55	69, 83
C22:6n-3	342	79	67, 91

4.5.5 System performance

Tables with results for all chromatography parameters used for describing system performance can be found in appendix 5. A short extract of the results is provided in this section.

The retention factor (*k*) increased with both increasing retention time and calibration level. Retention factor for identified FAMEs ranged from 1.06 to 15.22.

Peak width ($W_{50.0}$) increased with increasing calibration level. Peak width varied from 0.04 to 0.45. Plate number (*N*) clearly decreased for most of the identified FAMEs from calibration level 5, and for the remaining peaks from calibration level 6. Plate number ranged from 61518 to 716175.

The resolution factor (*R*) was >1.00 for all peaks in GLC #411 chromatogram from level 1-5. The closely eluting peaks for C20:1n-15, n-12 and n-9 had a resolution of 0.91 at level 6 and decreasing for the remaining higher levels.

Peak symmetry factors were positively related to concentration for all identified FAMEs in GLC #411, ranging from 0.57 to 6.11. All peaks had a symmetry factor beneath 2.5 for calibration level 1-5.

4.5.6 Precision and methodological variation

Three replicates of an intermediate concentration of GLC #411 (31 µg/ml of each FAME) was analyzed to determine the intraday analytical variation, expressed as precision of the GC-FID method. Mean area ratio for FAMEs, with respect to the internal standard, was calculated and the variability for each mean is presented as the relative standard deviation (RSD %) in Table 4.7.

Table 4.7 Analytical variation presented as the relative standard deviation for area ratios of a selection of FAMEs.

FAME	Mean area ratio	Std.dev	RSD %
C16:0	1.079	0.001	0.1
C18:0	1.127	0.002	0.1
C18:1	3.246	0.007	0.2
C18:2	1.119	0.001	0.1
C20:3n-6	1.110	0.004	0.3
C20:4n-6	1.088	0.002	0.2
C22:6n-3	1.022	0.007	0.7

The intraday repeatability for the sample preparation procedure and GC-FID analysis is expressed as methodological variation. The methodological variation was investigated by determining the mean area ratio of FAMEs in five prepared aliquots of the same serum sample. All five samples were prepared and analyzed in the same setup. The methodological variation is presented as RSD % and is listed in Table 4.8.

Table 4.8 Intraday methodological variation presented as relative standard deviation (RSD %) for a selection of FAMEs.

FAME	Mean area ratio	Std.dev	RSD %
C16:0	2.755	0.127	4.6
C18:0	1.877	0.080	4.2
C18:1	1.255	0.063	5.1
C18:2n-6	2.421	0.118	4.9
C20:3 n-6	0.308	0.016	5.2
C20:4 n-6	0.947	0.051	5.3
C20:5 n-3	0.159	0.014	8.5
C22:5 n-3	0.097	0.007	7.5
C22:6 n-3	0.477	0.026	5.5

4.5.7 External control of obtained analytical results

Nine carefully selected serum samples representing the variation of the study population were analyzed at an external, GMP certified chemical analysis contract laboratory (as Vitas, Oslo, Norway) to confirm analytical results achieved in this study. Nine representative FAMEs from each sample were compared and a percentage difference ranging from 0.0-4.0 % was observed within serum phospholipid fatty acid composition for individual samples (appendix 8).

4.6 Participant characteristics

At baseline, participants had a median age of 35 with a range from 22 to 61 years, and 62.3 % were overweight or obese according to WHO criteria listed in Table 1.1. Median BMI was 26.6 (18.8-62.7) kg/m^2. Table 4.9 presents the baseline characteristics for men attending this study divided in three groups based on their BMI. When results are further described in the text, they will be referred to as; group 1 (BMI 18.5-24.9 kg/m^2), group 2 (BMI 25.0-29.9 kg/m^2) and group 3 (BMI ≥30.0 kg/m^2). Ethnicity is not listed in the table because 99.3 % of the men were Caucasian.

Table 4.9 Baseline characteristics of men attending the study, divided into three groups according to BMI.

	BMI, kg/m²									
	1: 18.5-24.9			2: 25.0-29.9			3: ≥30.0			
	n	Median (range)		n	Median (range)		n	Median (range)		*p*-value[a]
Age, years	22	28	(24-51)	17	35	(22-58)	19	40	(22-61)	**0.005**[bc]
BMI, kg/m^2	22	22.9	(18.8-24.9)	17	26.8	(25.0-29.0)	19	43.5	(30.0-62.7)	<**0.001**[bcd]
Body fat, %	22	18.2	(7.2-27.1)	16	26.2	(10.6-33.7)	18	39.8	(21.8-51.7)	<**0.001**[bcd]
Abstinence, days	22	4	(1-7)	17	3	(2-9)	18	4	(2-14)	0.148

[a]Obtained from Kruskal Wallis Test for comparing medians.
[b]Group 2 significantly different (p<0.05) from group 1 tested with Mann-Whitney U Test.
[c]Group 3 significantly different (p<0.05) from group 1 tested with Mann-Whitney U Test.
[d]Group 3 significantly different (p<0.05) from group 2 tested with Mann-Whitney U Test.

Men in group 2 and 3 had both a significantly higher median age than men in group 1 (p=0.005). As expected, BMI and percent body fat were significantly higher for men in each group compared to men in the former group(s), with p<0.001 for both parameters. Abstinence time before semen sample delivery was not significantly different between participants in the three groups (p=0.148).

4.7 BMI in relation to semen quality

In crude analysis, BMI was investigated for associations with semen quality parameters for men in the three BMI groups (Table 4.10). A significant difference was observed between men in the groups for the semen quality parameters semen volume (p=0.005), total sperm count (p=0.009), sperm concentration (p=0.035), total sperm motility (p=0.008), total PR count (p=0.005), normal sperm morphology (p=0.012) and total normal sperm morphology count (p=0.001). Sperm vitality was the only parameter that did not reach statistical significance (p=0.362).

Table 4.10 Semen quality parameters of participants divided into three groups based on BMI at baseline.

	BMI, kg/m²						
	1: 18.5-24.9		2: 25.0-29.9		3: ≥30.0		
Semen quality parameters	n	Median (range)	n	Median (range)	n	Median (range)	*p*-value[a]
Semen volume (ml)	22	4.9 (2.9-8.0)	17	3.8 (1.4-7.6)	19	3.1 (0.8-8.4)	**0.005**[bc]
Total sperm count (10^6 cells)	21	400 (81-808)	16	183 (13-497)	19	125 (30-1127)	**0.009**[bc]
Sperm concentration (10^6 sperm/ml)	21	80 (13.4-187)	16	42.5 (7.2-184)	19	50 (8.3-155.5)	**0.035**
Vitality (%)	21	90.0 (75.0-97.0)	14	90.0 (53.0-97.0)	19	87.0 (47-95)	0.362
Total motility (PR+NP) (%)	21	85.0 (50.0-90.0)	13	75.0 (19.0-87.0)	7	58.0 (38.0-83.0)	**0.008**[c]
Total PR count (10^6sperm)	21	234.3 (15.4-557.5)	13	63.4 (5.5-310.1)	7	31.2 (11.7-185.1)	**0.005**[bc]
Normal morphology (%)	21	5.0 (0.0-8.0)	14	4.0 (0.0-10.0)	18	2.0 (1.0-7.0)	**0.012**[c]
Total normal morphology count (10^6 sperm)	21	17.7 (0.0-64.6)	14	9.6 (0.0-19.9)	18	3.9 (0.3-45.1)	**0.001**[bc]

[a]Obtained from Kruskal Wallis Test for comparing medians
[b]Group 2 significantly different (p<0.05) from group 1 tested with Mann-Whitney U test.
[c]Group 3 significantly different (p<0.01) from group 1 tested with Mann-Whitney U test.

Median values for the significant variables were compared with Mann-Whitney U Test and revealed that men in group 3 did not differ significantly from men in group 2 for any of the semen quality parameters (p>0.05). Men in group 2 and 3 had significantly decreased semen volume, total sperm count, total PR count and total normal sperm morphology count compared to men in group 1 (p<0.05 and p<0.01, respectively). Men in group 3 showed a significant decrease compared to men in group 1

for percentage normal sperm morphology and percentage total motile sperm (PR+NP) as well (p<0.01).

As mentioned earlier semen quality is affected by age and abstinence time. The comparisons of men in the three BMI groups were therefore repeated with adjustment for the two confounders (Table 4.11). After adjustment, semen volume and total normal morphology count were no longer significantly different for men in group 2 compared to men in group 1. Total normal morphology presented a significant decrease for men in group 3 compared to group 2 after adjustment (p=0.017). The same trend was seen in crude analysis, without reaching statistical significance (p=0.063). Sperm concentration showed a significant decrease for men in group 3 compared to men in group 1 after adjustment, while the difference did not reach statistical significance in crude analysis (p=0.003 and p=0.070, respectively). All other significant differences depicted in crude analysis remained statistically significant after adjustment for age and abstinence time; men in group 2 and 3 still had significantly decreased total sperm count (p=0.024 and p=<0.001) and total PR count (p=0.049 and p=0.009) compared to men in group 1. Men in group 3 still showed significantly decreased total sperm motility (PR+NP) and normal sperm morphology compared to men in group 1 (p=0.032 and p=0.033).

Table 4.11 Semen analysis for men in the three BMI groups were compared by using multiple linear regression with semen quality parameters as dependent continuous variables and BMI groups as an independent dichotomous variable, while adjusting for age and abstinence time (n = n listed in Table 4.10).

	BMI groups compared					
	1 vs 2		1 vs 3		2 vs 3	
Semen analysis	B[d]	*p*	B[d]	*p*	B[d]	*p*
Semen volume (ml)	-0.8	0.105	-1.3	**0.019**	-0.3	0.610
Total sperm count[a] (10^6 sperm)	-4.8	**0.024**	-8.0	**<0.001**	-2.1	0.349
Sperm concentration[a] (10^6 sperm/ml)	-1.5	0.131	-2.9	**0.003**	-0.6	0.514
Vitality (%)	-0.9	0.809	-0.7	0.848	1.3	0.730
Total motility (PR+NP)[b] (%)	-0.9	0.201	-1.8	**0.032**	-1.0	0.288
Total PR count[a] (10^6sperm)	-4.4	**0.049**	-6.9	**0.009**	-2.8	0.358
Normal morphology (%)	-0.1	0.944	-2.0	**0.033**	-1.5	0.119
Total normal morphology count[c] (10^6 sperm)	-0.3	0.109	-0.8	**<0.001**	-0.5	**0.017**

[a]Square root transformed to meet the distributional assumptions of linear regression.
[b]Reflected and square root transformed to meet the distributional assumptions of linear regression.
[c]Log transformed to meet the distributional assumptions of linear regression.
[d]Unstandardized B-coefficient achieved with multiple linear regression.

Multiple linear regression was also used to assess the relationship between BMI as a continuous independent variable and the semen quality parameters as continuous dependent variables while adjusting for age and abstinence time (Table 4.12). After the adjustment BMI was still negatively correlated with semen volume (p=0.030), total sperm count (p=0.009), total PR count (p=0.042) and total normal sperm morphology count (p=0.019). Total sperm count, sperm concentration, sperm vitality and total PR count were transformed to meet the distributional assumptions of linear regression.

Table 4.12 Multiple linear regressions were used to assess the relationship between BMI as a continuous independent variable and the semen quality parameters as continuous dependent variables while adjusting for age and abstinence time.

Semen quality parameters	n	Unstandardized B-coefficient	*p*-value
Semen volume (ml)	58	-0.043	**0.030**
Total sperm count[a] (10^6 sperm)	57	-0.210	**0.009**
Sperm concentration[a] (10^6 sperm/ml)	57	-0.061	0.097
Vitality[b] (%)	55	-0.002	0.695
Total motility (%)	42	-0.386	0.129
Total PR count (10^6 sperm)	42	-0.192	**0.042**
Normal morphology (%)	53	-0.042	0.216
Total normal morphology count (10^6 sperm)	54	-0.453	**0.019**

[a]Square root transformed to meet the distributional assumptions of linear regression.
[b]Reflected and log transformed to meet the distributional assumptions of linear regression.

4.8 FAME composition in serum phospholipids

The FAME composition in serum for all participants (Table 4.13) is displayed the same tendency with PUFAs (median 47.6 % (43.7-51.9)) > SFAs (39.9 % (36.2-42.7)). When PUFAs were divided into n-6 and n-3 FAMEs all participants showed a higher amount of n-6 FAMEs (35.5 % (29.2-39.2)) compared to n-3 FAMEs (11.7 % (8.3-19.6)). In most participant sera the most abundant single fatty acid was C16:0 with median 26.6 % (24.0-29.9). Other major FAME contributors in serum were C18:0 and C18:2n-6 with median 13.2 % (10.6-16.9) and 21.6 % (17.4-27.2), respectively. Together, these three FAMEs constituted approximately 60 % of total serum phospholipid FAMEs detected in participant samples.

Table 4.13 Serum phospholipid FAME composition for all participants

	All participants
FAME	Median % (range)
PUFA	47.6 (43.7-51.9)
n-6	35.5 (29.2-39.2)
C18:2n-6	21.6 (17.4-27.2)
C20:3n-6	3.8 (2.4-5.6)
C20:4n-6	9.6 (4.7-13.8)
n-3	11.7 (8.3-19.6)
C20:5n-3	2.8 (1.1-8.3)
C22:5n-3	2.8 (0.8-3.8)
C22:6n-3	6.3 (3.9-9.5)
MUFA	
C18:1	12.2 (10.4-16.1)
SFA	39.9 (36.2-42.7)
C16:0	26.6 (24.0-29.9)
C18:0	13.2 (10.6-16.9)
n-6/n-3-ratio	2.9 (1.5-4.5)
PUFA/SFA-ratio	1.2 (1.0-1.4)

4.8.1 BMI in relation to serum phospholipid FAME composition

Participants were divided into three groups based on BMI for comparison of single and grouped FAMEs measured at baseline, and median percentage (range) is listed in Table 4.14.

Table 4.14 Serum phospholipid FAME composition for participants divided into three groups based on BMI.

	BMI, kg/m²			
	1: 18.5-24.9 (n=22)	2: 25.0-29.9 (n=16)	3: ≥30.0 (n=18)	
FAME (%)	Median (range)	Median (range)	Median (range)	*p*-value[a]
PUFA	47.7 (43.7-50.1)	47.4 (44.5-51.9)	47.3 (44.9-48.7)	0.649
n-6	35.0 (29.7-37.9)	35.3 (29.2-38.4)	35.8 (30.1-39.2)	0.553
C18:2n-6	22.0 (17.9-27.2)	21.7 (17.4-27.2)	21.3 (17.4-23.2)	0.256
C20:3n-6	3.4 (2.4-5.6)	3.6 (2.4-5.5)	4.6 (3.0-5.4)	**0.001**[bc]
C20:4n-6	9.3 (4.7-12.2)	8.9 (6.1-12.7)	10.4 (6.9-13.8)	0.081
n-3	11.9 (8.4-19.6)	12.9 (8.6-17.8)	11.0 (8.3-18.6)	0.336
C20:5n-3	2.6 (1.2-8.3)	3.0 (1.1-6.9)	2.8 (1.7-8.0)	0.582
C22:5n-3	3.1 (2.4-3.8)	2.9 (2.2-3.3)	2.7 (2.2-3.1)	**0.006**[b]
C22:6n-3	6.4 (3.9-9.4)	7.0 (4.5-9.5)	6.0 (4.2-7.9)	0.172
MUFA				
C18:1	13.1 (10.6-16.1)	12.3 (11.3-15.0)	11.9 (10.4-14.1)	**0.007**[b]
SFA	39.3 (37.9-42.0)	39.7 (36.2-42.2)	40.9 (39.2-42.7)	**0.001**[bc]
C16:0	26.2 (24.4-29.9)	26.7 (24.0-29.3)	26.3 (24.7-28.4)	0.852
C18:0	12.8 (10.8-15.0)	13.1 (10.6-14.7)	14.2 (11.6-16.9)	**0.002**[bc]
n-6/n-3-ratio	2.8 (1.5-4.4)	2.7 (1.6-4.5)	3.3 (1.6-4.4)	0.368
PUFA/SFA-ratio	1.2 (1.0-1.3)	1.2 (1.1-1.4)	1.2 (1.1-1.2)	0.055

[a]Obtained from Kruskal Wallis Test for comparing medians.
[b]Group 3 significantly different from group 1 tested with Mann-Whitney U Test.
[c]Group 3 significantly different from group 2 tested with Mann-Whitney U Test.

There were significant differences between the median percentages for men in the three BMI groups with regard to C18:0 (p=0.002), C18:1 (p=0.007), C20:3n-6 (p=0.001), C22:5n-3 (p=0.006) and total SFA (p=0.001). The PUFA/SFA-ratio showed a decreasing trend, but did not reach statistical significance (p=0.055). Median values for the significant variables were compared with Mann-Whitney U Test and revealed that group 2 did not differ significantly from group 1 for any of the FAMEs (p>0.05). Men in group 3 had a significantly higher median percentage for C20:3n-6, C18:0 and total SFA compared to men in both group 1 and 2 (p<0.05). When comparing group 2 and 3 the latter group showed a lower median percentage for C22:5n-3 and C18:1 (p<0.05).

4.8.2 Serum phospholipid FAME composition in relation to semen quality

Multiple linear regressions were performed to investigate relationships between serum phospholipid FAMEs and semen quality parameters after adjustment for age and abstinence time. Semen volume showed a significant positive association with increasing percentage of C18:2n-6 (p=0.038), and a negative association was seen for semen volume and C20:4n-6 (p=0.006). No significant associations were found for sperm concentration or sperm vitality, as depicted in Table 4.15.

Table 4.15 Multiple linear regressions were used to assess the relationship between serum phospholipid FAMEs as continuous independent variables and the semen quality parameters as continuous dependent variables, while adjusting for age and abstinence time.

	Semen volume (ml) n=57		Tot. sperm count[a] (10^6 sperm) n=57		Sperm concentration[a] (10^6 sperm/ml) n=57		Vitality (%) n=55	
FAMEs (%)	B	*p*	B	*p*	B	*P*	B	*p*
PUFA	-0.1	0.482	-0.1	0.861	0.1	0.759	<0.05	0.435[b]
n-6	-0.1	0.426	-0.6	0.067	-0.1	0.378	<0.05	0.210[b]
C18:2n-6	0.2	**0.038**	-0.2	0.604	-0.1	0.472	<0.05	0.414[b]
C20:3n-6	-0.4	0.066	-1.0	0.283	-0.1	0.865	-0.1	0.708[b]
C20:4n-6	-0.3	**0.006**	-0.6	0.185	<0.05	0.798	-0.1	0.568[b]
n-3	<0.05	0.751	0.4	0.129	0.1	0.340	0.5	0.323
C20:5n-3	<0.05	0.921	0.5	0.280	0.2	0.479	<0.05	0.393[b]
C22:5n-3	0.8	0.068	4.4	**0.009**	1.1	0.172	3.7	0.216
C22:6n-3	<0.05	0.953	0.6	0.270	0.2	0.448	0.1	0.058[b]
MUFA								
C18:1	0.2	0.276	1.1	0.091	0.3	0.321	-0.1	0.241[b]
SFA	<0.05	0.897	-1.0	0.154	-0.4	0.161	0.8	0.497
C16:0	0.1	0.413	-0.2	0.813	-0.4	0.249	-0.1	0.914[b]
C18:0	-0.1	0.408	-0.7	0.238	-0.1	0.727	0.6	0.596
n-6/n-3-ratio	-0.2	0.375	-1.8	0.087	-0.4	0.369	-0.1	0.118[b]
PUFA/SFA-ratio	-0.9	0.745	6.7	0.559	4.4	0.394	0.3	0.715[b]

[a]Square root transformed to meet the distributional assumptions of linear regression.
[b]Reflected and log transformed to meet the distributional assumptions of linear regression.

The three sperm motility parameters listed in Table 4.16 all presented a inverse association with n-6 FAMEs (p=0.045, p=0.023 and p=0.023) and the n-6/n-3-ratio (p=0.041, p=0.012 and p=0.008), while a positive association was observed with C22:5n-3 (p=0.016, p=0.003 and p<0.001). Total sperm motility and total PR count was positively associated with n-3 FAMEs (p=0.039 and p=0.034), and percentage progressively motile sperm showed the same trend without reaching statistical significance (p=0.071). C18:0 and percentage progressively motile sperm also had a significant negative association (p=0.038), without achieving the same strength of association with the two other motility parameters.

Table 4.16 Multiple linear regressions were used to assess the relationship between serum phospholipid FAMEs as a continuous independent variable and the sperm motility parameters as continuous dependent variables while adjusting for age and abstinence time (n=42).

	Progressive motility (%)		Total motility (NP+PR) (%)		Total PR count (10^6 sperm)	
FAME (%)	B	*p*	B	*p*	B	*p*
PUFA	<0.05	0.976[a]	0.1	0.947	<0.05	0.862[c]
n-6	-2.3	**0.045**	-2.1	**0.023**	-0.1	**0.023**[c]
C18:2n-6		ND	-1.2	0.279	-13.5	0.219
C20:3n-6	-0.2	0.620[a]	-2.5	0.413	-0.1	0.199[c]
C20:4n-6	-2.1	0.197	-1.8	0.170	-0.6	0.260[b]
n-3	1.9	0.071	1.8	**0.039**	<0.05	**0.034**[c]
C20:5n-3	2.8	0.130	2.2	0.158	25.1	0.090
C22:5n-3	15.6	**0.016**	15.5	**0.003**	0.2	**<0.001**[c]
C22:6n-3	2.7	0.253	3.2	0.102	0.6	0.419[b]
MUFA						
C18:1	0.2	0.384[a]	0.1	0.662[a]	<0.05	0.680[c]
SFA	-0.2	0.349[a]	-0.6	0.767	-0.7	0.369[b]
C16:0		ND	0.3	0.273[a]	<0.05	0.313[c]
C18:0	-0.5	**0.038**[a]	-2.8	0.130	-0.1	0.297[c]
n-6/n-3-ratio	-8.0	0.041	-7.9	0.012	-0.1	**0.008**[c]
PUFA/SFA-ratio	1.5	0.738[a]	3.0	0.932	<0.05	0.987[c]

[a]Reflected and square root transformed to meet the distributional assumptions of linear regression.
[b]Square root transformed to meet the distributional assumptions of linear regression.
[c]Log transformed to meet the distributional assumptions of linear regression.
ND = Residuals did not achieve the distributional assumptions of linear regression.

Total normal sperm morphology count showed a negative association with n-6 FAMEs, and a positive association with C18:1. Percentage normal sperm morphology had a negative association with total SFAs and the same trend was observed for total normal sperm morphology count, without reaching statistical significance (*p*=0.088) (Table 4.17).

Table 4.17 Multiple linear regressions were used to assess the relationship between serum phospholipid FAMEs as continuous independent variables and the sperm morphology parameters as continuous dependent variables while adjusting for age and abstinence time (n=54).

	Normal morphology (%)		Total normal morphology count (10^6 sperm)	
FAMEs (%)	B	*p*	B	*P*
PUFA	0.1	0.773	<0.05	0.964[b]
n-6	-0.1	0.284	-0.2	**0.023**[a]
C18:2n-6	-0.2	0.200	-0.1	0.551[b]
C20:3n-6	-0.3	0.540	-0.2	0.098[b]
C20:4n-6	0.1	0.776	-0.1	0.409[b]
n-3	0.1	0.266	<0.05	0.138[b]
C20:5n-3	0.2	0.371	1.8	0.136[b]
C22:5n-3	0.2	0.771	0.3	0.089[b]
C22:6n-3	0.3	0.203	0.1	0.139[b]
MUFA				
C18:1	0.5	0.111	0.1	**0.026**[b]
SFA	-0.6	**0.043**	-0.4	0.088[a]
C16:0	<0.05	0.933	-0.1	0.554[b]
C18:0	-0.5	0.073	-0.1	0.098[b]
n-6/n-3-ratio	-0.5	0.251	-0.2	0.086[b]
PUFA/SFA-ratio	6.0	0.213	1.4	0.203[b]

[a]Square root transformed for normal distribution of residuals.
[b]Log transformed for normal distribution of residuals.

4.9 The effect of weight loss

Participants were divided into three groups; < 10 % (low) weight loss, ≥10 % (high) weight loss or bariatric surgery with a following weight loss. Semen quality and serum phospholipid FAME composition at baseline and after weight loss were compared within groups. Median BMI at baseline was 30.6 kg/m^2, ranging from 26.0-56.5 kg/m^2, 36.0 (29.0-46.6) kg/m^2 and 49.4 (43.5-62.7) kg/m^2, respectively. Corresponding median age was 46 (35-51) years, 49 (32-59) years and 40.5 (33-51) years. After weight loss the median BMI was 29.5 (24.0-53.3) kg/m^2, 32.2 (25-41.9) kg/m^2 and 39.4 (32.3-48.0) kg/m^2.

4.9.1 A comparison of semen quality

The results from semen quality comparison at baseline and after weight loss for men in the low percentage weight loss group are listed in Table 4.18; no significant changes were observed.

Table 4.18 A comparison of semen quality parameters at baseline and after low (<10 %) percentage weight loss.

		Median (25-75 percentile)				
Semen quality parameter	n	Baseline		After weight loss		*p*-value[1]
Vitality (%)	7	82	(53.0-92.0)	85	(82.6-87.0)	0.612
Sperm concentration (10^6 sperm/ml)	8	51.4	(36.6-129.6)	53	(31.5-114.7)	0.779
Total sperm count (10^6 sperm)	8	178.5	(92.3-424.0)	195	(61.8-301.6)	0.575
Semen volume (ml)	8	3.4	(2.3-4.1)	2.9	(1.9-4.5)	0.401
Normal morphology (%)	3	3	(1.0-6.0)	5	(1.5-6.0)	0.180
Total normal morphology count (10^6 sperm)	3	7	(0.7-13.4)	8.8	(0.9-15.1)	0.102
Progressive motility (%)	3	49	(10.0-58.0)	22	(12.0-36.0)	0.285
Total motility (%)	3	83	(58.0-85.0)	61	(48.0-72.0)	0.285
Total PR count (10^6 sperm)	3	84.3	(19.9-157.6)	32.1	(26.0-115.9)	0.273

[1]*p*-value from Wilcoxons Signed Rank Test.

The results from semen quality comparison at baseline and after weight loss for men in the high percentage weight loss group are listed in Table 4.19. Data for motility and morphology was only available for two of the participants and the results are listed as separate cases in Table 4.20. There were no significant changes in semen quality after a high percentage weight loss, but a decreasing trend was observed.

Table 4.19 A comparison of semen quality parameters at baseline and after high (≥10 %) percentage weight loss

		Median (25-75 percentile)				
Semen quality parameter	n	Baseline		After weight loss		*p*-value[1]
Vitality (%)	4	93.5	(75.8-94.6)	86.9	(68.8-90.9)	0.068
Sperm concentration (10^6 sperm/ml)	4	107.95	(48.3-131.1)	75.4	(29.6-100.7)	0.068
Total sperm count (10^6 sperm)	3	315	(85.0-540.0)	182.2	(87.5-277.7)	0.285
Semen volume (ml)	4	3	(2.1-4.1)	2.7	(1.9-4.4)	0.715

[1]*p*-value from Wilcoxons Signed Rank Test.

Table 4.20 A comparison of semen quality parameters at baseline and after high (≥10 %) percentage weight loss for two cases (NA=not analyzed).

	case 1		case 2	
Semen quality parameter	Baseline	After weight loss	Baseline	After weight loss
Normal morphology (%)	NA	NA	1.0	0.0
Total normal morphology count (10^6 sperm)	NA	NA	0.9	0.0
Progressive motility (%)	60.0	33.0	19.0	3.0
Total motility (%)	85.0	75.0	16.2	2.6
Total PR count (10^6 sperm)	189.0	60.1	44.0	21.0

NA = not analyzed

The results from semen quality comparison at baseline and after weight loss for men who underwent bariatric surgery are listed in Table 4.21. Sperm motility and morphology data after weight loss were

not available for these participants at the time of statistical analyses. No significant changes in semen quality were observed after weight loss.

Table 4.21 A comparison of semen quality parameters at baseline and after weight loss due to bariatric surgery (n=4).

	Median (25-75 percentile)				
Semen quality parameter	Baseline		After weight loss		p-value[1]
Vitality (%)	88.5	(87.0-90.0)	84.5	(76.0-89.0)	0.144
Sperm concentration (10^6 sperm/ml)	41.4	(14.4-64.0)	31.6	(6.8-68.6)	1.000
Total sperm count (10^6 sperm)	90	(38.5-150.5)	99.7	(64.5-218.1)	0.273
Semen volume (ml)	3.2	(1.2-4.6)	3.1	(1.6-7.7)	0.715

[1]*p*-value from Wilcoxons Signed Rank Test.

4.9.2 A comparison of serum phospholipid FAME composition

The percentage composition of FAMEs in serum phospholipids at baseline and after weight loss was compared within the three groups. The proportion of n-3 FAMEs has increased significantly (p=0.033) for men in the <10 % weight loss group (Table 4.22), with an increase in C22:6n-3 as the largest contributor. A decrease in the n-6/n-3-ratio can be seen for men in the same group, without reaching statistical significance (p=0.075).

Table 4.22 Within-group comparison of percent of total FAMEs before and after a weight loss < 10 % (n=11).

	Median % (25-75 percentile)				
FAME (%)	Baseline		<10 % weight loss		*p*-value[1]
PUFA	47	(46.6-48.4)	48.3	(46.6-49.1)	0.286
n-6	34.5	(33.3-36.3)	33.2	(31.7-34.0)	0.155
C18:2n-6	20.3	(17.6-21.6)	20.2	(17.5-21.3)	0.248
C20:3n-6	4.1	(3.6-4.7)	3.4	(2.9-4.8)	0.091
C20:4n-6	9.9	(8.5-11.7)	10.1	(7.6-12.4)	0.722
n-3	12.5	(10.9-15.3)	14.0	(11.0-16.3)	**0.033**
C20:5n-3	2.8	(2.3-4.5)	3.7	(2.6-4.9)	0.155
C22:5n-3	2.7	(2.5-3.1)	2.9	(2.6-3.1)	0.182
C22:6n-3	6.9	(6.2-7.3)	7.0	(6.0-8.9)	0.075
MUFA					
C18:1	12.0	(10.8-13.4)	12.0	(11.4-12.7)	0.594
SFA	40.5	(39.9-41.6)	40.2	(39.4-41.3)	0.131
C16:0	26.7	(25.9-28.0)	26.9	(26.1-28.0)	0.534
C18:0	13.2	(12.8-15.6)	13.3	(12.2-15.0)	0.182
n-6/n-3-ratio	2.9	(2.2-3.4)	2.3	(1.9-3.0)	0.075
PUFA/SFA-ratio	1.2	(1.1-1.2)	1.2	(1.2-1.2)	0.213

[1]p-value from Wilcoxons Signed Rank Test.

There were no significant changes in serum phospholipid FAME composition observed for the group who lost ≥10 % of their body weight. The proportion of SFAs showed a decreasing trend after weight loss, with an increasing trend for the PUFA/SFA-ratio, without being statistically significant (Table 4.23).

Table 4.23 Within-group comparison of percent of total FAMEs before and after weight loss of ≥ 10 % (n=4).

	Median (25-75 percentile)				
FAMEs (%)	Baseline		≥10 % weight loss		*p*-value[1]
PUFA	48.2	(47.4-48.9)	48.3	(47.6-49.4)	0.715
n-6	35.6	(30.0-37.7)	35.0	(32.3-37.0)	1.000
C18:2n-6	20.7	(18.2-22.8)	21.0	(19.6-22.2)	0.465
C20:3n-6	4.3	(3.3-5.3)	4.1	(3.5-4.3)	0.715
C20:4n-6	9.9	(8.0-11.8)	9.8	(7.9-11.9)	0.715
n-3	12.5	(10.3-17.3)	13.6	(11.0-16.3)	0.715
C20:5n-3	2.7	(1.8-6.7)	3.7	(1.8-5.1)	1.000
C22:5n-3	2.8	(2.5-3.0)	2.9	(2.5-3.0)	0.715
C22:6n-3	7.3	(5.6-7.8)	7.4	(5.9-8.5)	0.273
MUFA					
C18:1	11.5	(10.9-11.8)	12.1	(11.5-13.0)	0.144
SFA	40.1	(39.4-41.4)	39.2	(38.6-40.5)	0.068
C16:0	26.6	(26.2-27.4)	25.7	(25.1-26.3)	0.068
C18:0	13.5	(12.6-15.0)	13.8	(12.5-14.9)	0.715
n-6/n-3-ratio	2.9	(1.8-3.7)	2.7	(2.0-3.3)	0.465
PUFA/SFA-ratio	1.2	(1.2-1.2)	1.2	(1.2-1.3)	0.068

[1]*p*-value from Wilcoxons Signed Rank Test.

No significant changes were revealed for the serum phospholipid FAME composition in participants who lost weight after bariatric surgery (Table 4.24). The proportion of PUFAs, n-6 FAMEs and SFAs showed a decreasing trend and an increasing trend was observed for C18:1, but either were statistically significant.

Table 4.24 Within-group comparison of percent of total FAMEs before and after weight loss due to bariatric surgery (n=4).

	Median (25-75 percentile)				
FAMEs (wt%)	Baseline		After surgery		*p*-value[1]
PUFA	46.7	(45.4-46.9)	44.5	(41.3-46.1)	0.068
n-6	35.2	(34.6-36.6)	33.2	(32.6-34.3)	0.068
C18:2n-6	22.3	(21.7-23.1)	19.4	(17.2-23.3)	0.144
C20:3n-6	4.6	(4.1-4.9)	4.4	(3.0-4.8)	0.715
C20:4n-6	8.5	(7.2-10.0)	9.2	(7.7-11.0)	0.144
n-3	10.6	(10.0-12.0)	11.4	(7.0-13.4)	0.715
C20:5n-3	2.8	(2.2-3.1)	2.6	(2.1-3.2)	0.715
C22:5n-3	2.7	(2.6-3.0)	3	(0.7-3.1)	0.715
C22:6n-3	5.1	(4.8-6.2)	5.7	(4.1-7.1)	0.715
MUFA					
C18:1	12	(11.6-13.1)	14.8	(14.5-17.7)	0.068
SFA	41.4	(41.2-41.5)	40.1	(39.3-41.4)	0.068
C16:0	27	(25.8-28.2)	29	(26.3-30.2)	0.144
C18:0	14.4	(13.3-15.5)	11.3	(10.6-13.9)	0.068
n-6/n-3-ratio	3.3	(2.9-3.6)	2.9	(2.4-5.2)	0.715
PUFA/SFA-ratio	1.1	(1.1-1.1)	1.1	(1.0-1.2)	0.273

[1]*p*-value from Wilcoxons Signed Rank Test.

5 DISCUSSION, CONCLUSION AND FUTURE REMARKS

The prevalence of overweight and obesity has increased over the past years (1), together with an observed decline in semen quality (2, 3). A BMI above the normal range (>24.9 kg/m^2) has been associated with an altered hormone balance and lowered semen quality, though affected semen quality parameters varies (4, 11) and results are conflicting (28). Dietary fat intake has shown an association with semen quality. The proportion of saturated fat had an inverse relation to sperm concentration and total sperm count in two recent studies (94, 95). Serum phospholipid fatty acid composition can be used as a marker of short-term dietary fat intake (134). Non-dietary aspects such as endogenous metabolism, genetics and other lifestyle factors must be considered when results from fatty acid analysis are interpreted, because they may affect the fatty acid composition (86). There are few studies on serum phospholipid fatty acid composition in men in relation to semen quality, and changes in both parameters after weight loss. Case-studies on semen quality before and after bariatric surgery with a following weight loss have described a temporarily worsening of semen quality for the first two years postoperative, but an improvement after 24 months is suggested (139, 140). A study of semen quality and reproductive hormones after lifestyle changes with following weight loss indicated an improvement of both parameters for severely obese men (6).

The general aim of the HiOA study is to investigate several aspects of overweight and obesity in men, and the effect on male reproduction function. The aim of this master study was establish a qualitative and quantitative method for serum phospholipid FAME analyses, and to compare the qualitative performance of FAME analyses on gas chromatography coupled with flame-ionization detector (GC-FID) and mass spectrometer (GC-MS). The established GC-FID method was used to analyze serum phospholipid FAME composition in men with varying BMI at baseline, and for a selection of participants after weight loss. Semen analysis for the participants had already been performed at HiOA or other collaborate laboratories. Semen quality data was used in this master study to investigate associations with BMI, and with serum phospholipid FAME compositions, at baseline. The serum phospholipid FAME composition and semen quality parameters at baseline were compared with results after weight loss for participants who lost <10 % or ≥10 % of their weight, or underwent bariatric surgery prior to weight loss.

5.1 Discussion of material and methods

5.1.1 Long term sample storage and fatty acid stability

Serum samples for participants in this study have been stored in -80 °C for a time period of maximum three years. Matthan et al. (2010) showed that the serum phospholipid fatty acid composition

measured one year after collection and after 8-10 years of storage in -80 °C was approximately the same. Observed differences were likely caused by technical improvements in GC methodology rather than sample degradation (75). Thus, degradation of sample material due to storage in this study cannot be excluded, but is not likely.

5.1.2 Recovery

Expected recovery reported for FAME analyses using sample preparation techniques based on the established Folch extraction method is between 80-100 % (oral communication with professor emeritus Hans J. Grav, April 15th 2013). Recovery of the internal standard in this study was 30-70 %. The poor recovery may result in loss of phospholipid fatty acids present in low quantities in serum. When a sample preparation method involves many steps, there are several factors that may contribute to loss of sample material. The Folch method is shown to yield 97 % of total lipids in the extraction. Depending of the water and inorganic salt present during the aqueous washing step, the more polar glycerophospholipids, such as phosphatidyl serine and phosphatidyl ethanolamine, are in some degree carried to the aqueous phase. Folch and coworkers stated that approximately 0.6 % were lost in the aqueous phase, and it is a selective loss, not proportional to the amount of different lipids groups present in original sample material (98).

The fractionation method used in this study is well-established and should in theory not lead to any significant loss of sample material. Agren et al. (1992) reported a recovery >98 % after solid phase extraction (141). Firl et al. (2012) evidenced a substantial co-elution of a phospholipid standard (PC C15:0) in the neutral lipid fraction when being eluted with chloroform/2-propanol (2:1, v/v), and recommended a reduced amount of 2-propanol or pure chloroform to avoid loss of phospholipids (142).

The acid-catalysed transmethylation of isolated phospholipid fatty acids was performed at room temperature overnight. In relevant literature it is stated that complete transmethylation with methanolic HCl requires heating, preferably a temperature of 50° C overnight (96). The low reaction temperature may have resulted in a lower percent of fatty acids transmethylated and contributed to the observed low recovery of the internal standard. Burdge et al. (2000) reported a recovery of a C17:0 standard added to serum prior to sample preparation of 74.2 %, with a RSD = 10.1 %. Burdge et al. used a sample preparation similar to the procedure used in this study, except for transmethylation with H_2SO_4 in methanol with heated incubation (143).

The recovery of FAMEs is not usually taken into account as long as an internal standard method is used for quantification (oral communication with prof. emeritus Hans J. Grav, April 15th 2013). As mentioned, low recovery involves a risk of losing low quantity fatty acids during sample preparation, and recovery should be determined when a method is developed and optimized as a part of the method quality control. All participant chromatograms showed a similar FAME profile, and the sample with

lowest recovery had the same number of detected FAMEs as the sample with the highest recovery. For statistical analysis a selected number of nine FAMEs detected in participant samples were regarded to equal 100 % to be able to compare FAME composition between subjects, without being affected by varying recovery.

The internal standard consists of a phosphatidyl choline containing two C17:0 fatty acid equivalents (1,2-diheptadecanoyl-sn-glycero-3-phosphatidylcholine). The different phospholipid classes have varying chemical properties, and in reality our internal standard only reflects the recovery of FAMEs from the phosphatidyl choline fraction in the sample material. The recovery of FAMEs from the other phospholipid classes is in practice not measured. Phosphatidyl choline is by far the most abundant of the different phosphatidyl fractions and this internal standard is widely used within the field of phospholipid fatty acid analyses. The use of several internal standards representing at least both phosphatidyl choline and phosphatidyl ethanolamine (the two largest fractions) should be evaluated.

5.1.3 Response factors

A common assumption when lipid analyses are performed with GC-FID is that the detectors relative responses to all FAMEs are equal (115). In theory, the number of CHO^+ ions produced when organic compounds are burned in the flame of H_2 and air, is proportional to the effective number of carbon atoms in the compound. Carbonyl carbons (R-COOH in fatty acids) are not detected by FID and not included in the effective carbon number (108). Figure 4.3 clearly illustrates this predicted detector response for C10:0 to C18:0. The theoretical increase in RRFs is shown to be reliable in several earlier studies, and reduced relative response factors for C20-C24 indicate a not fully optimized sample preparation or injection technique (96). The lack of an optimized sample handling results in a proportion of the more volatile FAMEs in the serum sample not being loaded on the analytical column. The decreasing RRF for FAMEs with increasing number of double bonds in Figure 4.4 is as expected, because carbon atoms participating in a double bond have a slightly lowered detector response compared to a carbon atom with no double bonds (107).

In this study the GC-FID method was completely calibrated and the accurate response factors for FAMEs were determined; hence the observed deviation from theoretical relative response factor did not affect the results.

5.1.4 Calibration and limits of detection and quantification

Since the GC-FID method was intended for quantitative purposes, a full calibration procedure was performed. The correlation coefficients (R^2) were >0.99 for all FAMEs except C20:1n-15, in accordance with or improved compared to published data (71). The method was calibrated for nine concentration levels covering a concentration range from approximately 8-200 µg/ml and GC-FID had a linear response over the entire concentration range examined.

After analyzing participant serum samples it was observed that FAME concentrations span over a large concentration range. To achieve precise quantification of all present phospholipid FAMEs it would be better to obtain calibration curves for two linear concentration ranges, for example 0.02-50.0 µg/ml and 50-200 µg/ml for GC-FID, and to add more than one internal standard. C21:0 is an example of a later eluting FAME that has been used for quantitative analyses and would improve quantification of FAMEs with a chain length of C20 and longer (115).

The GC-FID method was calibrated before samples were analyzed and recalibrated after eight weeks of analyzing to examine the within laboratory reproducibility of the calibration curve. Area ratios for FAMEs obtained at the two time points were compared with linear regression. The curves where area ratios for C20:1n-15, n-12 and n-9, C22:1n-9 and C22:2n-6 measured at the two time points were compared, had a slope significantly different from 1.0 at a 5 % level. At the two highest concentration levels fronting was observed, which led to a decreased separation of the three 20:1 peaks. Fronting probably caused the difference in area ratios because of small variations in integration of the five listed peaks between the two calibrations. Fronting is caused by decreased retention capacity in the stationary phase, for example by overloading the column, and should be avoided. Fronting give less symmetric peaks and for closely eluting peaks, decreased resolution (100). Peaks with fronting may lead to a greater quantitative uncertainty because of lower quality of peak integration. Integration for all concentration levels was manually controlled and approved. For the detected and quantified FAMEs in participant sera the quantitative quality was not affected by fronting, and the slope for the curves comparing area ratio at the two calibrations were not significantly different from 1.0. Intercept confidence intervals all contain the value 0.0 and are considered not significantly different between for the two calibrations.

Higher areas were measured for the same concentrations at the second calibration compared to the first. Five aliquots of the nine concentration levels of GLC #411 used for calibration were prepared at the same time, and the four remaining aliquots were stored in 100µl crimp vials at -80 °C until repeated calibration. Vaporization of hexane leading to increased concentration of the standard solution may be the cause of the larger areas measured. The vaporization theory was strengthened by a small storage experiment where aliquots of 1 µg/ml GLC #411 were stored in -20 °C and -80 °C for 30 days and compared with the same solution analyzed directly after preparation (appendix 9). The stored samples showed larger areas compared to the sample analyzed directly after preparation. Two improvements that will contribute to minimize vaporization problems are; 1) Prepare fresh concentration levels from stock solutions of standards for each calibration and 2) store stock solutions of standards in appropriate containers in -80 °C. All samples were analyzed the day after completed preparation and are not affected by vaporization due to storage.

Limits of detection and quantification

Limits of detection achieved in this master study is equal or improved compared to published results (115). The limit of detection (LOD) and quantification (LOQ) calculated for GC-FID was in general higher compared to LOD and LOQ calculated for MS, as depicted in Tables 4.4 and 4.5. The signal-to-noise ratio (S/N-ratio) was used for calculating LOD and LOQ. S/N-ratio for GC-FID was given by the ChemStation software, while S/N-ratio for GC-MS was manually calculated to be able to compare the two detectors. Results from comparing the two detectors may have been different if both S/N-ratios were calculated by the same software. MS in TIC-mode showed the lowest LOD and LOQ for FAMEs with a chain length up to C20, while FID showed lowest LOD and LOQ for C22-C24. S/N-ratio for the two MS modes TIC and SIM are both manually calculated and comparable, and SIM show the clearly lowest LOD and LOQ of the two, in accordance to published results (115). SIM was performed by monitoring three mass-to-charge ratios in the same analysis, so the calculated S/N-ratio would probably be higher, and the following LOD and LOQ lower, if only one *m/z*-value was monitored at the time. SIM mode showed enhancement of the signal-to-noise ratio and is recommended for quantitative analyses with MS based on the considerably lowered LOD and LOQ compared to GC-MS TIC and GC-FID.

Validating the GC-FID method

After calibrating a method the next step would be to analyze known concentrations of FAMEs to confirm that the calibration curve reports accurate calculated amounts. A typical control sample would be serum spiked with known concentrations of analytical fatty acid reference standards. The stability and accuracy of the method should be measured at each analysis sequence to confirm that the calibration curve is valid. Typically, solutions with low, intermediate and high concentration within the concentration range of the calibration curve would be used.

It was a challenge to find analytical standards with a quantitative quality. The standard solution used for calibration, GLC #411, is delivered from the manufacturer with a concentration >100 mg, and is per se not a quantitative standard. GC-FID is a stable, well-known and used method for analyses of fatty acids, with small variations in analytical performance over time. When fatty acid analysis with GC-FID is performed for research purposes and the analytical variations is under control, the use of control samples is not common practice within the field (referring to oral communication with prof. emeritus Hans J. Grav, April 15th 2013).

5.1.5 System performance

A satisfying separation of the FAMEs in the standard solution GLC #411 resulted in a long analysis time (76.5 min). Long analysis time leads to high retention factors (*k*), in this study from 1.06-15.22. A shorter analysis time can be achieved if two or more GC-methods are optimized for different fatty

acid chain lengths, for example focus on separation of C8-C18 or C20-C24 with two different methods or even two columns with varying resolution capabilities.

The theoretical plate number for C14:0 given by the column manufacturer is approximately 3000 N/column meter, which results in 180000 N. Plate number observed in this study is higher, at least for calibration level 1-7. Plate number is automatically calculated by the ChemStation software and the deviation from the expected may be due to the calculation method.

A resolution >1.5 is required for adequate quantitative results. All FAMEs in GLC #411 achieved a satisfying resolution except the closely eluting C20:1 n-15, n-12 and n-9, and C20:3n-3 and C24:0 for calibration levels 6-9. The decreased resolution is due to fronting, which occurred at the highest concentration levels for late eluting FAMEs. Fronting also led to an observed deviation from optimal peak symmetry. Fronting, and its influence on the quality of quantitation, are discussed in the previous section and were not considered to have a noticeable effect on the quantitative results obtained in this study.

5.1.6 Precision and methodological variation

After retention time locking the GC-FID method, five aliquots of a serum sample were analyzed. The calculated RSD for variation in retention times was 0.018 % at the most. This is higher than promised from the manufacturer, which state a RSD <0.008 %. The RSD % observed in this study is anyhow satisfactory and similar or improved compared to other published results (122).

The precision was determined by analyzing three replicates of an intermediate concentration of the standard solution GLC #411. Achieved analytical variation for area ratios with the GC-FID method was less than 1 % RSD. The precision is satisfactory and consistent with published data (115). Three replicates for determining precision may be inadequate and the analytical variation should be validated before analyzing additional participant samples.

The methodological repeatability was determined by preparing and analyzing five aliquots of the same serum sample. The RSD % for variation in area ratios was ≤8.5 %, which is satisfactory considering the manual sample preparation method, and it is consistent with published results on RSD % for repeated analyses (84).

5.1.7 External control of serum phospholipid fatty acid composition

Nine representative serum samples were analyzed at an external laboratory. Serum phospholipid fatty acid compositions were compared. A variation of maximum 4.0 % was observed for the proportion of a single FAME in an individual profile. Considering the methodological repeatability achieved in this study, the observed variation was accepted. Possible contributing factors to the varying results are not further investigated. Information on sample preparation methods, precision and recovery has been

requested from the laboratory that performed the external control, but a response is not received upon the deadline of this thesis. Knowledge of those factors is needed for a satisfying comparison of results.

5.1.8 GC-FID versus GC-MS for FAME analyses

GC-MS as a FAME identification tool

GC-MS provided multidimensional information about an analyte, both retention time and mass spectra were used for FAME identification. Spectra for all integrated peaks in GLC #411 were compared with common features and rules previously characterized (71, 122). All listed features matched with spectra obtained in this study except *m/z* 108 <107 for n-3 FAMEs with three or more double bonds, which showed to be the opposite for all analyzed n-3 FAMEs.

Four participant samples were analyzed with both GC-FID and GC-MS. The peak identified as C20:1n-9 by GC-FID, turned out to be contamination in all four samples analyzed with GC-MS. C20:1n-9 detected in participant samples was, based on this discovery, excluded from result calculations. In theory C20:3n-3 should elute before C20:4n-6 on a polar column such as BPX70 (96). The mass spectra of the two closely eluted peaks indicate that C20:4n-6 elutes between C20:3n-6 and C20:3n-3 and that was the order used in this study. This supports the advantage of GC-MS over GC-FID when analyzing FAMEs in complex sample materials.

GC-FID versus GC-MS for FAME analyses

GC-FID performance in this study confirms the well-known GC-FID hallmarks of a broad range of linear response, excellent retention time precision and a low LOD. Analyses of standards and serum samples with GC-MS show significant advantages considering identification of FAMEs and the ability to reveal possible contamination identified as FAMEs based on its retention time. Co-eluting FAMEs with different number of double bonds, varying from none to three, can easily be separated by their distinct base peaks. GC-MS also provide the ability to separate analyte peaks from contamination if they co-elute, and MS performed in SIM-mode results in a remarkable improvement in LOD compared to GC-FID.

Dodds et al. (2005) concluded that quantification with GC-MS demands appropriate calibration, but if these demands are fulfilled, GC-MS is the preferable alternative for FAME analyses compared to GC-FID (115). GC-MS was not fully exploited in this study, but the preliminary results support this conclusion.

5.2 Discussion of the analytical results

5.2.1 BMI in relation to semen quality

The use of BMI as a parameter to categorize participants as normal, overweight or obese is controversial (144). A large muscle mass may lead to BMI higher than the normal range. Participants placed in the wrong BMI-group based on their muscle mass could erroneously affect significant associations of overweight and obesity on semen quality. Percentage body fat and/or waist circumference should be registered to avoid this misplacement. All participants had their percentage body fat measured at each visit, and in Table 4.9 it is shown that percentage body fat significantly increases with increasing BMI, validating our use of BMI to categorize participants.

Several semen quality parameters were investigated for association with BMI after adjusting for age and abstinence time. The men were categorized into three groups based on their BMI. Obesity was negatively associated with semen volume, total sperm count, sperm concentration, the two motility parameters (percentage motile sperm and total progressive motility count), and the two morphology parameters (percentage normal morphology and total normal morphology count) compared to men with BMI within the normal range. Total sperm count and total progressive motility count were also negatively associated with an increase in BMI from the normal range to the overweight range. These findings partly corroborate results reported by Jensen et al. (25), where high BMI was associated with reduced total sperm count and sperm concentration, but not with motility and morphology. Hammoud et al. (26) report both decreased total sperm count and total progressive motility count in association with obesity, and they observed the same trend for percentage normal morphology, in consistency with findings in this study. Decreased semen volume and percentage sperm with normal morphology for obese men is also reported earlier (27, 30). A recent meta-analysis of BMI in relation to sperm count found that overweight and obesity were associated with decreased total sperm count, but not with sperm concentration (4). Aggerholm et al. (5) failed to show any significant differences in semen quality between BMI groups, but morphology was not reported in the study. The population investigated in the different studies mentioned here varies. Jensen et al. (25) included a younger population with a narrower age range (76 % were <20 years) and a lower average BMI (22.4 kg/m^2) compared to this study. Hammoud et al. (26) and Shayeb et al. (27) recruited men from a fertility clinic and results may not reflect semen quality in the general population, which is represented in this master study. The meta-analysis (4) excluded a high number of studies showing an inverse relationship between BMI and sperm parameters, which may have led to underestimation of the effect of BMI on semen quality.

Semen quality may be affected by other confounders than the two adjusted for in this study (age and abstinence time). Alcohol and smoking is known to have a negative effect on semen quality (145, 146) and should be adjusted for when investigating BMI and semen quality. A sedentary lifestyle is

negatively associated with sperm concentration and total sperm count (147). A sedentary lifestyle is also related to an increased BMI (1) and therefore may apply to lifestyle for overweight and obese participants in this study. Data on alcohol use and smoking habits were not available at the time when statistical analyses were performed, but are collected for all participants and should be adjusted for in further studies on semen quality.

Semen quality measurements involve a high uncertainty because of inter-observer variability. Semen quality also provides only limited information about the sperm function. Fertilization outcome may be assessed with other functional tests addressing sperm ability to fuse with and fertilize an egg cell.

5.2.2 Serum phospholipid FAME composition for men in three BMI groups

Dietary fat intake in the Western world today contains an increased n-6/n-3-ratio due to modern industrial food production and increased consumption of vegetable oils. The role of dietary fat in adult human obesity has been controversial, but recent findings suggest that PUFAs in the n-6 and n-3 series are not equally potent in promoting adipose tissue development, and a high n-6/n-3-ratio promote development of adipose tissue (148). Diets rich in saturated fat have shown to increase risk of achieving a BMI >25 kg/m^2 (149, 150). The same trends are found in this study when comparing serum phospholipid FAME composition (Table 4.14). Overweight and obese participants showed a higher proportion of C20:3n-6 and SFAs (mainly due to C18:0) compared to men with normal BMI. The obese participants also showed a decreased proportion of C22:5n-3 compared to men with normal BMI.

Participants enrolled in this study have not provided dietary data. Observed differences in serum phospholipid FAME composition may be related to both differences in dietary intake and/or metabolic differences between obese and normal weight participants. An altered estimated desaturase activity (enzymes participating in metabolism of fatty acids, Figure 1.11) has previously shown to be associated with obesity (151), and metabolic syndrome (86). Similar differences seen for the serum phospholipid FAME composition in this study were also shown in obese adolescents compared to age-matched lean controls, with a decrease in n-3 fatty acids and an increase in SFAs (152), which indicates that the observed variations are consistent with the development of obesity. Based on the differences for plasma fatty acid composition and desaturase activity observed for subjects with metabolic syndrome compared to non-metabolic syndrome controls (86), it would be interesting for further investigations to divide participants in this study after presence of metabolic syndrome and repeat the comparisons of serum phospholipid FAME composition.

5.2.3 Serum phospholipid FAME composition and semen quality

Men in this study showed a negative association between the proportion of serum phospholipid n-6 FAMEs and both sperm motility parameters and total normal sperm morphology count (Table 4.16-4.17). Sperm motility parameters also had an inverse association with the n-6/n-3-ratio. All three

motility parameters showed a positive relationship with the proportion of n-3 FAMEs, although percentage progressive motile sperm did not reach statistical significance (p=0.071). The association seemed mostly due to increasing amount of C22:5n-3.

The proportion of total SFAs was negatively associated with percentage sperm with percentage normal morphology and total normal morphology count. Percentage C18:0 was associated with a decrease in percentage progressively motile sperm (Table 4.16).

Percentage C18:2n-6 and C20:4n-6 presented opposite effect on semen volume. C18:2n-6 shows the weakest significance and may be due to multiple testing and not biological mechanisms, although the possibility cannot be ruled out (Table 4.15).

Motility patterns, and to some extent normal morphology, are shown to closely correlate the rate of natural pregnancy (153). It is not clear which mechanisms are involved in regulation of sperm motility or morphology, but several studies have shown a positive correlation between spermatozoa C22:6n-3 and the motility and morphology, and a negative association in between n-6/n-3-ratio and two semen quality parameters (67, 68). To our knowledge, there are only one study is reporting phospholipid fatty acid composition in serum, seminal plasma and spermatozoa membrane in relation to semen quality in normozoospermic vs. asthenozoospermic males (82). Conquer et al. (82) concluded that the two groups of men have similar serum phospholipid fatty acid composition of C22:6n-3, suggesting a similar dietary intake, while C22:6n-3 was lower in seminal plasma and spermatozoa of the asthenozoospermic males. A C22:6n-3 supplementation study was performed by the same research group, and supplementation did not affect C22:6n-3 incorporation in spermatozoa membrane or sperm motility (90). A study in rabbits showed that a diet rich in n-3 fatty acids led to rearrangements in sperm membrane fatty acid composition at a subcellular level (91), and a recent study in rats found that a balanced n-3/n-6-ratio of approximately 1.52 gave increased sperm concentration and sperm motility (93). A n-3/n-6-ratio of 1.52 equals a n-6/n-3-ratio of 0.7. Participants in this master study had a much higher n-6/n-3-ratio than 0.7 (~3), which in the rat study led to a decrease in both motility and concentration, and a tendency to increased sperm deformity rate. These findings are in agreement with semen quality results in this master study.

Two recent studies on dietary fat intake and semen quality showed that a high intake of saturated fat was associated with decreased sperm concentration and total sperm count (94, 95). Serum phospholipid SFAs were negatively associated with the two parameters in this study, but did not reach statistical significance (Table 4.15). The relationship between dietary intake of SFA and corresponding levels in serum phospholipids is weaker than for PUFAs (9). This may be the reason why this study did not reveal the same associations. The dietary studies also showed a positive relationship with intake of n-3 fatty acids and/or MUFAs and normal sperm morphology, supporting earlier findings (92), and the same trend was observed here. The correlations of MUFAs in diet and serum

phospholipids are even weaker than for SFAs; hence the observation might also be due to multiple testing.

There are several mechanisms in which food intake can affect semen quality, without necessarily being reflected in serum phospholipid fatty acids. Lipophilic environmental chemicals have been found to accumulate in high-fat food items, and this chemicals may have endocrine-disrupting functions and lead to a decline in semen quality (52). A high saturated fat intake from fat-rich dairy and meat processed products seen in a typical Scandinavian diet (94) may contribute to the observed decrease in semen quality. A healthy diet with a high intake of lettuce, tomatoes and some fruits is associated with increased semen quality (52, 154). Oxidative stress with increased ROS production and decreased antioxidant capacity in the testicular environment is associated with decreased sperm quality. The healthy diet described in papers (52, 154) and by the Norwegian Directory of Health (155) is consistent with an increased intake of antioxidants, and may have contributed to the higher semen quality observed for men in the normal BMI group. These theories are based on speculations, due to the lack of dietary data in this study.

5.2.4 The effect of weight loss

Participants were categorized after percentage weight loss (<10 % or ≥10 %) or bariatric surgery, and semen quality and serum phospholipid FAME composition were investigated for changes after weight loss. Results are listed in Table 4.18-4.24.

Semen quality

Semen quality at base line and after weight loss was compared within groups. Weight loss showed no significant effect on semen quality. The lack of significant results may be due to small groups (n=3-8). Furthermore, non-parametric statistic tests were used to compare results within groups. Non-parametric tests demand a greater effect to reach statistical significance compared to their corresponding parametric tests. I therefore may have failed in detecting actual differences between results at baseline and after weight loss.

Men in the three groups had different BMI at baseline; the low percentage weight loss group had a median BMI of 30.6 kg/m^2, the high percentage weight loss group had a median BMI of 36.0 kg/m^2 and participants who went through bariatric surgery had a median BMI of 49.4 kg/m^2. Men in the low percentage weight loss group were split between BMI group 2 and 3, while men who had a high percentage weight loss or bariatric surgery were all in BMI group 3. This may indicate that men who lost <10 % of their body weight had an overall better semen quality at baseline compared to men in the two other weight loss groups, when looking at semen quality compared for different BMI groups in Table 4.11. Semen quality for men with BMI categorized as normal and overweight showed little significant difference, and this may explain the lack of effect of weight loss on semen quality for men

in the low percentage weight loss group. BMI for men in the three groups after weight loss remained in the range categorized as overweight and obese, and may explain why there was no significant improvement in semen quality.

Four men in this study underwent bariatric surgery to achieve weight loss, while the remaining participants achieved weight loss by lifestyle changes only. Three case studies suggested that bariatric surgery and a following rapid weight loss give a severe worsening of semen quality in months after surgery (139, 140, 156). These findings were challenged in a study by Reis et al. (157), who found no decrease in semen quality in men experiencing weight loss after bariatric surgery. Sermondade et al. (139) observed improved semen quality for one of their reported cases 24 months after surgery, and Reis et al. (157) did not test semen quality until 20 months after surgery, so Reis' group might have missed out on detecting a temporarily worsening in semen quality for their participants. Studies have observed an improvement in the male hormone balance after weight loss due to bariatric surgery, with an increase in testosterone (158, 159) and a decrease in estradiol. The suggestion that weight loss after bariatric surgery lead to severe worsening of semen quality in the time period when participants in this study delivered their second semen sample (approximately 12 months after surgery), was not supported by findings in this master study. Participants did not show any obvious worsening of semen quality after bariatric surgery and following weight loss, but it was a small sample size, and further research in this field is required. In the HiOA study, participants who return after their bariatric surgery with following weight loss should be invited to a third sample delivery 24 months postoperative; to see if an improvement of semen quality is observed.

Serum phospholipid FAME composition

Men in the low percentage weight loss group presented a significantly increased proportion of n-3 FAMEs and a trend to decreased n-6/n-3 ratio after weight loss. Men in the high percentage weight loss group showed no significant changes in FAME composition, but a decreasing trend was observed for the proportion of SFAs (mostly due to a decrease in C16:0) after weight loss. The group of participants who went through bariatric surgery showed a decreasing trend for the proportion of PUFAs, n-6 FAMEs and SFAs. The proportion of C18:1 showed an increase, but none of the observed changes reached statistical significance.

The observed changes in serum phospholipid FAME composition are consistent with nutritional recommendations for a healthier lifestyle from The Norwegian Directory of Health (155). They define a healthier diet as increased intake of vegetables, fruits and berries, fish and whole grain, and a limited intake of processed meat, red meat, salt, sugar and saturated fat. It is likely that participants who have lost weight by lifestyle changes have been following these or similar recommendations to improve the quality of their diet and lose weight. Johnson and coworkers (160) observed that patients who have been through bariatric surgery had a reduced intake of vegetables and fish postoperative compared to

their diet before surgery. The same study presented that participants in a lifestyle intervention program showed a more favorable diet in general after a one year follow-up compared to bariatric patients (160).

The intra-individual variation of serum phospholipid FAME composition is not known for the participant group in this master study. The natural variation may be a contributing factor to the observed trends, more than a distinctively changed diet. Losing weight induces several lifestyle changes in addition to diet alterations. A sedentary lifestyle is associated with higher scrotal temperature, which may lead to decreased semen quality (147). A higher activity level related to a weight loss process may have a positive effect on semen quality (147). There is a well-established relationship between male obesity and an altered reproductive hormone profile (25) and this might be a contributor to the observed decreased semen quality associated with increasing BMI in this study. Whether the hormonal profile was improved by weight loss for the participants in this study is not known. Findings in a related study (6) may indicate that further weight loss to reach the normal BMI range is needed for normalization of hormone levels, and to see if the assumed negative hormone related effect on semen quality is reversed.

5.2.5 Statistics and selection bias

The major limitations in this study are the small sample size, especially the limited number of participants who lost weight, and the multiple statistical tests performed. The small sample size led to wide ranges for the results, and findings must therefore be interpreted with caution. With the number of statistical tests performed, there are chances of false significant results. With a significance level of 0.05, 5 % percent of tests performed can theoretically give a false positive result. Approximately 25 % of performed tests in this study resulted in a significant *p*-value, which exceeds the 5 % possibly false results. A solution to reduce the possibility of chance findings with multiple testing is to perform a Bonferroni correction. The Bonferroni correction method is considered highly conservative for large numbers of comparisons (161) and was not performed in this study. The low *p*-values and biologically plausible results strengthen the findings in this thesis, in spite of the multiple testing.

One cannot exclude a selection effect among the participants entering such a study; they may be interested in semen quality analysis because they have experienced trouble conceiving. This possible selection bias is however present for all participants, both normal weight, overweight and obese, and it is unlikely that it has contributed to the results presented in this thesis. The age difference observed between normal and overweight participants is unfortunate because semen quality is age dependent, and actions must be done to eliminate the age difference when recruiting more men. When semen quality was investigated in this study, all results were adjusted for age and are therefore valid despite the age bias.

5.3 Conclusion

The GC-FID method used for analyses of serum FAMEs in this study need to be further optimized. An observed deviation from results obtained by an external laboratory was within accepted variation, but a low recovery and deviating response factors indicate that the GC-method used in this study needs further improvements. The calculated response factors for FAMEs with chain lengths >C18:0 deviated from the expected, probably due to loss of more volatile FAMEs during transfer of sample from injection to the column inlet. The calibrated GC-FID method must be validated with the use of reference standards or other control sample material with known concentrations of fatty acids before analyzing more samples, and storage conditions for calibration standards must be optimized as well, preferably stored in appropriate containers in -80 °C. GC-MS provided a more secure identification of FAMEs, and a remarkably lower limit of detection compared to GC-FID, when SIM mode was applied.

The results presented in this study show a significant negative association between BMI and semen quality. Men with a BMI ≥30 kg/m^2 had significantly decreased semen volume, sperm concentration, total sperm count, total motility, total progressively motile sperm count, percentage normal morphology and total normal morphology count compared to a group of men with a BMI of 18.5-24.9 kg/m^2. Total sperm count and total progressively motile sperm count were significantly lowered for participants with a BMI in the overweight range (25.0-29.9 kg/m^2) as well, indicating that those two parameters are more sensitive to a small increase in BMI than the other mentioned semen quality parameters.

The serum phospholipid FAME composition was altered for men with a BMI categorized as overweight and obese compared to men with a normal BMI. The overweight and obese men presented a higher proportion of C20:3n-6 and SFAs, the latter mostly due to an increased proportion of C18:0, when they were compared with men in the normal BMI range. Obese men also had a significantly lower proportion of C22:5n-3 compared to men with a normal BMI.

Semen quality was investigated in relation to serum phospholipid FAME composition. The proportion of n-6 FAMEs was negatively related to sperm motility and normal sperm morphology parameters. An increasing n-6/n-3 ratio was inversely associated with sperm motility parameters and the same trend was observed for percentage sperm with normal morphology, without reaching statistical significance. The proportion of n-3 FAMEs showed a significantly positive association with sperm motility parameters, while the proportion of SFA showed a negative association normal sperm morphology.

A <10 % weight loss led to an increase in the proportion of n-3 FAMEs, and a trend to decreasing n-6/n-3 ratio. Losing ≥10.0 % weight by lifestyle changes was associated with a trend of decreasing

proportion of SFAs. An increasing trend was observed for C18:1, with a decreasing trend for the proportion of PUFAs, n-6 FAMEs and SFAs for the men who lost weight after bariatric surgery, without reaching statistical significance. Weight loss was not associated with any significant changes in semen quality for either of the weight loss groups. The lack of significant effects may be due to small groups and that participants remained in the overweight and obese BMI groups after weight loss.

This study supports earlier observations that being overweight and obese has a negative effect on semen quality. A high proportion of SFAs and n-6 FAMEs, and a high n-6/n-3 ratio in serum phospholipids seem to have a negative association with semen quality, especially sperm motility and normal morphology. Overweight and obese men showed a higher proportion of SFAs, and changes in single n-6 (increased) and n-3 (decreased) FAMEs, but a clear link between BMI, serum phospholipids FAMEs and semen quality was not established.

5.4 Future remarks

In further studies on the serum phospholipid FAME composition and semen quality, dividing overweight and obese men separated in groups with or without metabolic syndrome should be considered, due to observed variations in metabolic activity and semen quality compared to men without the syndrome (31, 86). It would be interesting to see if reversed metabolic syndrome after weight loss lead to an improvement in semen quality. Ideally, participants who lose weight should be followed further until they reach a stable BMI within the normal range to confirm if weight loss lead to improved semen quality and male reproduction function.

6 REFERENCES

1. World Health Organization. Fact sheet N°311 Obesity and overweight European region: World Health Organization; 2012 [cited 2012 1104]. Available from: http://www.who.int/mediacentre/factsheets/fs311/en/
2. Carlsen E, Giwercman A, Keiding N, Skakkebaek NE. Evidence for decreasing quality of semen during past 50 years. BMJ (Clinical research ed). 1992 Sep 12;305(6854):609-13. PubMed PMID: 1393072. Pubmed Central PMCID: PMC1883354. Epub 1992/09/12. eng.
3. Jorgensen N, Asklund C, Carlsen E, Skakkebaek NE. Coordinated European investigations of semen quality: results from studies of Scandinavian young men is a matter of concern. International journal of andrology. 2006 Feb;29(1):54-61; discussion 105-8. PubMed PMID: 16466524. Epub 2006/02/10. eng.
4. Sermondade N, Faure C, Fezeu L, Shayeb AG, Bonde JP, Jensen TK, et al. BMI in relation to sperm count: an updated systematic review and collaborative meta-analysis. Human reproduction update. 2013 Dec 12;19(3):221-31. PubMed PMID: 23242914.
5. Aggerholm AS, Thulstrup AM, Toft G, Ramlau-Hansen CH, Bonde JP. Is overweight a risk factor for reduced semen quality and altered serum sex hormone profile? Fertility and sterility. 2008 Sep;90(3):619-26. PubMed PMID: 18068160.
6. Hakonsen LB, Thulstrup AM, Aggerholm AS, Olsen J, Bonde JP, Andersen CY, et al. Does weight loss improve semen quality and reproductive hormones? Results from a cohort of severely obese men. Reproductive health. 2011;8:24. PubMed PMID: 21849026. Pubmed Central PMCID: 3177768. Epub 2011/08/19. eng.
7. Hammoud AO, Meikle AW, Reis LO, Gibson M, Peterson CM, Carrell DT. Obesity and male infertility: a practical approach. Seminars in reproductive medicine. 2012 Dec;30(6):486-95. PubMed PMID: 23074007. Epub 2012/10/18. eng.
8. Vucenik I, Stains JP. Obesity and cancer risk: evidence, mechanisms, and recommendations. Annals of the New York Academy of Sciences. 2012 Oct;1271:37-43. PubMed PMID: 23050962. Pubmed Central PMCID: PMC3476838. Epub 2012/10/12. eng.
9. Vessby B. Dietary fat, fatty acid composition in plasma and the metabolic syndrome. Current opinion in lipidology. 2003 Feb;14(1):15-9. PubMed PMID: 12544656.
10. Kaul K, Tarr JM, Ahmad SI, Kohner EM, Chibber R. Introduction to diabetes mellitus. Advances in experimental medicine and biology. 2012;771:1-11. PubMed PMID: 23393665. Epub 2013/02/09. eng.
11. Du Plessis SS, Cabler S, McAlister DA, Sabanegh E, Agarwal A. The effect of obesity on sperm disorders and male infertility. Nature reviews Urology. 2010 Mar;7(3):153-61. PubMed PMID: 20157305.
12. Buchwald H, Oien DM. Metabolic/bariatric surgery Worldwide 2008. Obesity surgery. 2009 Dec;19(12):1605-11. PubMed PMID: 19885707.
13. Hofso D, Nordstrand N, Johnson LK, Karlsen TI, Hager H, Jenssen T, et al. Obesity-related cardiovascular risk factors after weight loss: a clinical trial comparing gastric bypass surgery and intensive lifestyle intervention. European journal of endocrinology / European Federation of Endocrine Societies. 2010 Nov;163(5):735-45. PubMed PMID: 20798226. Pubmed Central PMCID: PMC2950661. Epub 2010/08/28. eng.
14. Ashrafian H, Athanasiou T, Li JV, Bueter M, Ahmed K, Nagpal K, et al. Diabetes resolution and hyperinsulinaemia after metabolic Roux-en-Y gastric bypass. Obesity reviews : an official journal of the International Association for the Study of Obesity. 2011 May;12(5):e257-72. PubMed PMID: 20880129. Epub 2010/10/01. eng.
15. Jungwirth A, Giwercman A, Tournaye H, Diemer T, Kopa Z, Dohle G, et al. European Association of Urology guidelines on Male Infertility: the 2012 update. European urology. 2012 Aug;62(2):324-32. PubMed PMID: 22591628. Epub 2012/05/18. eng.

16. World Health Organization. Health topics:Infertility European region: World Health Organization; 2012 [cited 2012 1609]. Available from: http://www.who.int/topics/infertility/en/.
17. Kocelak P, Chudek J, Naworska B, Bak-Sosnowska M, Kotlarz B, Mazurek M, et al. Psychological disturbances and quality of life in obese and infertile women and men. International journal of endocrinology. 2012;2012:236217. PubMed PMID: 22844280. Pubmed Central PMCID: 3403244. Epub 2012/07/31. eng.
18. Ramlau-Hansen CH, Thulstrup AM, Nohr EA, Bonde JP, Sorensen TI, Olsen J. Subfecundity in overweight and obese couples. Human reproduction (Oxford, England). 2007 Jun;22(6):1634-7. PubMed PMID: 17344224. Epub 2007/03/09. eng.
19. Jensen TK, Scheike T, Keiding N, Schaumburg I, Grandjean P. Fecundability in relation to body mass and menstrual cycle patterns. Epidemiology. 1999 Jul;10(4):422-8. PubMed PMID: 10401878. Epub 1999/07/13. eng.
20. Gesink Law DC, Maclehose RF, Longnecker MP. Obesity and time to pregnancy. Human reproduction (Oxford, England). 2007 Feb;22(2):414-20. PubMed PMID: 17095518. Pubmed Central PMCID: 1924918. Epub 2006/11/11. eng.
21. Rikshospitalet. Velkommen til Seksjon for barnløshet og assistert befruktning. In: Kvinneklinikken, editor.: Oslo University Hospital.
22. Norman RJ, Noakes M, Wu R, Davies MJ, Moran L, Wang JX. Improving reproductive performance in overweight/obese women with effective weight management. Human reproduction update. 2004 May-Jun;10(3):267-80. PubMed PMID: 15140873. Epub 2004/05/14. eng.
23. Sallmen M, Sandler DP, Hoppin JA, Blair A, Baird DD. Reduced fertility among overweight and obese men. Epidemiology. 2006 Sep;17(5):520-3. PubMed PMID: 16837825. Epub 2006/07/14. eng.
24. Nguyen RH, Wilcox AJ, Skjaerven R, Baird DD. Men's body mass index and infertility. Human reproduction (Oxford, England). 2007 Sep;22(9):2488-93. PubMed PMID: 17636282. Epub 2007/07/20. eng.
25. Jensen TK, Andersson AM, Jorgensen N, Andersen AG, Carlsen E, Petersen JH, et al. Body mass index in relation to semen quality and reproductive hormones among 1,558 Danish men. Fertility and sterility. 2004 Oct;82(4):863-70. PubMed PMID: 15482761. Epub 2004/10/16. eng.
26. Hammoud AO, Wilde N, Gibson M, Parks A, Carrell DT, Meikle AW. Male obesity and alteration in sperm parameters. Fertility and sterility. 2008 Dec;90(6):2222-5. PubMed PMID: 18178190. Epub 2008/01/08. eng.
27. Shayeb AG, Harrild K, Mathers E, Bhattacharya S. An exploration of the association between male body mass index and semen quality. Reproductive biomedicine online. 2011 Dec;23(6):717-23. PubMed PMID: 22019618. Epub 2011/10/25. eng.
28. MacDonald AA, Herbison GP, Showell M, Farquhar CM. The impact of body mass index on semen parameters and reproductive hormones in human males: a systematic review with meta-analysis. Human reproduction update. 2010 May-Jun;16(3):293-311. PubMed PMID: 19889752. Epub 2009/11/06. eng.
29. Pauli EM, Legro RS, Demers LM, Kunselman AR, Dodson WC, Lee PA. Diminished paternity and gonadal function with increasing obesity in men. Fertility and sterility. 2008 Aug;90(2):346-51. PubMed PMID: 18291378. Pubmed Central PMCID: 2597471. Epub 2008/02/23. eng.
30. Chavarro JE, Toth TL, Wright DL, Meeker JD, Hauser R. Body mass index in relation to semen quality, sperm DNA integrity, and serum reproductive hormone levels among men attending an infertility clinic. Fertility and sterility. 2010 May 1;93(7):2222-31. PubMed PMID: 19261274. Pubmed Central PMCID: 2864498. Epub 2009/03/06. eng.
31. Leisegang K, Udodong A, Bouic PJ, Henkel RR. Effect of the metabolic syndrome on male reproductive function: a case-controlled pilot study. Andrologia. 2012 Dec 28. PubMed PMID: 23278477. Epub 2013/01/03. Eng.
32. Peterson M. Male factors: Human Reproduction; 1997 [updated 2000; cited 2013 0405]. Available from: http://library.med.utah.edu/kw/human_reprod/seminars/seminar2B.html.

33. Dohle GR. Male infertility in cancer patients: Review of the literature. International journal of urology : official journal of the Japanese Urological Association. 2010 Apr;17(4):327-31. PubMed PMID: 20202000.
34. Baazeem A, Belzile E, Ciampi A, Dohle G, Jarvi K, Salonia A, et al. Varicocele and male factor infertility treatment: a new meta-analysis and review of the role of varicocele repair. European urology. 2011 Oct;60(4):796-808. PubMed PMID: 21733620. Epub 2011/07/08. eng.
35. Aitken RJ. Sperm function tests and fertility. International journal of andrology. 2006 Feb;29(1):69-75; discussion 105-8. PubMed PMID: 16466526.
36. Nicopoullos JD, Gilling-Smith C, Almeida PA, Homa S, Norman-Taylor JQ, Ramsay JW. Sperm DNA fragmentation in subfertile men: the effect on the outcome of intracytoplasmic sperm injection and correlation with sperm variables. BJU international. 2008 Jun;101(12):1553-60. PubMed PMID: 18294305. Epub 2008/02/26. eng.
37. Fariello RM, Pariz JR, Spaine DM, Cedenho AP, Bertolla RP, Fraietta R. Association between obesity and alteration of sperm DNA integrity and mitochondrial activity. BJU international. 2012 Sep;110(6):863-7. PubMed PMID: 22300410. Epub 2012/02/04. eng.
38. Kort HI, Massey JB, Elsner CW, Mitchell-Leef D, Shapiro DB, Witt MA, et al. Impact of body mass index values on sperm quantity and quality. Journal of andrology. 2006 May-Jun;27(3):450-2. PubMed PMID: 16339454. Epub 2005/12/13. eng.
39. De Marchi E, Baldassari F, Bononi A, Wieckowski MR, Pinton P. Oxidative Stress in Cardiovascular Diseases and Obesity: Role of p66Shc and Protein Kinase C. Oxidative medicine and cellular longevity. 2013;2013:564961. PubMed PMID: 23606925. Pubmed Central PMCID: PMC3625561. Epub 2013/04/23. eng.
40. Makker K, Agarwal A, Sharma R. Oxidative stress & male infertility. The Indian journal of medical research. 2009 Apr;129(4):357-67. PubMed PMID: 19535829. Epub 2009/06/19. eng.
41. Kasturi SS, Tannir J, Brannigan RE. The metabolic syndrome and male infertility. Journal of andrology. 2008 May-Jun;29(3):251-9. PubMed PMID: 18222914. Epub 2008/01/29. eng.
42. Flesch FM, Gadella BM. Dynamics of the mammalian sperm plasma membrane in the process of fertilization. Biochimica et Biophysica Acta. 2000;1469:197-235.
43. Saalu LC. The incriminating role of reactive oxygen species in idiopathic male infertility: an evidence based evaluation. Pakistan journal of biological sciences: PJBS. 2010 May 1;13(9):413-22. PubMed PMID: 20973394. Epub 2010/10/27. eng.
44. Agarwal A, Makker K, Sharma R. Clinical relevance of oxidative stress in male factor infertility: an update. American journal of reproductive immunology. 2008 Jan;59(1):2-11. PubMed PMID: 18154591. Epub 2007/12/25. eng.
45. Tortora GJ. The endocrine system. Introduction to the human body. 4th ed: Biological Sciences Textbooks; 1997. p. 287-320.
46. Kerr JB, Millar M, Maddocks S, Sharpe RM. Stage-dependent changes in spermatogenesis and Sertoli cells in relation to the onset of spermatogenic failure following withdrawal of testosterone. The Anatomical record. 1993 Apr;235(4):547-59. PubMed PMID: 8385423. Epub 1993/04/01. eng.
47. Kerr JB, Savage GN, Millar M, Sharpe RM. Response of the seminiferous epithelium of the rat testis to withdrawal of androgen: evidence for direct effect upon intercellular spaces associated with Sertoli cell junctional complexes. Cell and tissue research. 1993 Oct;274(1):153-61. PubMed PMID: 8242704. Epub 1993/10/01. eng.
48. Zavos P. Male Infertility [cited 2013 0510]. Available from: http://www.homefertility.com/mi.html.
49. Guyton AC, Hall JE. Reproductive and hormonal functions of the male. Textbook of medical physiology. 10th ed. USA: W.B. Saunders Company; 2001. p. 916-27.
50. Roth MY, Amory JK, Page ST. Treatment of male infertility secondary to morbid obesity. Nature clinical practice Endocrinology & metabolism. 2008 Jul;4(7):415-9. PubMed PMID: 18523426. Pubmed Central PMCID: PMC2664380. Epub 2008/06/05. eng.
51. Hammoud AO, Griffin J, Meikle AW, Gibson M, Peterson CM, Carrell DT. Association of aromatase (TTTAn) repeat polymorphism length and the relationship between obesity and decreased

sperm concentration. Human reproduction (Oxford, England). 2010 Dec;25(12):3146-51. PubMed PMID: 20881004. Epub 2010/10/01. eng.
52. Mendiola J, Torres-Cantero AM, Moreno-Grau JM, Ten J, Roca M, Moreno-Grau S, et al. Food intake and its relationship with semen quality: a case-control study. Fertility and sterility. 2009 Mar;91(3):812-8. PubMed PMID: 18314116.
53. Oliva A, Spira A, Multigner L. Contribution of environmental factors to the risk of male infertility. Human reproduction (Oxford, England). 2001 Aug;16(8):1768-76. PubMed PMID: 11473980. Epub 2001/07/28. eng.
54. Luboshitzky R, Lavie L, Shen-Orr Z, Herer P. Altered luteinizing hormone and testosterone secretion in middle-aged obese men with obstructive sleep apnea. Obesity research. 2005 Apr;13(4):780-6. PubMed PMID: 15897488. Epub 2005/05/18. eng.
55. Cabler S, Agarwal A, Flint M, du Plessis SS. Obesity: modern man's fertility nemesis. Asian journal of andrology. 2010 Jul;12(4):480-9. PubMed PMID: 20531281.
56. Hjollund NH, Bonde JP, Jensen TK, Olsen J. Diurnal scrotal skin temperature and semen quality. The Danish First Pregnancy Planner Study Team. International journal of andrology. 2000 Oct;23(5):309-18. PubMed PMID: 11012789.
57. Karila T, Hovatta O, Seppala T. Concomitant abuse of anabolic androgenic steroids and human chorionic gonadotrophin impairs spermatogenesis in power athletes. International journal of sports medicine. 2004 May;25(4):257-63. PubMed PMID: 15162244. Epub 2004/05/27. eng.
58. Jorgensen N, Joensen UN, Jensen TK, Jensen MB, Almstrup K, Olesen IA, et al. Human semen quality in the new millennium: a prospective cross-sectional population-based study of 4867 men. BMJ open. 2012;2(4). PubMed PMID: 22761286. Pubmed Central PMCID: PMC3391374. Epub 2012/07/05. eng.
59. Slama R, Eustache F, Ducot B, Jensen TK, Jørgensen N, Horte A, et al. Time to pregnancy and semen parameters: a cross-sectional study among fertile couples from four European cities. Human Reproduction. 2002 February 1, 2002;17(2):503-15.
60. Cooper TG, Noonan E, von Eckardstein S, Auger J, Baker HW, Behre HM, et al. World Health Organization reference values for human semen characteristics. Human reproduction update. 2010 May-Jun;16(3):231-45. PubMed PMID: 19934213. Epub 2009/11/26. eng.
61. World Health Organization. WHO Laboratory Manual for the Examination and Processing of Human Semen. 5th ed. Cambridge: Cambridge University Press; 2010.
62. Dietrichs E, Hurlen P, Toverud KC. Det mannlige kjønnsorgan. Den forunderlige kroppen. 5. ed. Oslo: Gyldendal; 2006. p. 68-9.
63. Encyclopædia Britannica Inc. Image Gallery: The Human Reproductive System. Encyclopædia Britannica Inc; 2013.
64. De Jonge C, Barratt C. The sperm cell. New York, USA: Cambridge University Press; 2006.
65. Alberts, Johnson, Lewis, Raff, Roberts, Walter. Sexual reproduction:Meiosis, germ cells and fertilization. Molecular biology of the cell. 5th ed. USA: Garland Science; 2008. p. 1269-304.
66. Lenzi A, Picardo M, Gandini L, Dondero F. Lipids of the sperm plasma membrane: from polyunsaturated fatty acids considered as markers of sperm function to possible scavenger therapy. Human reproduction update. 1996 May-Jun;2(3):246-56. PubMed PMID: 9079417.
67. Gulaya NM, Margitich VM, Govseeva NM, Klimashevsky VM, Gorpynchenko, II, Boyko MI. Phospholipid composition of human sperm and seminal plasma in relation to sperm fertility. Archives of andrology. 2001 May-Jun;46(3):169-75. PubMed PMID: 11339641. Epub 2001/05/08. eng.
68. Aksoy Y, Aksoy H, Altinkaynak K, Aydin HR, Ozkan A. Sperm fatty acid composition in subfertile men. Prostaglandins, leukotrienes, and essential fatty acids. 2006 Aug;75(2):75-9. PubMed PMID: 16893631. Epub 2006/08/09. eng.
69. Mathews CK, van Holde KE, Ahern KG. Lipids, membranes and cellular transport. Biochemistry. 3rd ed. San Fransisco, CA, USA: Addison Wesley Longman Inc.; 2000. p. 315-52.
70. Alberts B, Johnson A, Lewis J, Raff M, Roberts K, Walter P. Membrane structure. Molecular biology of the cell. 5th ed. USA: Garland Science; 2008. p. 617-50.

71. Sanchez-Avila N, Mata-Granados JM, Ruiz-Jimenez J, Luque de Castro MD. Fast, sensitive and highly discriminant gas chromatography-mass spectrometry method for profiling analysis of fatty acids in serum. Journal of chromatography A. 2009 Oct 2;1216(40):6864-72. PubMed PMID: 19729166.
72. Gurr MI, Harwood JL, Frayn KN. Fatty acid structure and metabolism. Lipid biochemistry. 5th ed. Oxford, UK: Blackwell publishing; 2005. p. 13-91.
73. McMurry J. Biomolecules: Lipids and their metabolism. Organic biochemistry with biological applications. 2nd ed. Canada: Cengage Learning; 2011. p. 936-86.
74. Hodson L, Skeaff CM, Fielding BA. Fatty acid composition of adipose tissue and blood in humans and its use as a biomarker of dietary intake. Progress in lipid research. 2008 Sep;47(5):348-80. PubMed PMID: 18435934. Epub 2008/04/26. eng.
75. Matthan NR, Ip B, Resteghini N, Ausman LM, Lichtenstein AH. Long-term fatty acid stability in human serum cholesteryl ester, triglyceride, and phospholipid fractions. Journal of lipid research. 2010 Sep;51(9):2826-32. PubMed PMID: 20448292. Pubmed Central PMCID: PMC2918465. Epub 2010/05/08. eng.
76. Ma J, Folsom AR, Eckfeldt JH, Lewis L, Chambless LE. Short- and long-term repeatability of fatty acid composition of human plasma phospholipids and cholesterol esters. The Atherosclerosis Risk in Communities (ARIC) Study Investigators. The American journal of clinical nutrition. 1995 Sep;62(3):572-8. PubMed PMID: 7661119. Epub 1995/09/01. eng.
77. Simopoulos AP. The importance of the ratio of omega-6/omega-3 essential fatty acids. Biomedicine & pharmacotherapy = Biomedecine & pharmacotherapie. 2002 Oct;56(8):365-79. PubMed PMID: 12442909. Epub 2002/11/22. eng.
78. Gurr MI, Harwood JL, Frayn KN. Dietary lipids. Lipid biochemistry. 5th ed. UK: Blackwell publishing; 2005. p. 127-68.
79. Mathews CK, Van Holde KE, Ahern KG. Lipid metabolism 1: Fatty acids, triacylglycerols and lipoproteins. Biochemistry. 3rd ed. USA: Addison Wesley Longman; 2000. p. 627-65.
80. Simopoulos AP. Genetic variants in the metabolism of omega-6 and omega-3 fatty acids: their role in the determination of nutritional requirements and chronic disease risk. Experimental biology and medicine (Maywood, NJ). 2010 Jul;235(7):785-95. PubMed PMID: 20558833. Epub 2010/06/19. eng.
81. Thiebaut AC, Rotival M, Gauthier E, Lenoir GM, Boutron-Ruault MC, Joulin V, et al. Correlation between serum phospholipid fatty acids and dietary intakes assessed a few years earlier. Nutrition and cancer. 2009;61(4):500-9. PubMed PMID: 19838922. Epub 2009/10/20. eng.
82. Conquer JA, Martin JB, Tummon I, Watson L, Tekpetey F. Fatty acid analysis of blood serum, seminal plasma, and spermatozoa of normozoospermic vs. asthenozoospermic males. Lipids. 1999 Aug;34(8):793-9. PubMed PMID: 10529089. Epub 1999/10/21. eng.
83. Fekete K, Marosvolgyi T, Jakobik V, Decsi T. Methods of assessment of n-3 long-chain polyunsaturated fatty acid status in humans: a systematic review. The American journal of clinical nutrition. 2009 Jun;89(6):2070S-84S. PubMed PMID: 19420097. Epub 2009/05/08. eng.
84. Seppanen-Laakso T, Laakso I, Hiltunen R. Analysis of fatty acids by gas chromatography, and its relevance to research on health and nutrition. Analytica Chimica Acta. 2002 Mar 29;465:39-62.
85. Hite AH. Food frequency questionnaires: Small associations and large errors. Nutrition (Burbank, Los Angeles County, Calif). 2013 Jun;29(6):925-6. PubMed PMID: 23660170. Epub 2013/05/11. eng.
86. Mayneris-Perxachs J, Guerendiain M, Castellote AI, Estruch R, Covas MI, Fito M, et al. Plasma fatty acid composition, estimated desaturase activities, and their relation with the metabolic syndrome in a population at high risk of cardiovascular disease. Clinical nutrition (Edinburgh, Scotland). 2013 Mar 28. PubMed PMID: 23591154. Epub 2013/04/18. Eng.
87. Tavilani H, Doosti M, Nourmohammadi I, Mahjub H, Vaisiraygani A, Salimi S, et al. Lipid composition of spermatozoa in normozoospermic and asthenozoospermic males. Prostaglandins, leukotrienes, and essential fatty acids. 2007 Jul;77(1):45-50. PubMed PMID: 17693070. Epub 2007/08/21. eng.

88. Tavilani H, Doosti M, Abdi K, Vaisiraygani A, Joshaghani HR. Decreased polyunsaturated and increased saturated fatty acid concentration in spermatozoa from asthenozoospermic males as compared with normozoospermic males. Andrologia. 2006 Oct;38(5):173-8. PubMed PMID: 16961570. Epub 2006/09/12. eng.
89. Zalata AA, Christophe AB, Depuydt CE, Schoonjans F, Comhaire FH. The fatty acid composition of phospholipids of spermatozoa from infertile patients. Molecular human reproduction. 1998 Feb;4(2):111-8. PubMed PMID: 9542967. Epub 1998/05/23. eng.
90. Conquer JA, Martin JB, Tummon I, Watson L, Tekpetey F. Effect of DHA supplementation on DHA status and sperm motility in asthenozoospermic males. Lipids. 2000 Feb;35(2):149-54. PubMed PMID: 10757545. Epub 2000/04/11. eng.
91. Mourvaki E, Cardinali R, Dal Bosco A, Corazzi L, Castellini C. Effects of flaxseed dietary supplementation on sperm quality and on lipid composition of sperm subfractions and prostatic granules in rabbit. Theriogenology. 2010 Mar 15;73(5):629-37. PubMed PMID: 20034660. Epub 2009/12/26. eng.
92. Safarinejad MR. Effect of omega-3 polyunsaturated fatty acid supplementation on semen profile and enzymatic anti-oxidant capacity of seminal plasma in infertile men with idiopathic oligoasthenoteratospermia: a double-blind, placebo-controlled, randomised study. Andrologia. 2009 Feb;43(1):38-47. PubMed PMID: 21219381. Epub 2011/01/12. eng.
93. Yan L, Bai XL, Fang ZF, Che LQ, Xu SY, Wu D. Effect of different dietary omega-3/omega-6 fatty acid ratios on reproduction in male rats. Lipids in health and disease. 2013 Mar 13;12(1):33. PubMed PMID: 23497018. Epub 2013/03/19. Eng.
94. Jensen TK, Heitmann BL, Jensen MB, Halldorsson TI, Andersson AM, Skakkebaek NE, et al. High dietary intake of saturated fat is associated with reduced semen quality among 701 young Danish men from the general population. The American journal of clinical nutrition. 2013 Feb;97(2):411-8. PubMed PMID: 23269819.
95. Attaman JA, Toth TL, Furtado J, Campos H, Hauser R, Chavarro JE. Dietary fat and semen quality among men attending a fertility clinic. Human reproduction (Oxford, England). 2012 May;27(5):1466-74. PubMed PMID: 22416013. Pubmed Central PMCID: 3329193. Epub 2012/03/15. eng.
96. Eder K. Gas chromatographic analysis of fatty acid methyl esters. Journal of chromatography B, Biomedical applications. 1995 Sep 15;671(1-2):113-31. PubMed PMID: 8520689. Epub 1995/09/15. eng.
97. Folch J, Lees M, Sloane Stanley G. A simple method for the isolation and purification of total lipides from animal tissues. J Biol Chem. 1957;226(1):497-509.
98. Nelson GJ. Isolation and purification of lipids from animal tissue. Analysis of lipids and lipoproteins. 1975:1-22.
99. Kaluzny MA, Duncan LA, Merritt MV, Epps DE. Rapid separation of lipid classes in high yield and purity using bonded phase columns. Journal of lipid research. 1985 Jan;26(1):135-40. PubMed PMID: 3973509. Epub 1985/01/01. eng.
100. Braithwaite A, Smith FJ. Theoretical considerations. Chromatographic methods. 5th ed. The Netherlands: Kluwer Academic Publishers; 1999. p. 17-43.
101. Hoshi M, Williams M, Kishimoto Y. Esterification of fatty acids at room temperature by chloroform-methanolic HCl-cupric acetate. Journal of lipid research. 1973 Sep;14(5):599-601. PubMed PMID: 4729977. Epub 1973/09/01. eng.
102. Christie WW. Preparation of ester derivatives of fatty acids for chromatographic analysis: The AOCS Lipid Library; [cited 2012 1129]. Available from: http://lipidlibrary.aocs.org/topics/ester_93/index.htm#B.
103. Greibrokk T, Lundanes E, Rasmussen KE. Gasskromatografi. Kromatografi. 3rd ed. Norway: Universitetsforlaget; 1994.
104. Harris DC. Introduction to analytical separations. Quantitative chemical analysis. 7th ed. USA: W.H. Freeman and company; 2007. p. 501-27.

105. Sparkman OD, Penton ZE, Kitson FG. Gas chromatography. Gas chromatography and mass spectrometry, a practical guide. 2nd ed. Oxford, UK: Elsevier Inc.; 2011. p. 15-79.
106. TutorVista. Chromatography: TutorVista.com; 2010 [cited 2013 0323]. Available from: http://chemistry.tutorvista.com/analytical-chemistry/chromotography.html.
107. Braithwaite A, Smith FJ. Gas chromatography. Chromatographic methods. 5th ed. The Netherlands: Kluwer academic publishers; 1999. p. 165-257.
108. Harris DC. Gas chromatography. Quantitative chemical analysis. 7th ed. USA: W.H. Freeman and company; 2007. p. 528-55.
109. Sheffield Hallam University. Gas chromatography [cited 2013 0323]. Available from: http://teaching.shu.ac.uk/hwb/chemistry/tutorials/chrom/gaschrm.htm.
110. Technologies A. Guard columns or retention gap: Agilent Technologies; [cited 2012 0311]. Available from: http://www.chem.agilent.com/cag/cabu/guardcolretgap.htm.
111. Agilent Technologies. Capillary GC columns: Agilent; [cited 2013 0323]. Available from: http://www.chem.agilent.com/cag/cabu/capgccols.htm.
112. SGE Analytical Science. BPX High Performance Capillary Columns: SGE Analytical Science; [cited 2013 0324]. Available from: http://www.sge.com/support/training/columns/bpx---high-performance/high-temp/bpx-high-performance-capillary-columns.
113. Sire J. Molekylorbitaler og kovalent binding. Chemica. 2nd ed. Norway: Vigmostad og Bjørke AS; 1998. p. 411-33.
114. SGE Analytical Science. GC columns - BPX70: SGE Analytical Science; [cited 2013 0324]. Available from: http://www.sge.com/products/columns/gc-columns/bpx70.
115. Dodds ED, McCoy MR, Rea LD, Kennish JM. Gas chromatographic quantification of fatty acid methyl esters: flame ionization detection vs. electron impact mass spectrometry. Lipids. 2005 Apr;40(4):419-28. PubMed PMID: 16028722. Epub 2005/07/21. eng.
116. Giarrocco V, Quimby B, Klee M. Retention Time Locking: Concepts and Applications. DE, USA: 1997.
117. Sparkman OD, Penton ZE, Kitson FG. The fundamentals of GC/MS. Gas chromatography and mass spectrometry, a practical guide. 2nd ed. Oxford, UK: Elsevier Inc; 2011. p. 1-12.
118. Harris DC. Mass spectrometry. Quantitative chemical analysis. 7th ed. USA: W.H. Freeman and company; 2007. p. 474-500.
119. Sparkman OD. Mass spectrometry instrumentation. Gas chromatography and mass spectrometry, a practical guide. 2nd ed. Oxford, UK: Elsevier Inc; 2011. p. 89-148.
120. Sparkman OD. Mass spectral data interpretation. Gas chromatography and mass spectrometry, a practical guide. Oxford, UK: Elsevier Inc.; 2011. p. 149-206.
121. Christie WW. Methyl Esters - Archive of Mass Spectra: The AOCS Lipid Library; 2012 [cited 2013 0324]. Available from: http://lipidlibrary.aocs.org/ms/arch_me/me_sat/M0016.htm.
122. Hartig C. Rapid identification of fatty acid methyl esters using a multidimensional gas chromatography-mass spectrometry database. Journal of chromatography A. 2008 Jan 4;1177(1):159-69. PubMed PMID: 18037421.
123. Sparkman OD. Quantitation with GC/MS Gas chromatography and mass spectrometry, a practical guide. 2nd ed. Oxford, UK: Elsevier Inc.; 2011. p. 207-18.
124. Harris DC. Quality assurance and calibration methods. Quantitative chemical analysis. 7th ed. USA: W.H. Freeman and company; 2007. p. 78-95.
125. Dolan J. Back-To-Basics #1: Retention Factor: SeparationScience; 2012 [cited 2013 0208]. Available from: http://www.sepscience.com/Techniques/LC/Articles/314-/HPLC-Solutions-28-Back-to-Basics-1-Retention-Factor.
126. Christie WW. Gas chromatography: Theoretical aspects and instrumentation [cited 2012 1025]. Available from: http://lipidlibrary.aocs.org/gc_lipid/03_theor/index.htm.
127. Agilent Technologies Inc. Evaluating system suitability. Agilent ChemStation-understanding your ChemStation. 7th ed: Agilent Technologies; 2009.
128. Agilent Technologies Inc. Quantification. Agilent ChemStation-understanding your ChemStation. 7th ed: Agilent Technologies Inc; 2009.

129. Reis LO, Dias FG. Male fertility, obesity, and bariatric surgery. Reproductive sciences. 2012 Aug;19(8):778-85. PubMed PMID: 22534334. Epub 2012/04/27. eng.
130. Ministry of Health and Care Services. Helseforskningsloven 2008 [cited 2012 1014]. Available from: http://lovdata.no/cgi-wift/wiftldles?doc=/app/gratis/www/docroot/all/nl-20080620-044.html&emne=helse*&&.
131. Ministry of Education and Research. Forskningsetikkloven 2006 [cited 2012 1015]. Available from: http://lovdata.no/cgi-wift/wiftldles?doc=/app/gratis/www/docroot/all/nl-20060630-056.html&emne=forskningsetikk*&.
132. World Health Organization. WHO Laboratory Manual for the Examination of Human Semen and Sperm-Cervical Mucus Interaction. 4th ed. Cambridge: Cambridge University Press; 1999 May.
133. Barratt CLR, Björndahl L, Menkveld R, Mortimer D. ESHRE special interest group for andrology basic semen analysis course: a continued focus on accuracy, quality, efficiency and clinical relevance. Human Reproduction. 2011 September 28, 2011.
134. Arab L, Akbar J. Biomarkers and the measurement of fatty acids. Public health nutrition. 2002 Dec;5(6A):865-71. PubMed PMID: 12638594. Epub 2003/03/18. eng.
135. Almendingen K, Hostmark AT, Fausa O, Mosdol A, Aabakken L, Vatn MH. Familial adenomatous polyposis patients have high levels of arachidonic acid and docosahexaenoic acid and low levels of linoleic acid and alpha-linolenic acid in serum phospholipids. International journal of cancer Journal international du cancer. 2007 Feb 1;120(3):632-7. PubMed PMID: 17096349. Epub 2006/11/11. eng.
136. Levitas E, Lunenfeld E, Weiss N, Friger M, Har-Vardi I, Koifman A, et al. Relationship between the duration of sexual abstinence and semen quality: analysis of 9,489 semen samples. Fertility and sterility. 2005 Jun;83(6):1680-6. PubMed PMID: 15950636.
137. Levitas E, Lunenfeld E, Weisz N, Friger M, Potashnik G. Relationship between age and semen parameters in men with normal sperm concentration: analysis of 6022 semen samples. Andrologia. 2007 Apr;39(2):45-50. PubMed PMID: 17430422.
138. Bjørndal A, Hofoss H. Statistikk for helse- og sosialfagene. 3rd ed. Norway: Gyldendal Akademisk; 2008.
139. Sermondade N, Massin N, Boitrelle F, Pfeffer J, Eustache F, Sifer C, et al. Sperm parameters and male fertility after bariatric surgery: three case series. Reproductive biomedicine online. 2012 Feb;24(2):206-10. PubMed PMID: 22196889. Epub 2011/12/27. eng.
140. Lazaros L, Hatzi E, Markoula S, Takenaka A, Sofikitis N, Zikopoulos K, et al. Dramatic reduction in sperm parameters following bariatric surgery: report of two cases. Andrologia. 2012 Apr 28. PubMed PMID: 22540334. Epub 2012/05/01. Eng.
141. Agren JJ, Julkunen A, Penttila I. Rapid separation of serum lipids for fatty acid analysis by a single aminopropyl column. Journal of lipid research. 1992 Dec;33(12):1871-6. PubMed PMID: 1479296. Epub 1992/12/01. eng.
142. Firl N, Kienberger H, Hauser T, Rychlik M. Determination of the fatty acid profile of neutral lipids, free fatty acids and phospholipids in human plasma. Clinical chemistry and laboratory medicine : CCLM / FESCC. 2013 Apr;51(4):799-810. PubMed PMID: 23006900. Epub 2012/09/26. eng.
143. Burdge GC, Wright P, Jones AE, Wootton SA. A method for separation of phosphatidylcholine, triacylglycerol, non-esterified fatty acids and cholesterol esters from plasma by solid-phase extraction. The British journal of nutrition. 2000 Nov;84(5):781-7. PubMed PMID: 11177194. Epub 2001/02/15. eng.
144. Bergman RN, Stefanovski D, Buchanan TA, Sumner AE, Reynolds JC, Sebring NG, et al. A better index of body adiposity. Obesity (Silver Spring, Md). 2011 May;19(5):1083-9. PubMed PMID: 21372804. Pubmed Central PMCID: PMC3275633. Epub 2011/03/05. eng.
145. La Vignera S, Condorelli RA, Balercia G, Vicari E, Calogero AE. Does alcohol have any effect on male reproductive function? A review of literature. Asian journal of andrology. 2013 Mar;15(2):221-5. PubMed PMID: 23274392. Epub 2013/01/01. eng.

146. Ramlau-Hansen CH, Thulstrup AM, Aggerholm AS, Jensen MS, Toft G, Bonde JP. Is smoking a risk factor for decreased semen quality? A cross-sectional analysis. Human reproduction (Oxford, England). 2007 Jan;22(1):188-96. PubMed PMID: 16966350.
147. Gaskins AJ, Mendiola J, Afeiche M, Jorgensen N, Swan SH, Chavarro JE. Physical activity and television watching in relation to semen quality in young men. British journal of sports medicine. 2013 Feb 4. PubMed PMID: 23380634. Epub 2013/02/06. Eng.
148. Ailhaud G, Massiera F, Weill P, Legrand P, Alessandri JM, Guesnet P. Temporal changes in dietary fats: role of n-6 polyunsaturated fatty acids in excessive adipose tissue development and relationship to obesity. Progress in lipid research. 2006 May;45(3):203-36. PubMed PMID: 16516300.
149. Phillips CM, Kesse-Guyot E, McManus R, Hercberg S, Lairon D, Planells R, et al. High dietary saturated fat intake accentuates obesity risk associated with the fat mass and obesity-associated gene in adults. The Journal of nutrition. 2012 May;142(5):824-31. PubMed PMID: 22457394. Epub 2012/03/30. eng.
150. Pan DA, Hulbert AJ, Storlien LH. Dietary fats, membrane phospholipids and obesity. The Journal of nutrition. 1994 Sep;124(9):1555-65. PubMed PMID: 8089723. Epub 1994/09/01. eng.
151. Warensjo E, Ohrvall M, Vessby B. Fatty acid composition and estimated desaturase activities are associated with obesity and lifestyle variables in men and women. Nutrition, metabolism, and cardiovascular diseases : NMCD. 2006 Mar;16(2):128-36. PubMed PMID: 16487913.
152. Karlsson M, Marild S, Brandberg J, Lonn L, Friberg P, Strandvik B. Serum phospholipid fatty acids, adipose tissue, and metabolic markers in obese adolescents. Obesity (Silver Spring, Md). 2006 Nov;14(11):1931-9. PubMed PMID: 17135608. Epub 2006/12/01. eng.
153. Mortimer D, Pandya IJ, Sawers RS. Relationship between human sperm motility characteristics and sperm penetration into human cervical mucus in vitro. Journal of reproduction and fertility. 1986 Sep;78(1):93-102. PubMed PMID: 3761279. Epub 1986/09/01. eng.
154. Gaskins AJ, Colaci DS, Mendiola J, Swan SH, Chavarro JE. Dietary patterns and semen quality in young men. Human reproduction (Oxford, England). 2012 Oct;27(10):2899-907. PubMed PMID: 22888168. Pubmed Central PMCID: PMC3442634. Epub 2012/08/14. eng.
155. The Norwegian Directory of Health. Kostholdsråd 2011 [cited 2013 0504]. Available from: http://helsedirektoratet.no/folkehelse/ernering/kostholdsrad/Sider/default.aspx.
156. di Frega AS, Dale B, Di Matteo L, Wilding M. Secondary male factor infertility after Roux-en-Y gastric bypass for morbid obesity: case report. Human reproduction (Oxford, England). 2005 Apr;20(4):997-8. PubMed PMID: 15618249. Epub 2004/12/25. eng.
157. Reis LO, Zani EL, Saad RD, Chaim EA, de Oliveira LC, Fregonesi A. Bariatric Surgery Does not Interfere With Sperm Quality—A Preliminary Long-Term Study. Reproductive sciences. 2012 October 1, 2012;19(10):1057-62.
158. Hammoud A, Gibson M, Hunt SC, Adams TD, Carrell DT, Kolotkin RL, et al. Effect of Roux-en-Y gastric bypass surgery on the sex steroids and quality of life in obese men. The Journal of clinical endocrinology and metabolism. 2009 Apr;94(4):1329-32. PubMed PMID: 19174499. Pubmed Central PMCID: PMC2682482. Epub 2009/01/29. eng.
159. Woodard G, Ahmed S, Podelski V, Hernandez-Boussard T, Presti J, Jr., Morton JM. Effect of Roux-en-Y gastric bypass on testosterone and prostate-specific antigen. The British journal of surgery. 2012 May;99(5):693-8. PubMed PMID: 22302466. Epub 2012/02/04. eng.
160. Johnson LK, Andersen LF, Hofso D, Aasheim ET, Holven KB, Sandbu R, et al. Dietary changes in obese patients undergoing gastric bypass or lifestyle intervention: a clinical trial. The British journal of nutrition. 2012 Oct 30:1-8. PubMed PMID: 23110916. Epub 2012/11/01. Eng.
161. Altman D. Practical statistics for medical research. USA: CRC Press; 1999.

7 APPENDIX

List of appendixes

Appendix 1	Equipment, reagents, chemicals and commercial stock standard solutions
Appendix 2	Stepwise procedure for sample preparation of serum phospholipid fatty acids
Appendix 3	Contents of the commercial stock standard solution GLC #411 (Nu-ChekPrep, USA)
Appendix 4	Conversion of FAME results to FAME equivalents in serum
Appendix 5	System performance for GC-FID analysis of GLC #411 FAMEs
Appendix 6	Mass spectra for peaks representing the use of expected features for identification, and TIC and EIC displaying an unexpected elution order for C20:3 and C20:4
Appendix 7	Calibration curves obtained with GC-FID at two different time points
Appendix 8	External control of results from serum phospholipid FAME analyses
Appendix 9	Storage of standard solutions

Appendix 1: Equipment, reagents, chemicals and commercial stock standard solutions

Equipment

Equipment with supplier and ordering information, sorted by supplier.

Product name	Supplier	Ordering Information
7693A Automatic Liquid Sampler	Agilent Technologies	
7890A GC System	Agilent Technologies	
BPX70 GC Column	SGE Analytical Science	Part No: 054623
ThermoQuest Trace GC-MS	Thermo Scientific	
TriPlus Autosampler	Thermo Scientific	
Aluminum crimp cap fitted with a pre-cut blue silicone/PTFE seal.	Chromacol, Thermo Fisher Scientific	Part No. 8-AC-ST101
Crimp Top Round Bottom Vial 100 µl - Clear Gold Grade	Chromacol, Thermo Fisher Scientific	Part No. 01-CVG
Hand crimper for 8mm crimp caps.	Chromacol, Thermo Fisher Scientific	Part No. CR-8
9 inch Pasteur Pipets, Disposable, Bulk Pack, Non-Sterile, Unplugged	Corning®	Product No. 7095D-9
MICROLITER Syringe, model 710	Hamilton®	Part No. 7638-01
Disposable Glass Serological Pipets, Disposable, TD, Bulk Pack, Non-Sterile, Unplugged	Pyrex®, Corning®	Cat. No. 7079-1N
Quickfit® Ground socket conical	Pyrex®, SciLabware	Item No. BC24/C14T
Quickfit® Ground socket cylindrical	Pyrex®, SciLabware	Item No. MF24/1/5
Quickfit® Hollow-blown glass stopper B-length	Pyrex®, SciLabware	Item No. SB14
Quickfit® Hollow-blown glass stopper C-length	Pyrex®, SciLabware	Item No. 2595/03M
Supelclean™ LC-NH2 SPE Tube	Supelco, Sigma-Aldrich®	SKU 504483
Visidry™ Drying Attachment for use with Visiprep 12-port model	Supelco, Sigma-Aldrich®	SKU 57100-U
Visiprep™ SPE Vacuum Manifold, 12-port model	Supelco, Sigma-Aldrich®	SKU 57030-U

Reagents

Chloroform/methanol 2:1 (v/v)

Reagents

Chloroform, MERCK (Art.No. 1.02432.2500)

Methanol, Sigma-Aldrich (SKU 32213N)

Procedure

Components volumes and amounts to make chloroform/methanol 2:1

Components	Amount
Chloroform	600 ml
Methanol	300 ml

1. Measure 300 ml methanol
2. Add 600 ml chloroform
3. Store the mixture in 4-6 °C.

Chloroform/2-propanol 2:1 (v/v)

Reagents

Chloroform, MERCK (Art.No. 1.02432.2500)

2-propanol, Fluka Analytical (SKU 34965)

Procedure

Components volumes and amounts to make chloroform/2-propanol 2:1

Components	Amount
Chloroform	150 ml
2-propanol	75 ml

1. Measure 150 ml chloroform
2. Add 75 ml 2-propanol
3. Store the mixture in 4-6 °C

6 % Sodium bicarbonate

Reagents

Sodium bicarbonate, Sigma-Aldrich (SKU S5761)

Distilled water

Procedure

Components volumes and amounts to make 6 % sodium bicarbonate

Components	Amount
Sodium bicarbonate	30 g
Distilled water	470 ml

1. Scale in 30 g of sodium bicarbonate
2. Add 470 ml of distilled and mix well to get an homogenous solution
3. Store in room temperature.

2 % acetic acid in diethyl ether

Reagents

Diethyl ether, MERCK (Art.No. 1.00921.1000)

Glacial acetic acid, MERCK (Art.No. 8.18755.1000)

Procedure

Components volumes and amounts to make 2 % acetic acid in diethyl ether

Components	Amount
Diethyl ether	98 ml
Glacial acetic acid	2 ml

1. Measure up 98 ml of diethyl ether
2. Add 2 ml of glacial acetic acid
3. Store in 4-6 °C

Chemicals

Chemicals and reagents with supplier and ordering information, sorted alphabetically.

Chemical	Supplier	Ordering information
2,2-dimethoxypropane	Sigma-Aldrich®	SKU D136808
2-propanol	Fluka Analytical	SKU 34965
3M Metanolic HCl	Sigma-Aldrich®	SKU 33050-U
Acetone	Sigma-Aldrich®	SKU 32201N
Benzene	Sigma-Aldrich®	SKU 270709
Butylated hydroxytoluen 1 % in ethanol (BHT)	AppliChem	A1874.0010
Chloroform	MERCK	Art.No. 1.02432.2500
Diethyl ether	MERCK	Art.No. 1.00921.1000
Glacial acetic acid	MERCK	Art.No. 8.18755.1000
Hydrochloric acid Fuming Min. 37 %	MERCK	Art.No. 1.00317.9200
Methanol	MERCK	Art.No. 1.06011.2500
n-Hexane SupraSolv®	MERCK	Art.No.1.04371.2500
Sodium bicarbonate, BioXtra, 99.5-100.5 %	Sigma-Aldrich®	SKU S6297

Commercial stock standard solutions

Standard solution	Supplier	Ordering information
GLC #411	Nu-Chek-Prep	GLC-411
Methyl heptadecanoate (C17:0)	Fluka	51633-1G
1,2-Diheptadecanoyl-sn-Glycero (ISTD)	Larodan	37-1700-9
cis-5,8,11,14,17-eicosapentaenoic acid ME	Supelco	47571-U
Methyl cis-7,10,13,16,19-docosapentaenoate	Supelco	47563-U

Appendix 2: Stepwise procedure for sample preparation of serum phospholipid fatty acids

Lipid extraction:

1. Thaw serum samples in 4-6 °C.
2. Add 4 ml of chloroform/methanol (2:1, v/v) to conical test tubes.
3. Add 15 µl BHT 1 % in ethanol (antioxidant).
4. Add 30 µl ISTD and then 200 µl of a serum sample to each tube except the reagents blank.
5. Vortex for 30 sec and incubate in room temperature on bench for 30 min.
6. Add 800 µl 0.9 % NaCl and vortex for 30 sec at 1000...
7. Incubate at room temperature on bench for 10 min.
8. Centrifuge for 5 min at 2000 rpm.
9. Transfer the lower chloroform phase to new round test tubes and damp to dryness under a stream of N_2.
10. Dissolve in 300 µl chloroform and vortex for 20 sec.

Solid phase extraction (SPE):

1. Remove the needles from the Visidry attachment and place SPE columns on the Vacuum Manifold lid. Use low vacuum throughout the protocol.
2. Wash columns with 4x1 ml hexane.
3. Transfer the 200 µl sample to the columns, leave 100 µl in the test tube on ice for transmethylation.
4. Wash columns with 4x0.2 ml chloroform.
5. Elute neutral lipids with 4x1 ml chloroform/2-propanol (2:1).
6. Elute free fatty acids with 4x1 ml diethyl ether containing 2 % acetic acid.
7. Elute phospholipids into new round test tubes with 4x1 ml methanol.

Transmethylation

-both test tubes with separated phospholipids and total lipids:

1. Vaporize the phospholipid phase until dryness under N_2.
2. Add 1 ml benzene, 200 µl dimetoxy propane and 2 ml 3 M methanolic HCl in that order.
3. Vortex
4. Leave samples dark overnight in room temperature.

∞

5. Neutralize solutions by adding 4 ml $NaHCO_3$ resolved in destilled water. Vortex carefully, but thoroughly with the stopper losely fitted, be aware of gas. Tilt the test tubes until gas formation is over.
6. Extract phospholipids by adding 2 ml of n-hexane and tilt the tubes ten times.
7. Centrifuge samples for 3 min at 15 % U/min.
8. Transfer the lipid phase to new round tubes and place tubes under N_2.
9. Repeat point 5-7 three times to a total extraction volume of 6 ml and vaporize under N_2 until dryness.
10. Resolve samples by adding 200 µl n-hexane. 400 µl for blank samples.
11. Divide samples into two portions in special 100 µl tubes and replace air in the tubes with N_2 before capping. Samples are now ready for GC analysis. Store samples in -20 °C until analyzed.

Appendix 3: Contents of the commercial stock standard solution GLC #411 (Nu-ChekPrep, USA)

GLC REFERENCE STANDARD
SPECIAL PREPARATION
Item % By Weight

GLC # 411

CHAIN	ITEM	% BY WT.
C8:0	METHYL OCTANOATE	3.23
C10:0	METHYL DECANOATE	3.23
C12:0	METHYL LAURATE	3.23
C12:1	METHYL 11-DODECENOATE	3.23
C14:0	METHYL MYRISTATE	3.23
C14:1	METHYL MYRISTOLEATE	3.23
C16:0	METHYL PALMITATE	3.23
C16:1	METHYL PALMITOLEATE	3.23
C18:0	METHYL STEARATE	3.23
C18:1	METHYL OLEATE	3.23
C18:1	METHYL PETROSELINATE	3.23
C18:1	METHYL VACCENATE	3.23
C18:2	METHYL LINOLEATE	3.23
C20:0	METHYL ARACHIDATE	3.23
C18:3	METHYL LINOLENATE	3.23
C18:3	METHYL GAMMA LINOLENATE	3.23
C20:1	METHYL 5-EICOSENOATE	3.23
C20:1	METHYL 8-EICOSENOATE	3.23
C20:1	METHYL 11-EICOSENOATE	3.23
C20:2	METHYL 11-14 EICOSADIENOATE	3.23
C22:0	METHYL BEHENATE	3.23
C22:1	METHYL ERUCATE	3.23
C20:3	METHYL 11-14-17 EICOSATRIENOATE	3.23
C20:3	METHYL HOMOGAMMA LINOLENATE	3.23
C20:4	METHYL ARACHIDONATE	3.23
C22:2	METHYL 13-16 DOCOSADIENOATE	3.23
C22:3	METHYL 13-16-19 DOCOSATRIENOATE	3.23
C22:4	METHYL 7-10-13-16 DOCOSATETRAENOATE	3.23
C24:0	METHYL LIGNOCERATE	3.23.
C24:1	METHYL NERVONATE	3.23
C22:6	METHYL DOCOSAHEXAENOATE	3.23

Appendix 4: Conversion of FAME results to FAME equivalents in serum

Internal standard (ISTD): 1, 2-Diheptadecanoyl-sn-glycero-3-phosphatidylcholine. Amount ISTD added prior to sample preparation: 30 µl of a stock standard solution with concentration 1.00 mg/mL

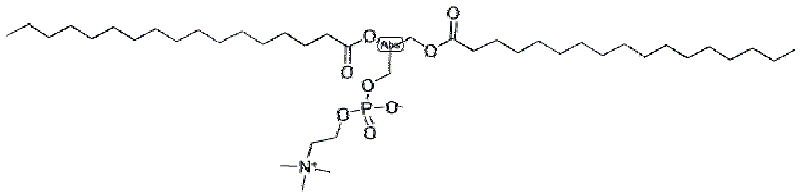

Physical data:

Molecular formula: $C_{42}H_{84}NO_8P$, molecular weight 762.09 g/mole.

ISTD contain two C17:0-FAME equivalents:

C17:0 – free fatty acid: $C_{17}H_{34}O_2$ 270.451 g/mole

C17:0 – FAME: $C_{18}H_{36}O_2$ 284.477 g/mole

Recovery of ISTD in analyzed samples:

Added ISTD at start: $30 \cdot 10^{-3} ml \cdot 1.00\ mg/mL = 0.030\ mg = \underline{30\ \mu g}$

Mole ISTD added: $\dfrac{30 \cdot 10^{-6} g}{762.06\ g/mole} = \underline{3.94 \cdot 10^{-8}\ mole}$

Grams of C17:0-fatty acid/FAME equivalents at start:

Mass, fatty acid-equivalents: $2 \cdot 3.94 \cdot 10^{-8}\ mole \cdot 270.451 g/mole = \underline{21.3 \mu g}$

Mass, FAME-equivalents: $2 \cdot 3.94 \cdot 10^{-8}\ mole \cdot 284.477 g/mole = \underline{22.4 \mu g}$

ISTD is added to 200 µl serum. Calculated concentration of C17:0 FAME in 200 µl serum:

$$C_{ISTD} = \frac{22.4 \mu g}{0.200\ ml} = \underline{112\ \mu g/ml}$$

In analyzed samples:

The total lipid fraction is split; 2/3 is fractionated to isolate the phospholipid fraction. Maximum amount of micrograms C17:0-FAME present in a prepared analytical sample:

$$2 \cdot 3.94 \cdot 10^{-8}\ mole \cdot 284.477\ g/mole \cdot \frac{0.200\ ml}{0.300\ ml} = 14.93 \cdot 10^{-6} g = \underline{14.9\ \mu g}$$

Concentration of C17:0-FAME in the analytical sample with a 100 % recovery:

$$C_{C17:0} = \frac{14.9\ \mu g}{0.200\ ml} = \underline{74.6\ \mu g/ml}$$

Appendix 5: System performance for GC-FID analysis of GLC #411 FAMEs

Retention factor (k)

Table A5-1 Retention factors for GLC #411 FAMEs obtained by GC-FID analysis.

	Calibration level								
FAME	1	2	3	4	5	6	7	8	9
C8:0	1.06	1.06	1.06	1.06	1.06	1.06	1.06	1.06	1.06
C10:0	1.80	1.80	1.80	1.80	1.80	1.80	1.80	1.80	1.81
C12:0	3.00	2.99	2.99	2.99	3.00	3.00	3.00	3.01	3.01
C12:1	3.48	3.48	3.48	3.48	3.48	3.49	3.49	3.50	3.50
C14:0	4.58	4.58	4.58	4.58	4.59	4.60	4.60	4.61	4.62
C14:1n-5	5.04	5.04	5.04	5.04	5.04	5.05	5.06	5.06	5.07
C16:0	6.34	6.34	6.34	6.34	6.35	6.36	6.37	6.38	6.39
C16:1n-7	6.70	6.71	6.71	6.71	6.72	6.73	6.74	6.75	6.76
C17:0	7.23	7.23	7.23	7.23	7.24	7.24	7.24	7.24	7.25
C18:0	8.10	8.10	8.11	8.11	8.13	8.14	8.16	8.18	8.19
C18:1	8.39	8.40	8.40	8.40	8.50	8.52	8.53	8.54	8.56
C18:2n-6	8.94	8.95	8.95	8.95	8.96	8.98	8.99	9.00	9.01
C18:3n-6	9.32	9.32	9.32	9.33	9.33	9.35	9.36	9.37	9.38
C18:3n-3	9.65	9.66	9.66	9.66	9.67	9.68	9.70	9.71	9.72
C20:0	9.86	9.87	9.88	9.88	9.91	9.94	9.97	10.00	10.02
C20:1n-9	10.05	10.06	10.06	10.07	10.09	10.11	10.14	10.17	10.20
C20:1n-15	10.14	10.15	10.15	10.16	10.18	10.21	10.23	10.26	10.28
C20:1n-12	10.21	10.22	10.22	10.23	10.25	10.28	10.30	10.32	10.34
C20:2n-6	10.86	10.86	10.87	10.87	10.89	10.91	10.93	10.94	10.96
C20:3n-6	11.28	11.29	11.29	11.30	11.31	11.33	11.35	11.36	11.38
C20:4n-6	11.57	11.58	11.58	11.58	11.60	11.62	11.63	11.65	11.66
C20:3n-3	11.67	11.68	11.68	11.68	11.70	11.72	11.74	11.75	11.77
C22:0	11.85	11.86	11.87	11.88	11.90	11.94	11.96	11.99	12.02
C22:1n-9	12.26	12.26	12.27	12.28	12.30	12.33	12.35	12.37	12.40
C22:2n-6	12.99	13.00	13.00	13.01	13.03	13.05	13.07	13.10	13.12
C22:3n3/C22:4n-6	13.89	13.90	13.90	13.91	13.93	13.96	13.98	14.00	14.02
C24:0	14.03	14.04	14.04	14.05	14.08	14.12	14.15	14.18	14.21
C24:1n-9	14.48	14.49	14.49	14.50	14.53	14.57	14.60	14.63	14.66
C22:6n-3	15.12	15.12	15.13	15.13	15.15	15.17	15.19	15.20	15.22

Peak width ($W_{50.0}$)

Table A5-2 Peak width for GLC #411 FAMEs obtained by GC-FID analysis.

	Calibration level								
FAME	1	2	3	4	5	6	7	8	9
C8:0	0.05	0.05	0.04	0.04	0.04	0.04	0.04	0.04	0.04
C10:0	0.06	0.05	0.05	0.05	0.05	0.05	0.05	0.06	0.06
C12:0	0.08	0.07	0.07	0.07	0.07	0.07	0.08	0.08	0.08
C12:1	0.08	0.08	0.08	0.08	0.08	0.08	0.08	0.08	0.09
C14:0	0.09	0.09	0.09	0.09	0.09	0.10	0.10	0.10	0.11
C14:1n-5	0.09	0.09	0.09	0.09	0.09	0.10	0.09	0.10	0.10
C16:0	0.10	0.10	0.10	0.10	0.11	0.11	0.12	0.12	0.13
C16:1n-7	0.10	0.10	0.10	0.10	0.10	0.10	0.11	0.12	0.12
C17:0	0.10	0.10	0.10	0.10	0.11	0.12	0.12	0.13	0.14
C18:0	0.10	0.10	0.10	0.10	0.12	0.14	0.15	0.18	0.20
C18:1	-	-	-	-	-	-	-	-	-
C18:2n-6	0.11	0.10	0.11	0.11	0.11	0.11	0.12	0.13	0.14
C18:3n-6	0.12	0.11	0.11	0.11	0.12	0.12	0.12	0.12	0.13
C18:3n-3	0.11	0.11	0.12	0.12	0.11	0.12	0.12	0.13	0.13
C20:0	0.12	0.12	0.12	0.13	0.15	0.19	0.21	0.24	0.37
C20:1n-9	0.12	0.12	0.13	0.14	0.14	0.18	0.22	0.25	0.35
C20:1n-15	0.12	0.12	0.12	0.12	0.14	0.16	0.18	0.17	0.22
C20:1n-12	0.12	0.12	0.12	0.12	0.13	0.12	0.12	0.12	0.15
C20:2n-6	0.13	0.13	0.13	0.13	0.14	0.15	0.15	0.17	0.19
C20:3n-6	0.14	0.13	0.14	0.13	0.13	0.14	0.15	0.16	0.18
C20:4n-6	0.14	0.13	0.14	0.13	0.14	0.14	0.15	0.15	0.16
C20:3n-3	0.14	0.14	0.14	0.13	0.14	0.14	0.14	0.15	0.16
C22:0	0.15	0.15	0.15	0.14	0.16	0.20	0.22	0.26	0.29
C22:1n-9	0.15	0.15	0.15	0.14	0.15	0.16	0.19	0.19	0.24
C22:2n-6	0.16	0.16	0.16	0.16	0.15	0.16	0.18	0.20	0.22
C22:3n-3/C22:4n-6	0.16	0.16	0.16	0.16	0.15	0.17	0.18	0.21	0.23
C24:0	0.16	0.17	0.17	0.17	0.17	0.20	0.22	0.25	0.29
C24:1n-9	0.17	0.16	0.17	0.17	0.15	0.17	0.20	0.20	0.23
C22:6n-3	0.17	0.17	0.17	0.17	0.17	0.16	0.17	0.18	0.18

Plate number (N)

Table A5-3 Plate number for GLC #411 FAMEs obtained by GC-FID analysis.

	Calibration level								
FAME	1	2	3	4	5	6	7	8	9
C8:0	100555	145241	165378	182710	206182	207993	202928	199666	193419
C10:0	211133	222802	228385	226947	222618	217307	207016	192847	181186
C12:0	230003	237183	230727	236102	225002	209226	195034	170494	152518
C12:1	263993	261412	268274	264824	257340	244148	224550	200279	182442
C14:0	307043	303697	310493	307101	280820	242862	206885	181946	152147
C14:1n-5	340005	347488	350159	341339	324054	291828	269060	228010	200821
C16:0	449939	439401	430842	423940	363017	290847	244090	197195	160472
C16:1n-7	477818	474650	478204	468922	425667	366153	321695	274848	239442
C17:0	498699	478421	472260	465095	408732	364895	331208	294634	259401
C18:0	615108	581101	556633	532034	383465	239993	172403	125363	97567
C18:1	133464	131890	130819	128271	601964	510437	454659	383225	335102
C18:2n-6	663974	664355	652522	644901	545657	475571	413856	350633	284420
C18:3n-6	645205	645598	649289	636675	583605	514201	458329	401631	353023
C18:3n-3	654661	672374	642062	642572	598847	516457	452195	391221	347103
C20:0	627503	576501	525779	483201	296858	176246	125324	93632	72326
C20:1n-9	579906	551666	524879	474970	308749	156868	89605	67518	73077
C20:1n-15	609889	602815	575887	556231	401359	238392	135576	110285	119023
C20:1n-12	637746	654419	644197	650380	577015	479729	403009	297764	303050
C20:2n-6	626806	604030	584076	605013	523313	401735	330618	257423	198892
C20:3n-6	635189	623178	617511	616592	541129	452028	383036	309553	256118
C20:4n-6	614566	656045	643623	629052	598514	516029	450672	400463	338639
C20:3n-3	625685	629013	629384	645144	580908	497307	456414	386482	328873
C22:0	615839	572421	570342	539383	373134	224285	163666	109709	80155
C22:1n-9	613307	603209	601145	574807	478408	350451	266869	210108	152512
C22:2n-6	628924	629340	611184	603018	522040	400919	332526	265483	200985
C22:3n-3/ C22:4n-6	657525	668934	655527	643055	547532	442073	359713	280999	233172
C24:0	648658	611328	609170	567054	421255	287448	213848	161718	118130
C24:1n-9	655703	651192	636436	629879	527568	406475	323301	267984	228837
C22:6n-3	713868	714214	708723	716175	655177	586172	508080	440529	391101

Resolution (R)

Table A5-4 Resolution for GLC #411 FAMEs obtained by GC-FID analysis.

	Calibration level								
FAME	1	2	3	4	5	6	7	8	9
C8:0	-1	-1	-1	-1	-1	-1	-1	-1	-1
C10:0	29.50	32.62	33.83	34.53	35.30	35.17	34.55	33.79	33.01
C12:0	41.22	42.16	42.07	42.32	41.64	40.62	39.43	37.38	35.72
C12:1	14.29	14.38	14.37	14.41	14.12	13.68	13.15	12.35	11.73
C14:0	29.09	29.00	29.36	29.19	28.37	8.64	8.34	8.21	7.87
C14:1n-5	11.18	11.19	11.29	11.18	10.78	10.08	9.46	8.77	8.13
C16:0	30.48	30.51	30.45	30.16	28.64	26.38	24.72	22.48	20.65
C16:1n-7	8.32	8.24	8.21	8.12	7.56	6.87	6.34	5.77	5.27
C17:0	11.54	11.38	11.31	11.19	10.49	9.66	9.02	8.32	7.56
C18:0	18.56	18.22	18.05	17.82	16.07	13.99	12.62	11.32	10.38
C18:1	-	-	-	-	-	-	-	-	-
C18:2n-6	7.25	7.19	7.13	7.07	9.04	8.32	7.76	7.07	6.43
C18:3n-6	7.46	7.44	7.40	7.35	6.86	6.39	5.98	5.53	5.07
C18:3n-3	6.44	6.49	6.42	6.38	6.15	5.73	5.39	5.03	4.72
C20:0	3.91	3.94	3.87	3.86	3.54	3.15	2.90	2.72	2.58
C20:1n-9	3.25	3.13	3.01	2.85	2.18	1.58	1.27	1.11	1.05
C20:1n-15	1.57	1.55	1.54	1.47	1.25	0.91	0.66	0.56	0.56
C20:1n-12	1.24	1.24	1.20	1.22	1.10	0.91	0.69	0.56	0.55
C20:2n-6	11.19	11.09	10.92	11.02	10.20	9.00	8.16	7.05	6.55
C20:3n-6	6.98	6.87	6.79	6.85	6.37	5.67	5.15	4.56	4.07
C20:4n-6	4.60	4.65	4.60	4.56	4.33	3.98	3.68	3.39	3.06
C20:3n-3	1.53	1.57	1.57	1.56	1.54	1.45	1.39	1.32	1.24
C22:0	2.79	2.81	2.85	2.87	2.66	2.35	2.20	1.97	1.82
C22:1n-9	6.05	5.89	5.87	5.71	4.92	3.94	3.34	2.77	2.34
C22:2n-6	10.62	10.55	10.43	10.29	9.44	8.11	7.21	6.41	5.46
C22:3n-3/C22:4n-6	12.44	12.50	12.34	12.23	11.34	10.10	9.15	8.12	7.23
C24:0	1.85	1.87	1.89	1.87	1.74	1.58	1.46	1.35	1.23
C24:1n-9	5.99	5.88	5.83	5.70	5.05	4.29	3.72	3.30	2.92
C22:6n-3	8.36	8.28	8.19	8.15	7.43	6.55	5.86	5.24	4.76

Peak symmetry

Table A5-5 Peak symmetry for GLC #411 FAMEs obtained by GC-FID analysis.

	Calibration level								
FAME	1	2	3	4	5	6	7	8	9
C8:0	0.57	0.82	0.92	0.97	1.08	1.16	1.21	1.28	1.36
C10:0	0.88	0.97	1.02	1.04	1.17	1.33	1.45	1.61	1.82
C12:0	0.96	1.00	1.07	1.11	1.37	1.63	1.87	2.20	2.49
C12:1	0.99	1.02	1.04	1.13	1.32	1.56	1.77	2.08	2.42
C14:0	0.96	1.12	1.12	1.15	1.44	1.93	2.28	2.74	3.19
C14:1n-5	0.96	1.03	1.07	1.12	1.45	1.77	1.93	2.19	2.85
C16:0	0.98	1.03	1.19	1.29	1.73	2.31	2.82	3.11	3.81
C16:1n-7	1.01	1.02	1.18	1.26	1.45	2.03	2.46	2.91	3.53
C17:0	1.38	1.34	1.32	1.36	1.44	1.28	1.19	1.10	0.94
C18:0	1.05	1.16	1.37	1.33	1.92	2.55	3.93	4.23	4.78
C18:1	-	-	-	-	-	-	-	-	-
C18:2n-6	0.99	1.12	1.16	1.20	1.55	2.05	2.61	3.05	3.53
C18:3n-6	1.04	1.13	1.11	1.23	1.45	1.92	2.41	2.62	3.32
C18:3n-3	1.01	1.17	1.13	1.20	1.53	1.91	2.45	2.77	3.37
C20:0	1.13	1.22	1.27	1.48	2.19	3.17	4.01	5.08	4.96
C20:1n-9	1.04	1.17	1.19	1.29	1.38	2.04	2.83	3.47	3.46
C20:1n-15	1.06	1.15	1.41	1.33	1.56	1.97	2.48	2.83	2.32
C20:1n-12	1.03	1.21	1.28	1.41	1.73	2.38	2.63	2.97	2.77
C20:2n-6	1.07	1.18	1.24	1.36	1.70	2.31	2.93	3.46	4.09
C20:3n-6	1.00	1.08	1.18	1.28	1.66	2.18	2.41	2.79	3.65
C20:4n-6	1.05	1.15	1.13	1.26	1.47	2.09	2.32	2.87	3.21
C20:3n-3	0.99	1.11	1.15	1.19	1.55	2.13	2.48	3.07	3.62
C22:0	1.07	1.25	1.44	1.56	2.25	3.27	4.37	5.36	6.11
C22:1n-9	1.04	1.15	1.36	1.39	1.94	2.78	3.28	3.20	4.68
C22:2n-6	1.02	1.14	1.21	1.35	2.00	2.28	3.04	3.67	4.25
C22:3n-3/C22:4n-6	1.10	1.18	1.19	1.32	1.95	2.89	3.39	3.78	4.62
C24:0	1.01	1.24	1.30	1.46	2.21	3.42	4.54	5.66	6.37
C24:1n-9	1.07	1.21	1.20	1.34	1.90	2.91	3.05	3.72	5.27
C22:6n-3	0.96	1.03	1.08	1.19	1.47	1.94	2.48	2.38	3.30

Appendix 6:Mass spectra for peaks representing the use of expected features for identification, and TIC and EIC displaying an unexpected elution order for C20:3 and C20:4.

Mass spectra for FAMEs with varying number of double bonds, representing the expected features used for identification.

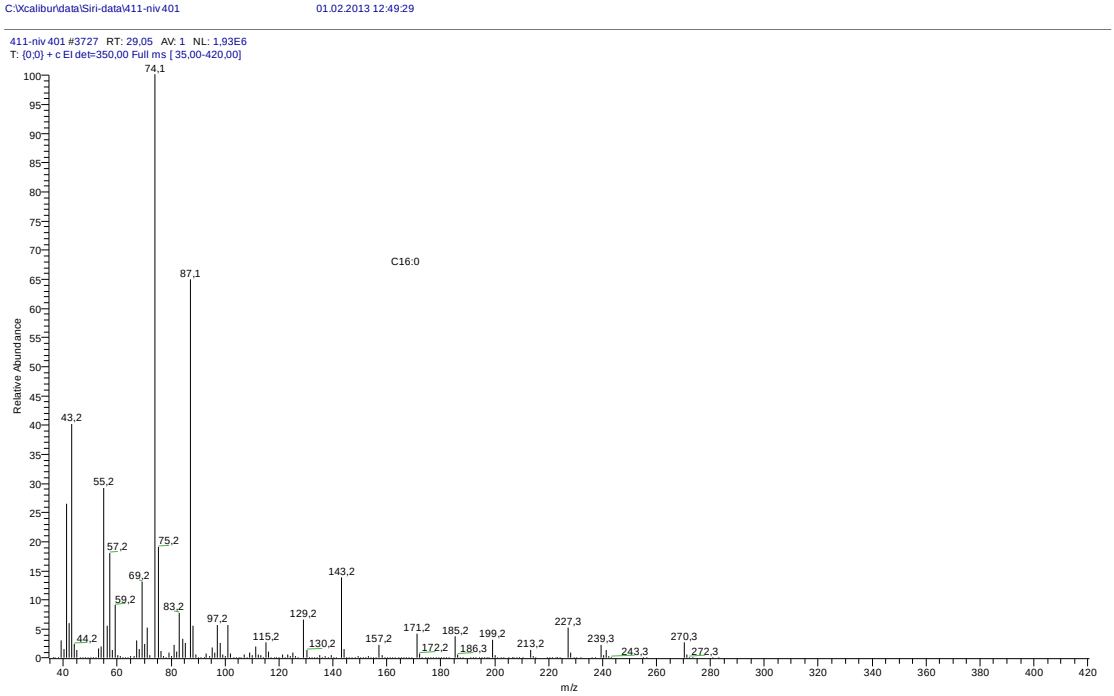

Figure A6-1 Mass spectrum for C16:0, a representative spectrum for saturated FAMEs.

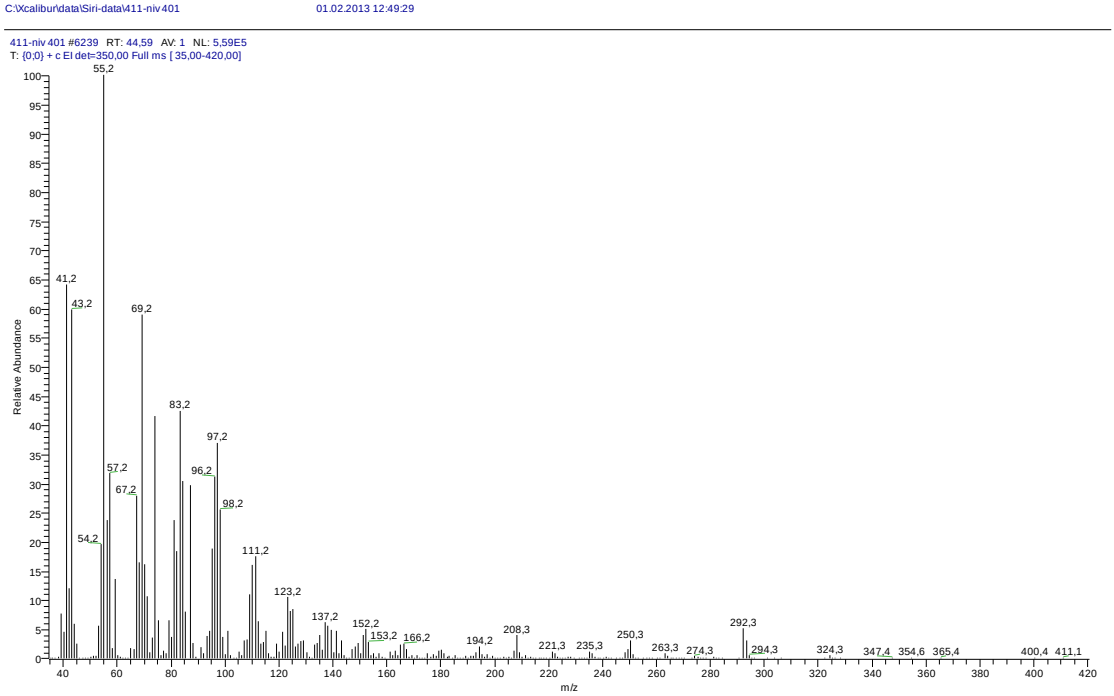

Figure A6-2 Mass spectrum for C20:1n-9, a representative spectrum for monounsaturated FAMEs.

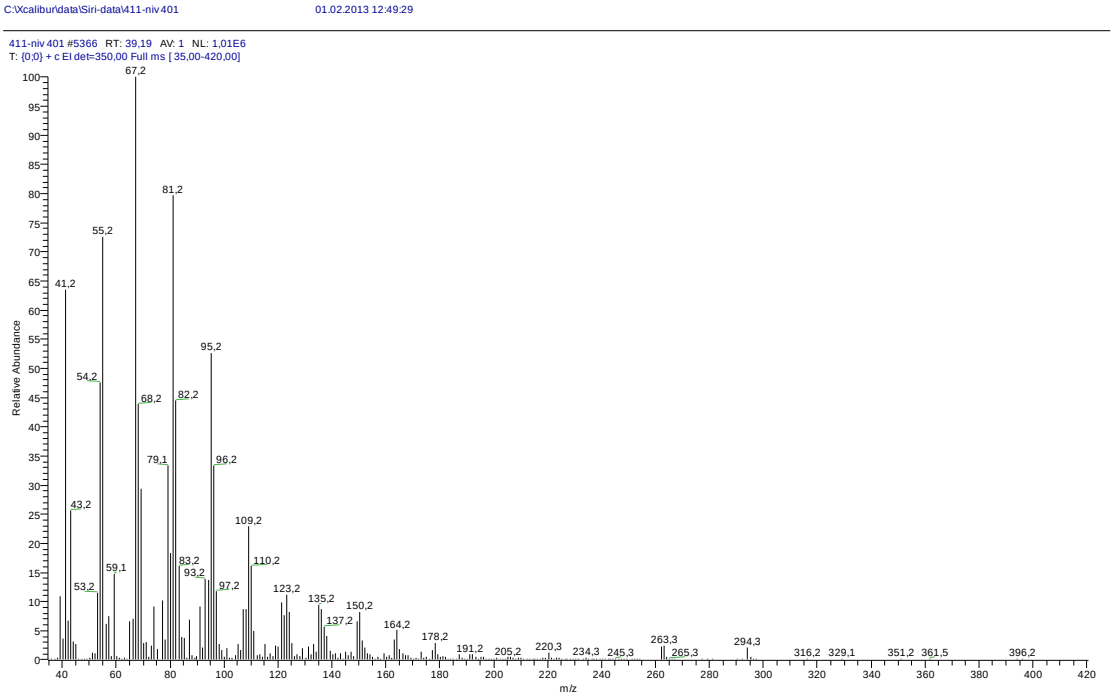

Figure A6-3 Mass spectrum for C18:2n-6, a representative spectrum for an unsaturated FAME with two double bonds.

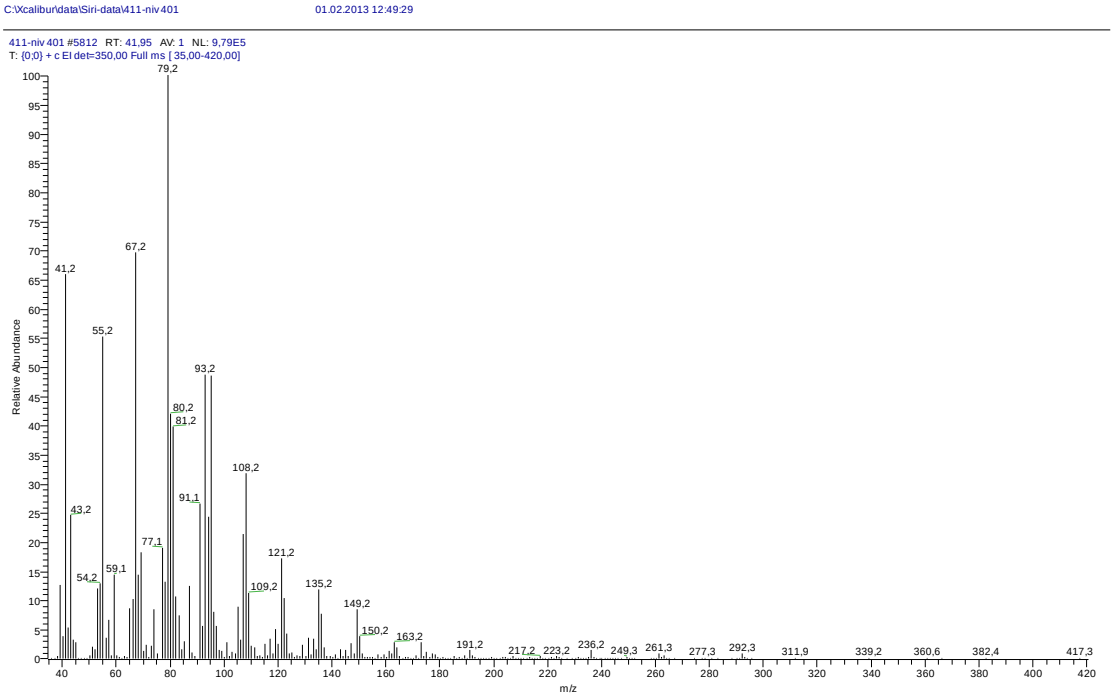

Figure A6-4 Mass spectrum for C18:3n-3, a representative spectrum for a unsaturated FAME with three double bonds.

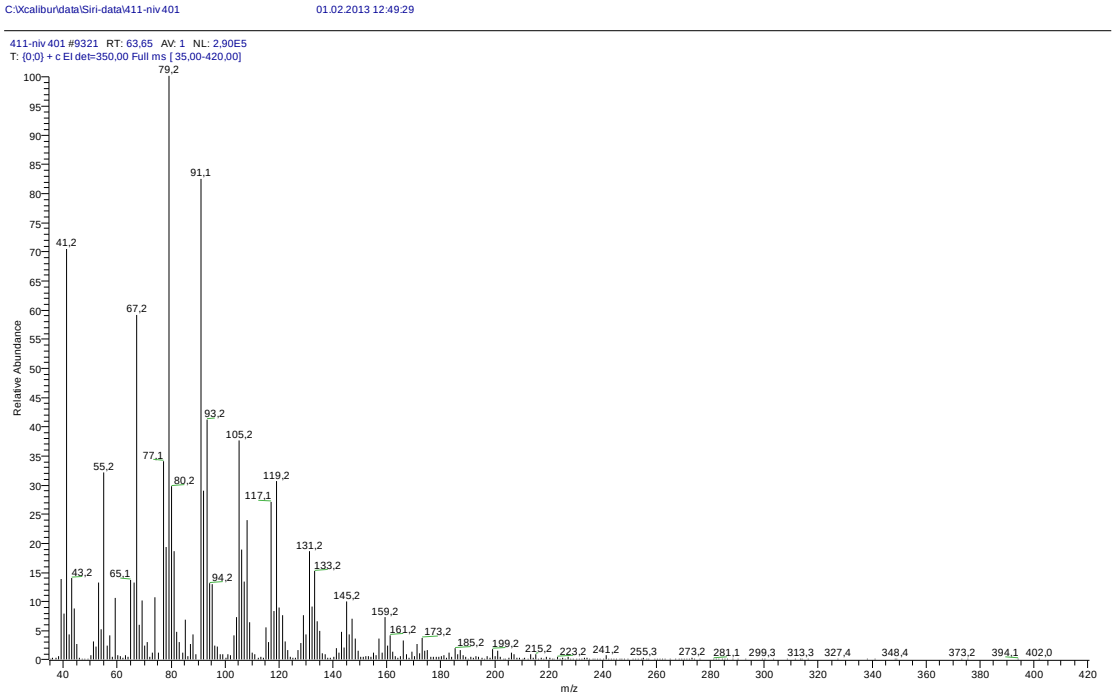

Figure A6-5 Mass spectrum for C22:6n-3, a representative spectrum for an unsaturated FAME with four or more double bonds.

Contamination identified as C20:1n-9 in a participant sample.

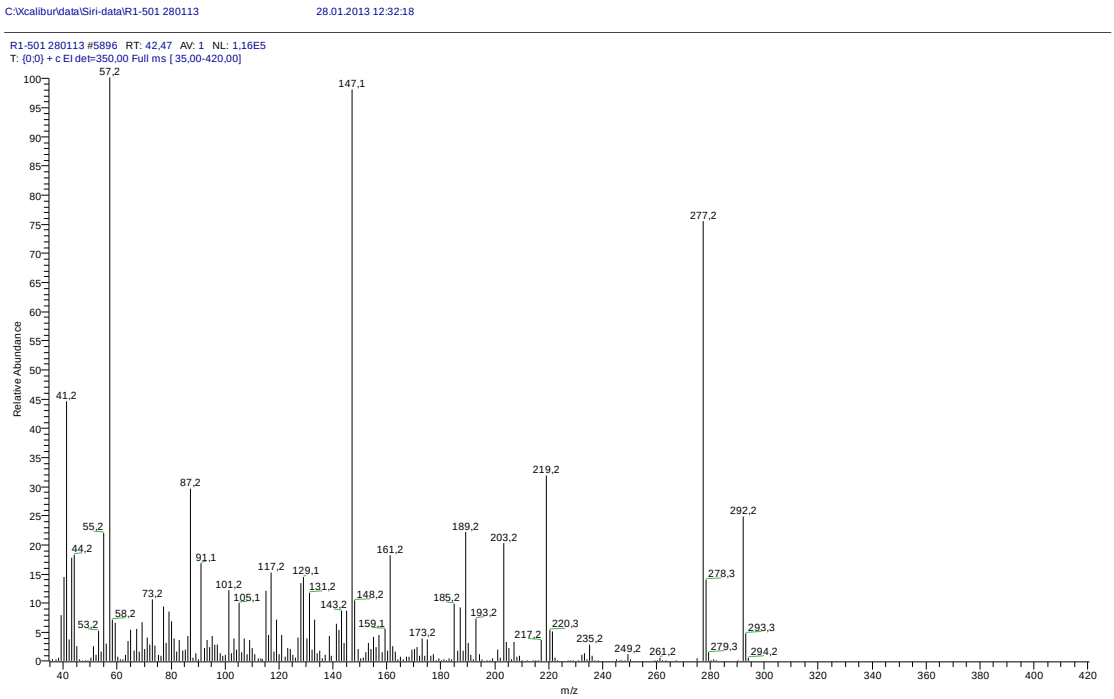

Figure A6-6 Mass spectrum for a contamination with identical retention time as the FAME C20:1n-9 discovered in a participant sample.

Extracted ion chromatogram for the FAME molecular ion for C20:3 (*m/z* 320)

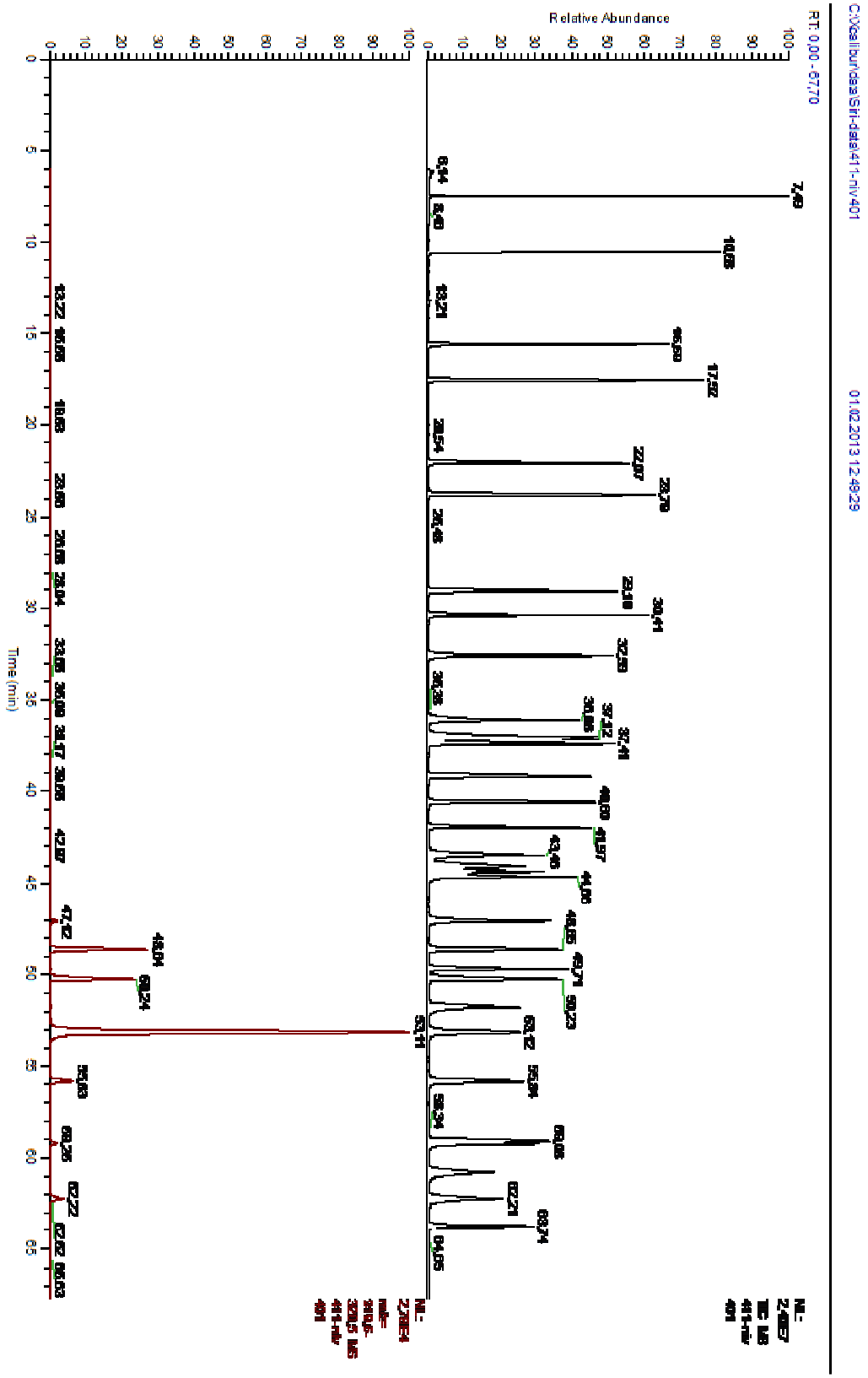

Figure A6-7 TIC and EIC for the molecular ion for C20:3 FAMEs (*m/z* 320).

Appendix 7: Calibration curves obtained with GC-FID at two different time points

Calibration curves for the first (left) and second (right) calibration of the GC-FID method

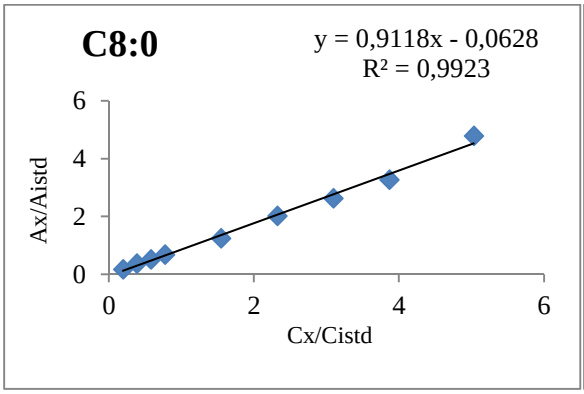

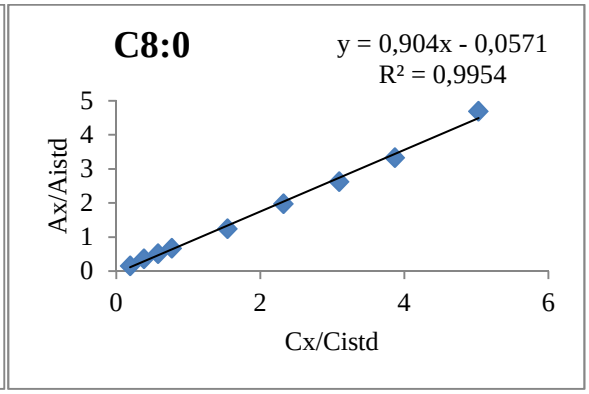

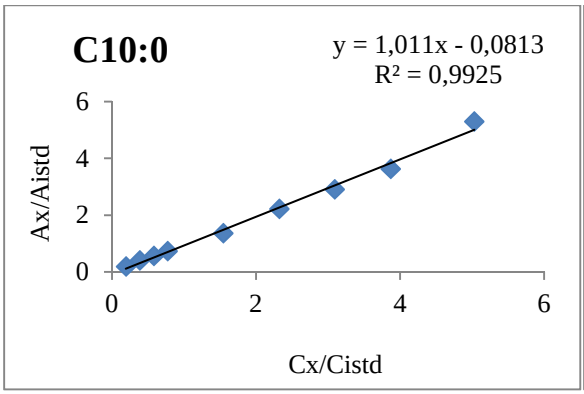

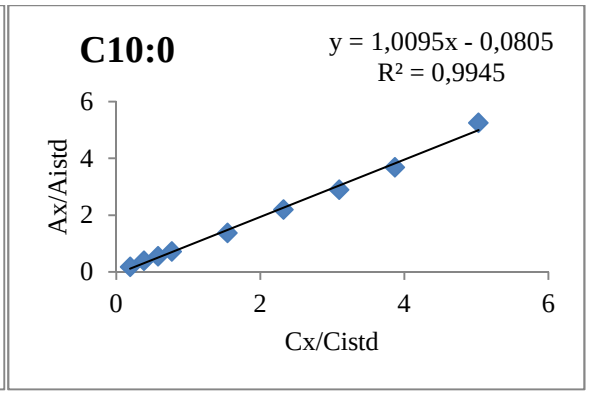

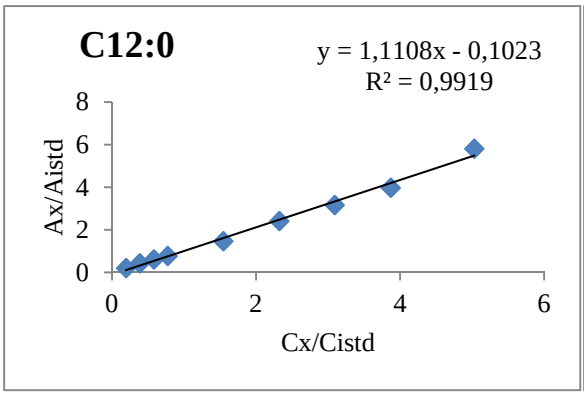

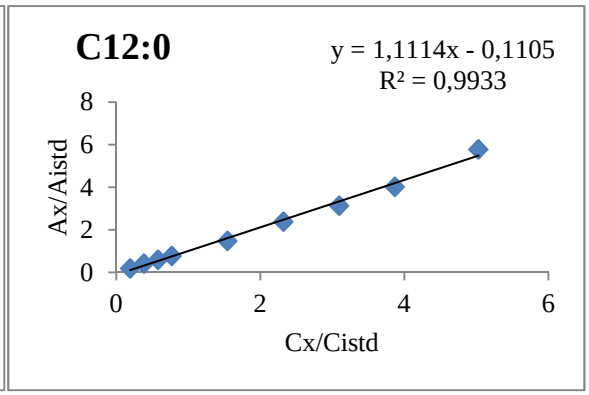

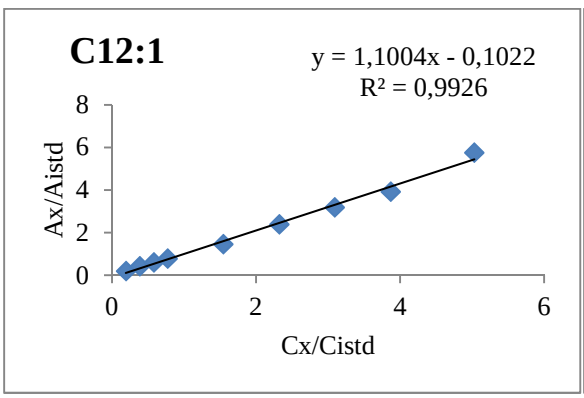

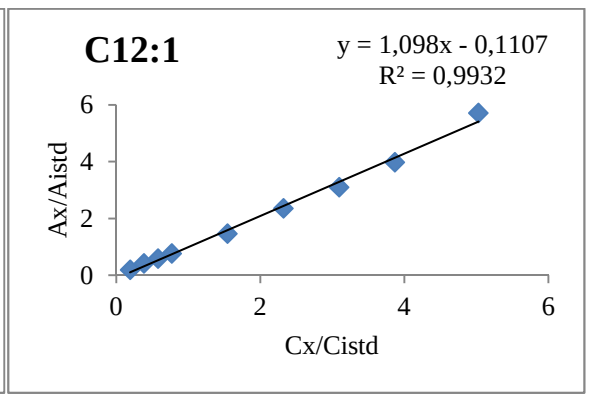

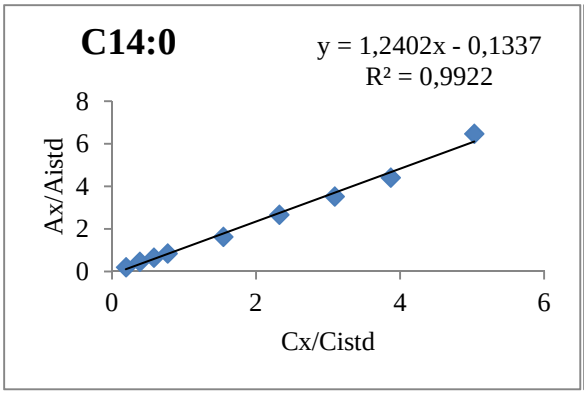
C14:0
y = 1,2402x - 0,1337
R² = 0,9922
Ax/Aistd
Cx/Cistd

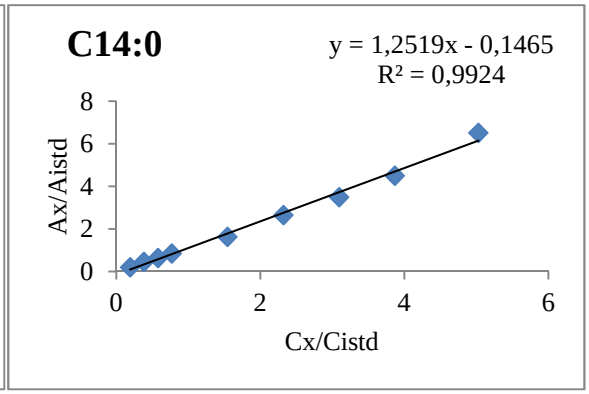
C14:0
y = 1,2519x - 0,1465
R² = 0,9924
Ax/Aistd
Cx/Cistd

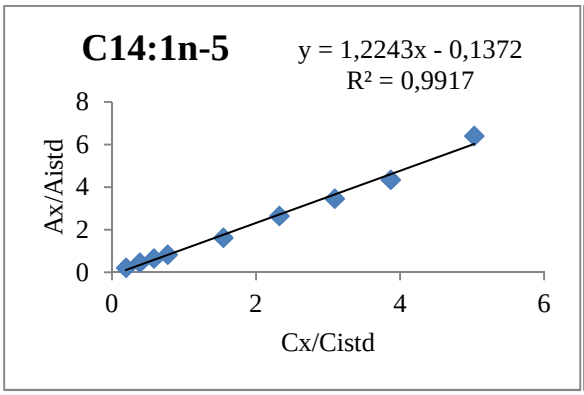
C14:1n-5
y = 1,2243x - 0,1372
R² = 0,9917
Ax/Aistd
Cx/Cistd

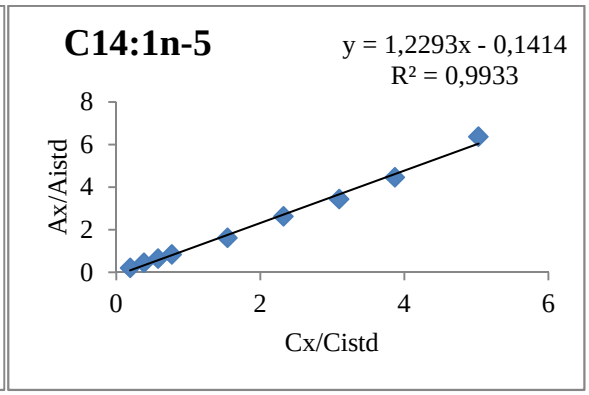
C14:1n-5
y = 1,2293x - 0,1414
R² = 0,9933
Ax/Aistd
Cx/Cistd

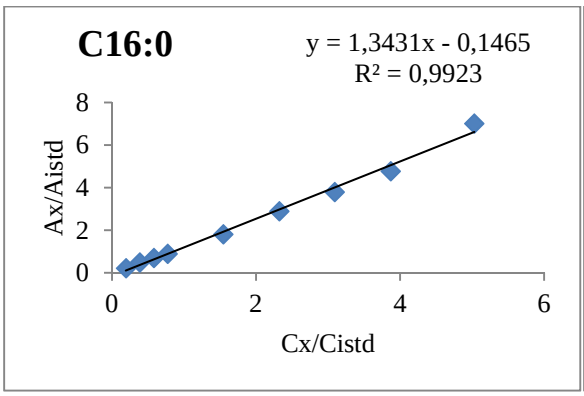
C16:0
y = 1,3431x - 0,1465
R² = 0,9923
Ax/Aistd
Cx/Cistd

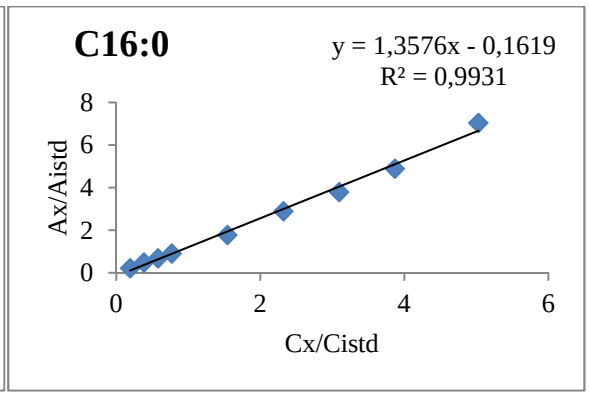
C16:0
y = 1,3576x - 0,1619
R² = 0,9931
Ax/Aistd
Cx/Cistd

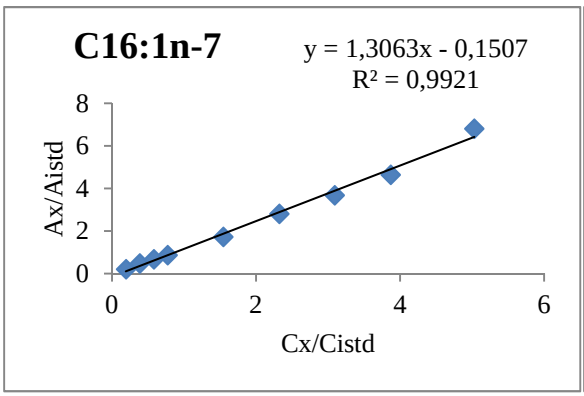
C16:1n-7
y = 1,3063x - 0,1507
R² = 0,9921
Ax/Aistd
Cx/Cistd

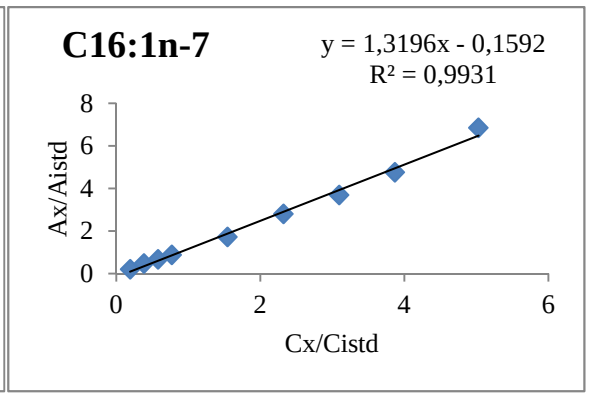
C16:1n-7
y = 1,3196x - 0,1592
R² = 0,9931
Ax/Aistd
Cx/Cistd

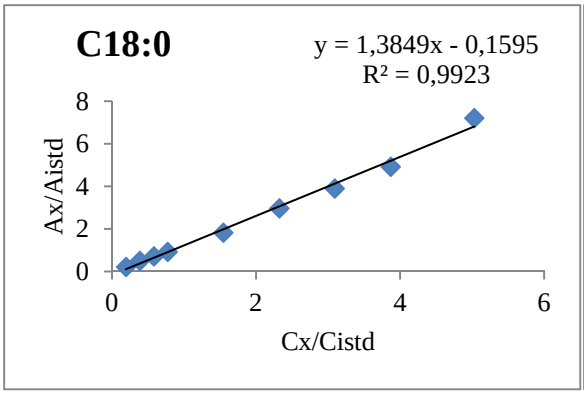
C18:0
y = 1,3849x - 0,1595
R² = 0,9923
Ax/Aistd
Cx/Cistd

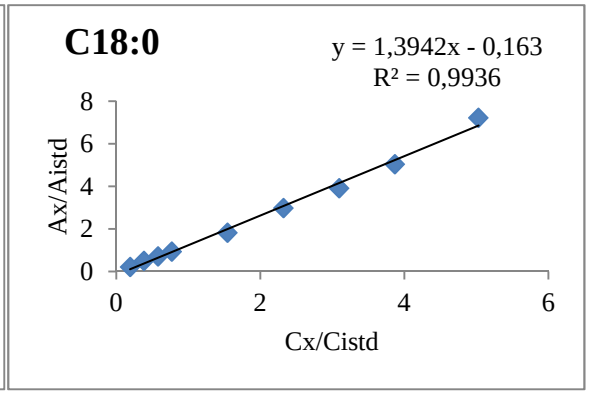
C18:0
y = 1,3942x - 0,163
R² = 0,9936
Ax/Aistd
Cx/Cistd

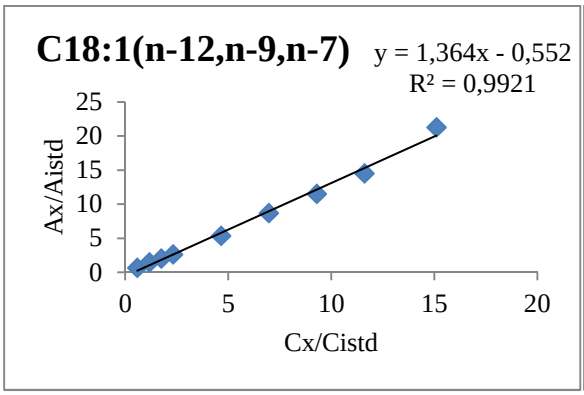
C18:1(n-12,n-9,n-7)
y = 1,364x - 0,552
R² = 0,9921
Ax/Aistd
Cx/Cistd

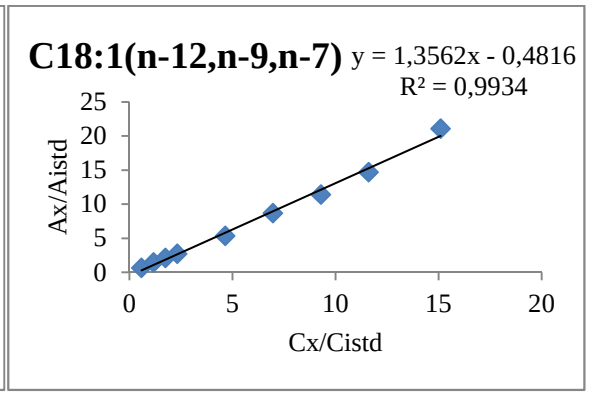
C18:1(n-12,n-9,n-7)
y = 1,3562x - 0,4816
R² = 0,9934
Ax/Aistd
Cx/Cistd

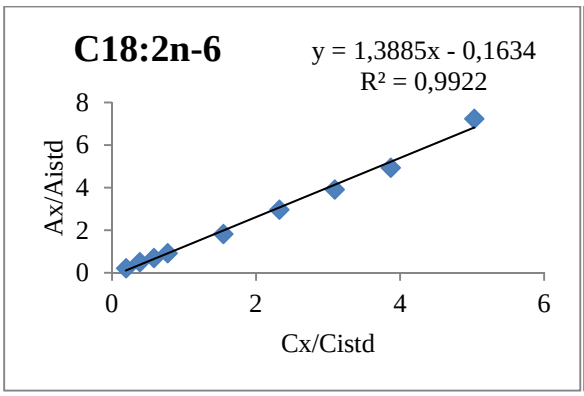
C18:2n-6
y = 1,3885x - 0,1634
R² = 0,9922
Ax/Aistd
Cx/Cistd

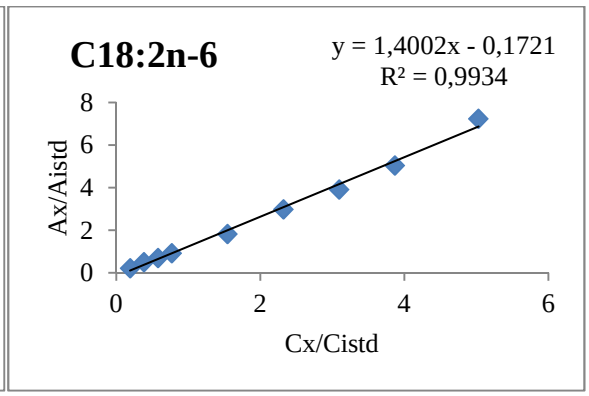
C18:2n-6
y = 1,4002x - 0,1721
R² = 0,9934
Ax/Aistd
Cx/Cistd

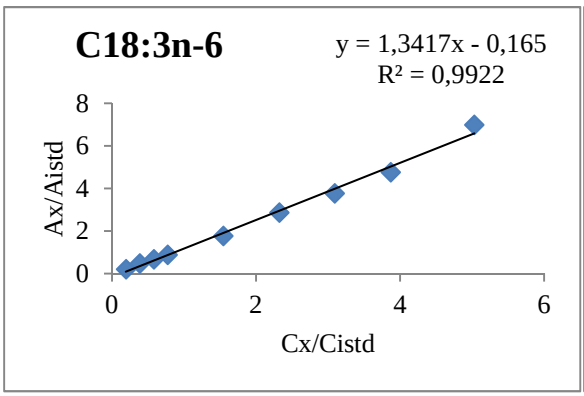
C18:3n-6
y = 1,3417x - 0,165
R² = 0,9922
Ax/Aistd
Cx/Cistd

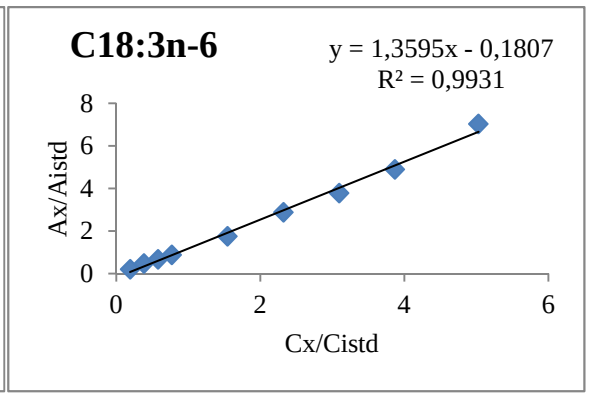
C18:3n-6
y = 1,3595x - 0,1807
R² = 0,9931
Ax/Aistd
Cx/Cistd

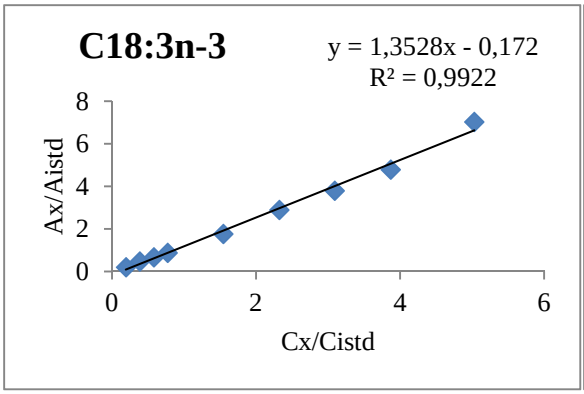
C18:3n-3
y = 1,3528x - 0,172
R² = 0,9922
Ax/Aistd
Cx/Cistd

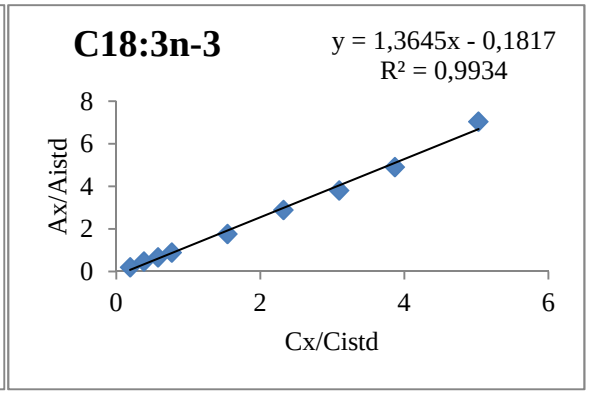
C18:3n-3
y = 1,3645x - 0,1817
R² = 0,9934
Ax/Aistd
Cx/Cistd

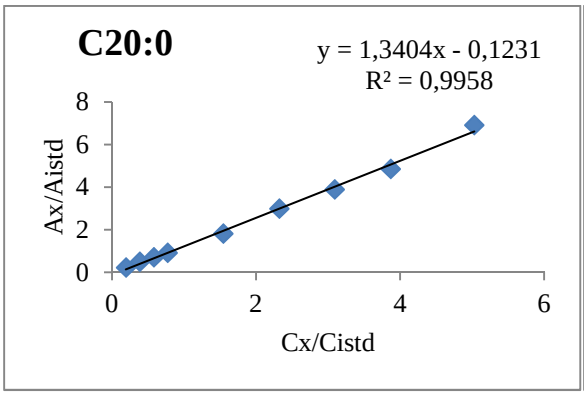
C20:0
y = 1,3404x - 0,1231
R² = 0,9958
Ax/Aistd
Cx/Cistd

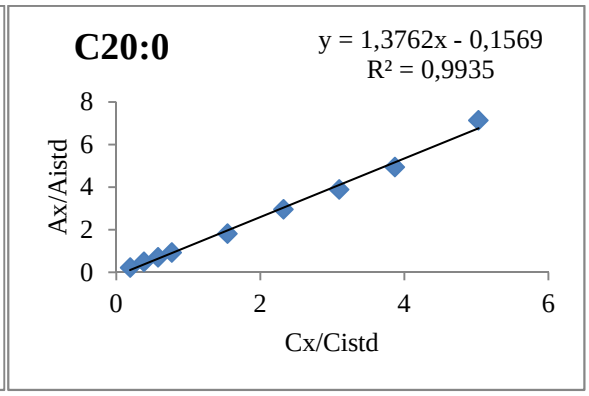
C20:0
y = 1,3762x - 0,1569
R² = 0,9935
Ax/Aistd
Cx/Cistd

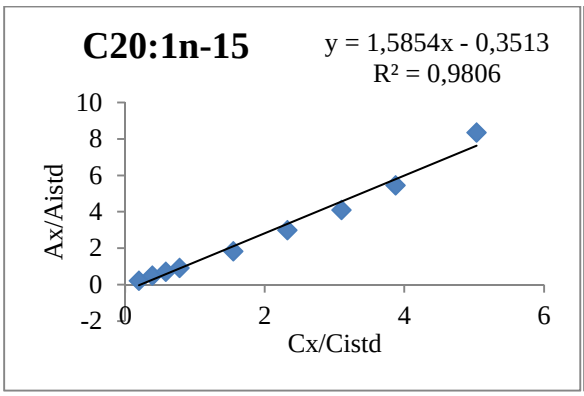
C20:1n-15
y = 1,5854x - 0,3513
R² = 0,9806
Ax/Aistd
Cx/Cistd

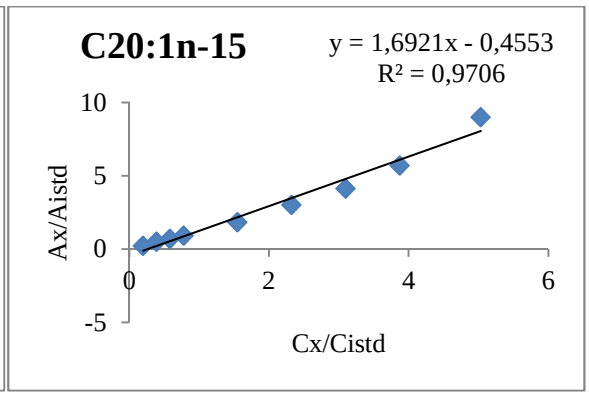
C20:1n-15
y = 1,6921x - 0,4553
R² = 0,9706
Ax/Aistd
Cx/Cistd

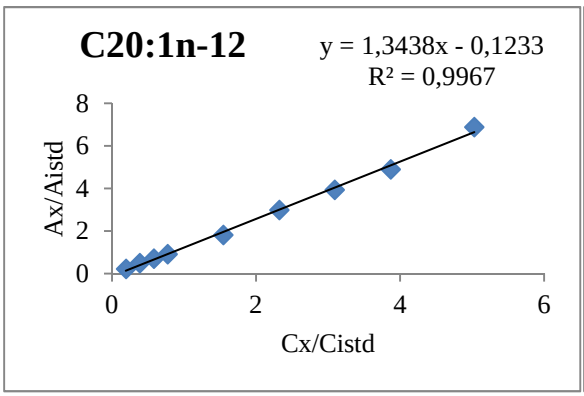
C20:1n-12
y = 1,3438x - 0,1233
R² = 0,9967
Ax/Aistd
Cx/Cistd

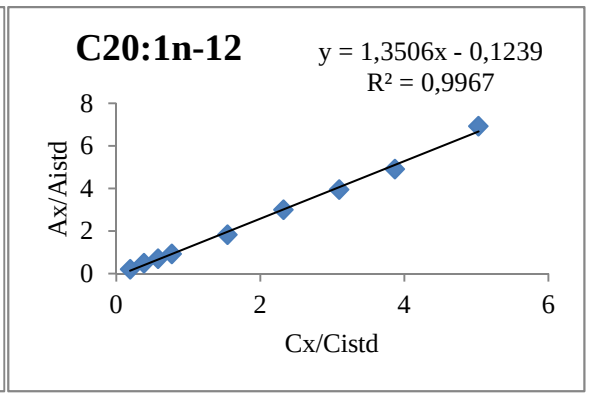
C20:1n-12
y = 1,3506x - 0,1239
R² = 0,9967
Ax/Aistd
Cx/Cistd

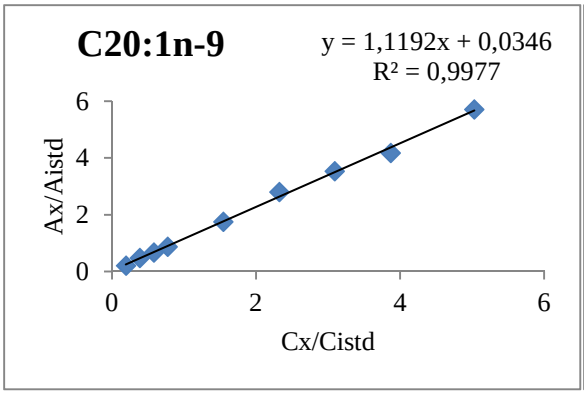
C20:1n-9
y = 1,1192x + 0,0346
R² = 0,9977
Ax/Aistd
Cx/Cistd

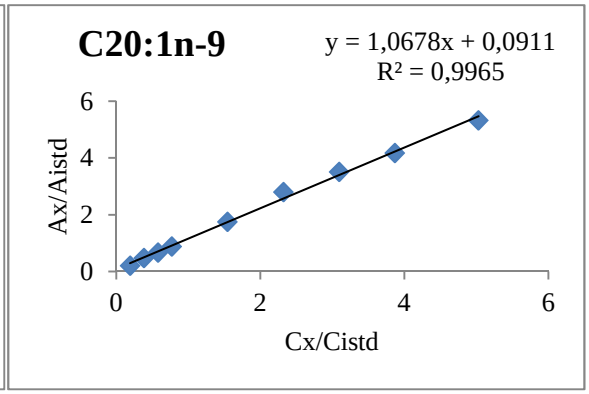
C20:1n-9
y = 1,0678x + 0,0911
R² = 0,9965
Ax/Aistd
Cx/Cistd

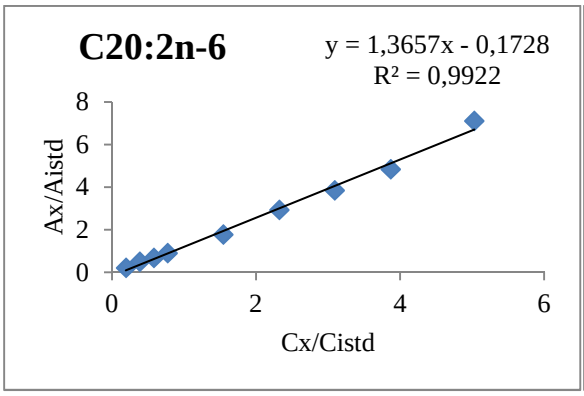
C20:2n-6
y = 1,3657x - 0,1728
R² = 0,9922
Ax/Aistd
Cx/Cistd

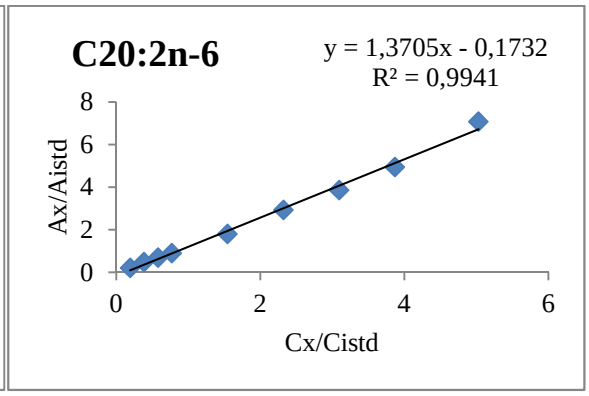
C20:2n-6
y = 1,3705x - 0,1732
R² = 0,9941
Ax/Aistd
Cx/Cistd

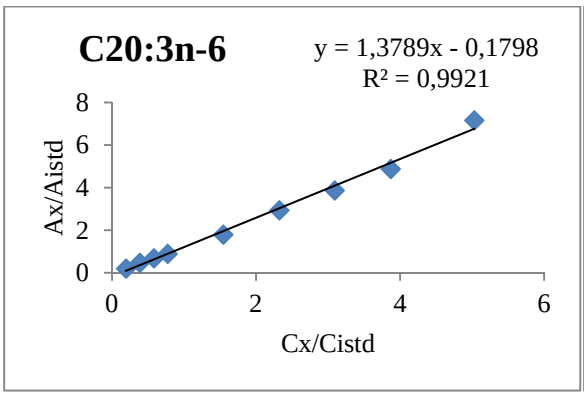
C20:3n-6
y = 1,3789x - 0,1798
R² = 0,9921
Ax/Aistd
Cx/Cistd

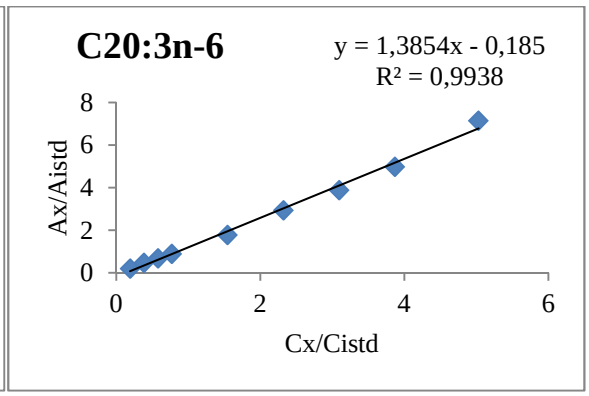
C20:3n-6
y = 1,3854x - 0,185
R² = 0,9938
Ax/Aistd
Cx/Cistd

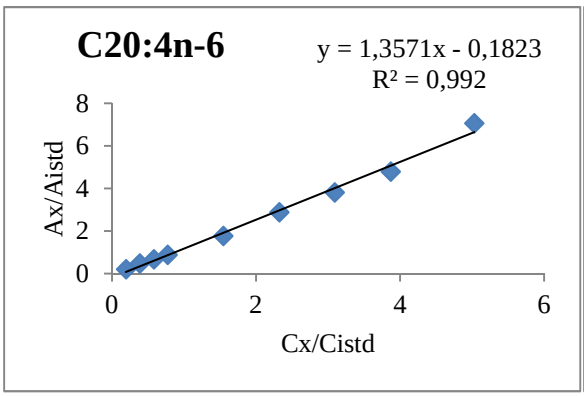
C20:4n-6
y = 1,3571x - 0,1823
R² = 0,992
Ax/Aistd
Cx/Cistd

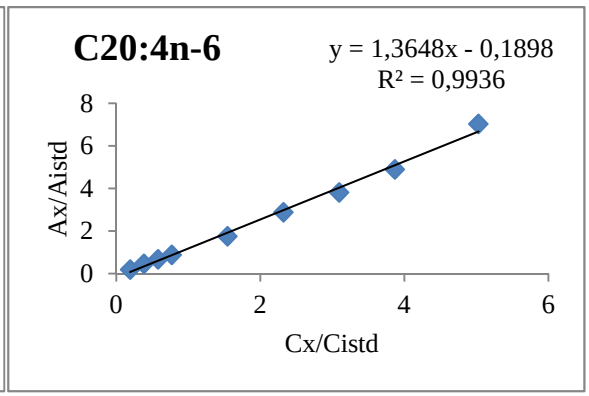
C20:4n-6
y = 1,3648x - 0,1898
R² = 0,9936
Ax/Aistd
Cx/Cistd

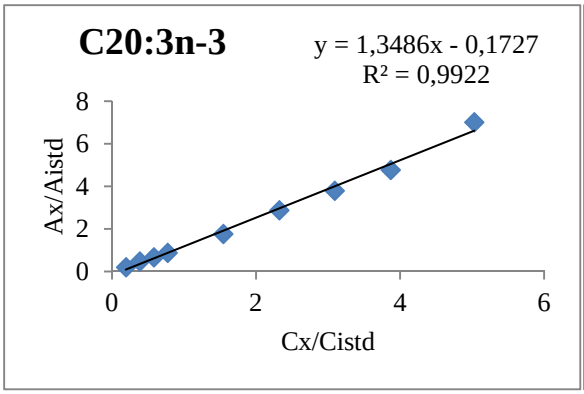
C20:3n-3
y = 1,3486x - 0,1727
R² = 0,9922
Ax/Aistd
Cx/Cistd

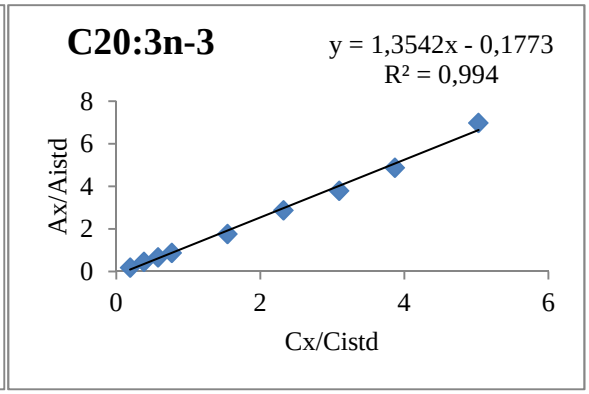
C20:3n-3
y = 1,3542x - 0,1773
R² = 0,994
Ax/Aistd
Cx/Cistd

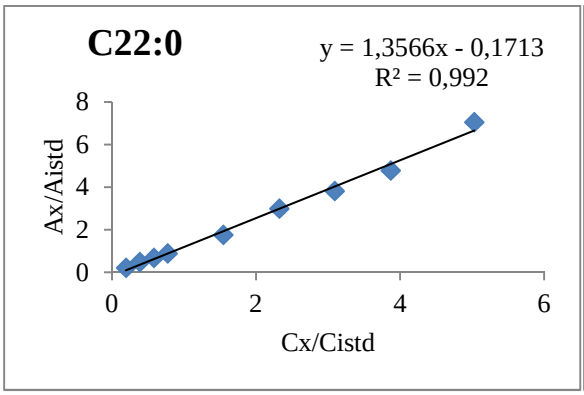
C22:0
y = 1,3566x - 0,1713
R² = 0,992
Ax/Aistd
Cx/Cistd

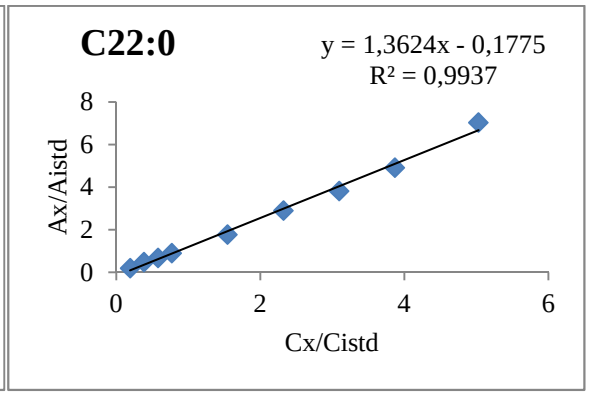
C22:0
y = 1,3624x - 0,1775
R² = 0,9937
Ax/Aistd
Cx/Cistd

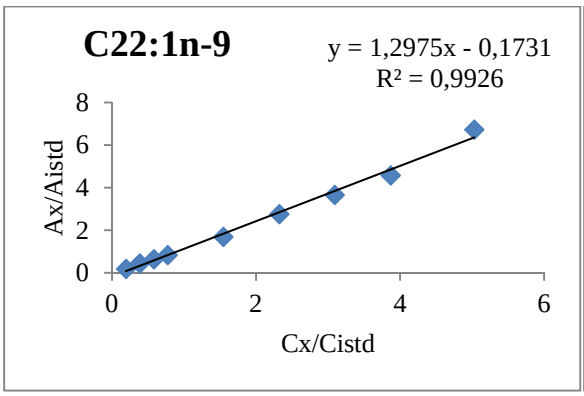
C22:1n-9
y = 1,2975x - 0,1731
R² = 0,9926
Ax/Aistd
Cx/Cistd

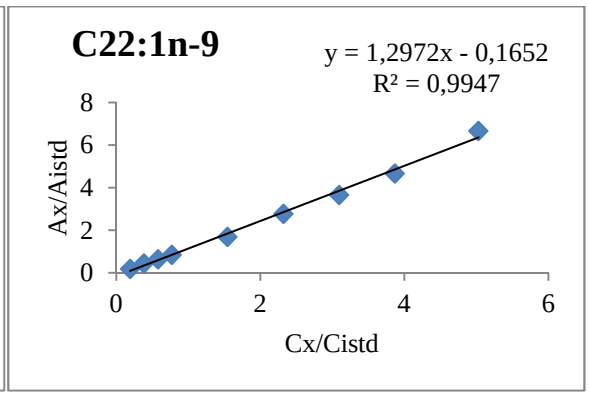
C22:1n-9
y = 1,2972x - 0,1652
R² = 0,9947
Ax/Aistd
Cx/Cistd

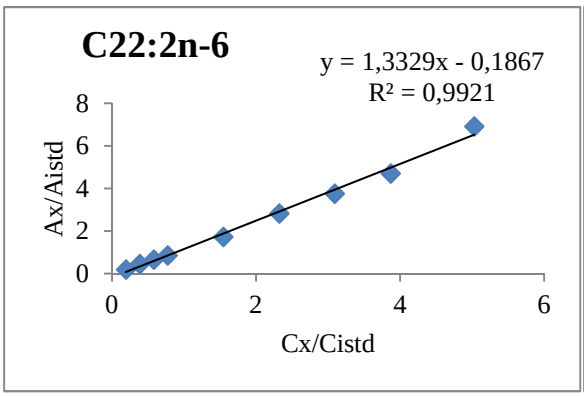
C22:2n-6
y = 1,3329x - 0,1867
R² = 0,9921
Ax/Aistd
Cx/Cistd

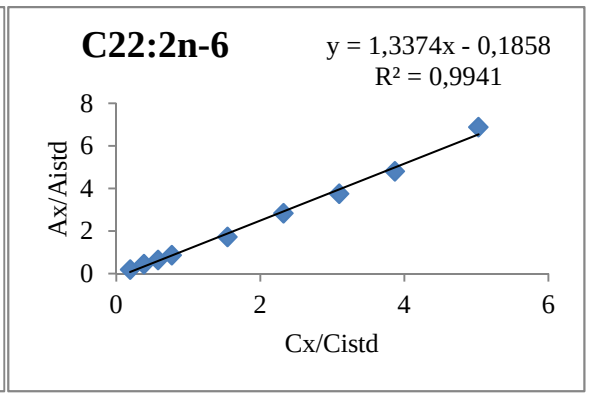
C22:2n-6
y = 1,3374x - 0,1858
R² = 0,9941
Ax/Aistd
Cx/Cistd

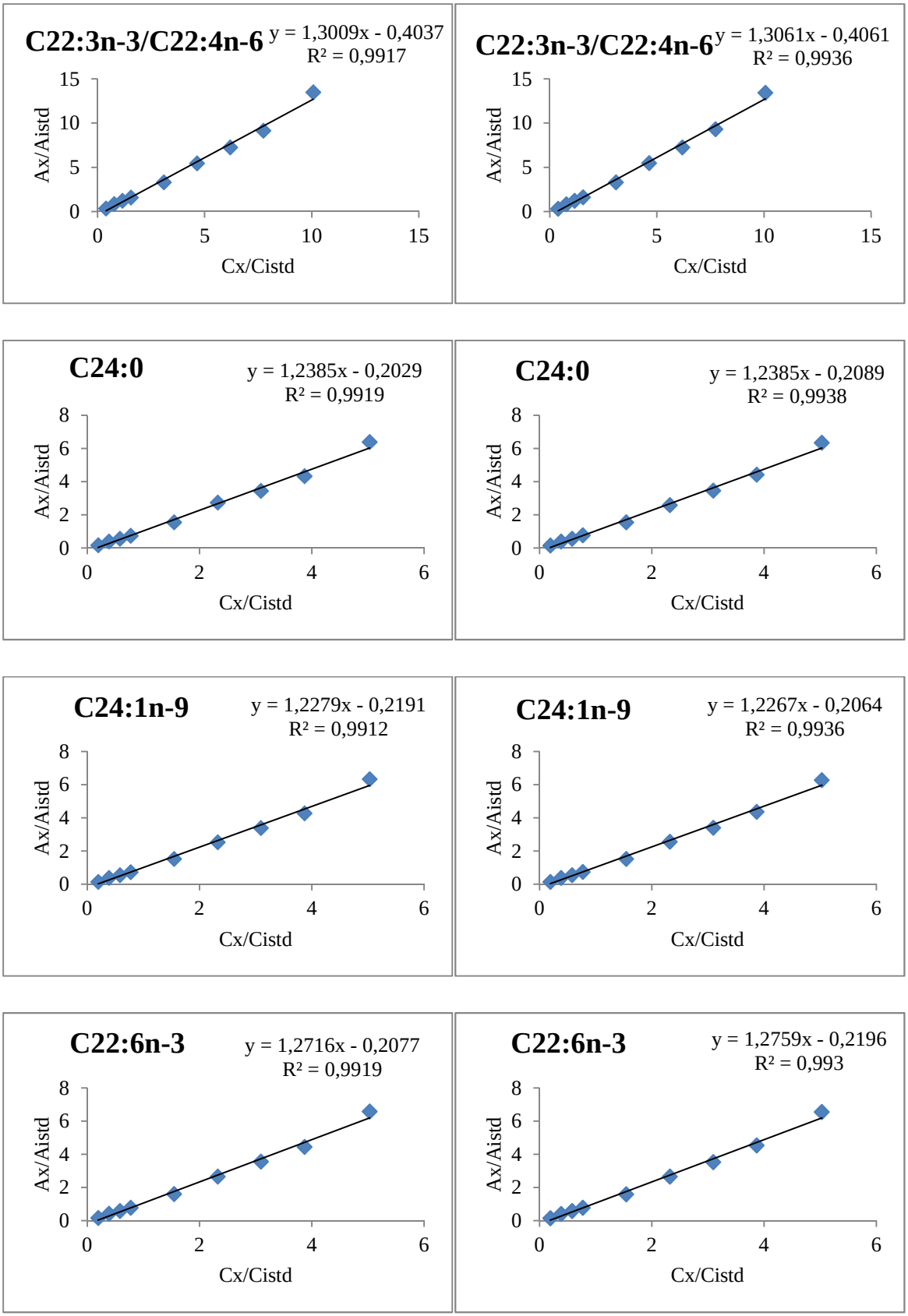

Figure A7-1 Calibration curves obtained with GC-FID for nine concentration levels of GLC #411 FAMEs. Curves from the first calibration to the left and curves for the repeated calibration 8 weeks later to the right.

Appendix 8: External control of results from serum phospholipid FAME analyses

Results for serum phospholipid FAME analyses achieved in this study were compared with results from an external laboratory. Numbers listed in the table is the difference between obtained percentages for single FAMEs out of total of 100 %.

$$Results_{master} - Results_{Vitas}$$

Table A8-1 Differences between obtained percentages for selected single FAMEs out of a total of 100 % for nine participant samples.

ID	C16:0	C18:0	C18:1	C18:2n-6	C20:3n-6	C20:4n-6	C20:5n-3	C22:5n-3	C22:6n-3
1	-3.8	-0.4	1.5	-1.2	0.9	0.3	1.6	1.7	-0.7
2	-3.8	-0.6	1.4	-1.1	0.7	0.1	1.3	1.5	0.3
3	-4.0	-0.6	1.7	-1.7	0.9	0.0	1.5	1.7	0.3
4	-3.1	-0.7	1.7	-1.3	0.6	0.3	0.9	1.4	0.3
5	-2.4	-1.1	1.4	-1.4	0.9	0.1	1.4	1.5	-0.4
6	-2.3	-0.9	0.8	-1.5	0.8	0.4	1.4	1.4	-0.2
7	-4.0	-1.5	1.5	-1.9	1.0	0.9	2.7	1.7	-0.3
8	-3.7	-1.5	3.3	-1.5	1.4	0.9	1.2	-1.0	1.3
9	-3.8	-2.2	2.4	-1.2	1.1	0.5	1.4	1.9	0.0

Appendix 9: Storage of standard solutions

Aliquots of 1 mg/ml total FAME concentration of GLC #411 analyzed after preparation and after one month storage in -20 and -80 °C. The experiment was performed to see if storage conditions and standard solution preparation procedures were adequate, because of observed increase in areas measured for stored standard solution compared to a freshly prepared standard solution.

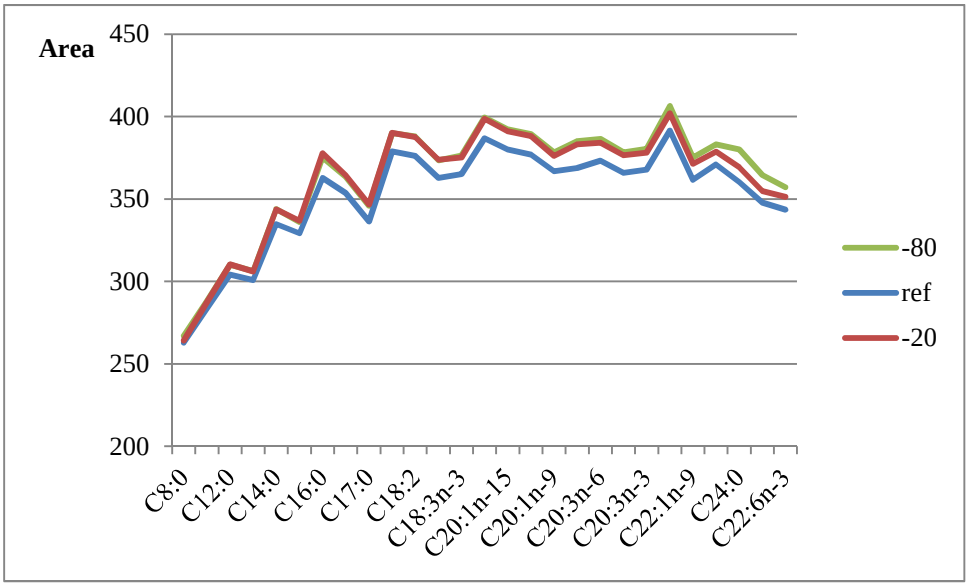

Figure A9-1 Aliquots of 1 mg/ml total FAME concentration of GLC #411 were analyzed directly after sample preparation (blue), or after one month storage in -20 °C (red) or -80 °C (green).